ISTITUTO ITALIANO
DI TECNOLOGIA

UNIVERSITÀ DEGLI STUDI
DI GENOVA

Thesis dissertation for the PhD course in neuroscience, curriculum Neuroscience and Neurotechnology cycle XXXVIII

Deciphering octopus arm and sucker control mechanisms for novel soft robotic applications

PhD Candidate:

Janina Leonie Röckner

Supervisors:

Letizia Zullo

Barbara Mazzolai

Table of Content

List of figures

List of tables

Abbreviations

A	Acetabulum
ANC	Axial nerve cord
AR	Arm reaction
BH, BE, EH	Marker pairs: Base to hand, Base to electrode, Electrode to Hand
BORIS	Behavioural Observation Research Interactive Software
C	Circular muscle
C12, C15, C25, C13, C24	Crystal pairs: 1-2, 1-5, 2-5, 1-3, 2-4
CA	Contraction Attachment
CCI	Co-contraction index
CD	Contraction Detachment
CI	Confidence interval
CNS	Central Nervous System
EMG	Electromyography
Glm.nb	Negative binomial regression
GLMMs	General linear mixed-effects-model
iEMG	Integrated electromyography
Int	Phase muscle activity
Int/s	Phase muscle activity/ time
IQR	Interquartile range
L	Longitudinal muscle
lme	Linear mixed effects
L/L0	Distance/ pre-pull distance
MaxDef	Maximum deformation
MBL	Marine biological laboratory
N	Number of replicates

n	Number of Trials
NR	No reaction
O; Fig. 2	Oblique muscle
O; Fig. 8	Orifice
OCA	Orientation-Contraction Attachment
OL	Optic lobe
PNS	Peripheral nervous system
rEMG	Rectified electromyography
SE	Standard error
SEM	Supraoesophageal mass
sEMG	Smoothed electromyography
SG	Sucker ganglion
SJ	Shrimp juice
Slope_diff	Slope drop magnitude
Slope_max	Local maximum
Slope_min	Local minimum
SR	Sucker reaction
StS	Sucker to Sucker
SUB	Suboesophageal mass
SW	Seawater
T	Transverse muscle
t	time
WLA	Wave-Like Attachment
WLD	Wave-Like Detachment

Abstract

Soft robotics has gained substantial popularity over the last ten years. As the name implies, these robots are mainly composed of soft materials. However, their biggest strength is also their biggest challenge: without rigid structures, movements can be performed with substantially more degrees of freedom than in regular robots. This large motion repertoire makes it hard to develop systems that can reliably predict and control movements. In nature, one model facing similar challenges is the octopus. Octopuses are among the most intelligent molluscs and have developed unique abilities to control all eight of their soft limbs. Each arm is a muscular hydrostat that creates movement through the local interplay of antagonistic muscles and connective tissues. This enables octopuses to perform motions like extension, shortening, bending and stiffening at any location along the arm. Although the arm can essentially move with infinite degrees of freedom, several octopus arm motions, such as extension and fetch, are performed following stereotypical patterns, suggesting that control can be simplified through distributed motor programmes. However, a cause-and-effect understanding linking muscle recruitment, deformation and behaviour remains incomplete.

This thesis investigates octopus arm and sucker control across three levels: (1) local motor control underlying stereotyped arm deformations, (2) role of sensory input at the sucker level in CNS-dependent action selection during retrieval, and (3) stereotyped sucker attachment and detachment strategies and their associated pressure dynamics. To address this, we combined *ex vivo* electromyography with kinematic tracking and muscle deformation measurements, behavioural and movement assays *in vivo* and *ex vivo*, and video- and pressure-based analyses of sucker attachment.

Our results show patterns of longitudinal and transverse muscle co-activation during electrically evoked arm extension and mechanically induced withdrawal-like resistance, consistent with a stabilising role of the proximal arm region and compatible with local stiffening. Muscle deformation measurements further indicate that neural activity can shape how strain is distributed during pulling. *In vivo*, octopuses adjusted retrieval decisions and kinematics based on stimulus value: Larger food items likely engage more chemo- and mechanotactile receptors at the

sucker-prey contact site and were associated with faster initiation and higher fetch velocities. Non-food items were unlikely to be retrieved, suggesting that the sucker chemosensory system contributes to brain action selection. Consistent with this, isolated arms did not differentiate between food and non-food items, indicating that chemosensory cues at the sucker level bias action selection primarily when central processing is available. Finally, we identified stereotyped patterns of sucker attachment and detachment. Moreover, pressure traces revealed strategy-dependent dynamics, including stepwise reinforcement, plateaus, and gradual versus abrupt release, consistent with active modulation of suction during attachment and detachment.

By linking local muscle recruitment, sucker sensory-driven action selection and sucker attachment dynamics, this thesis provides biological principles for reducing control complexity in compliant systems and may inform soft robotic designs that integrate distributed sensing with robust, damage-minimising attachment.

1 Introduction

1.1 Context and motivation

Over the last decade, the field of soft robotics has gained in popularity (Raman and Laschi 2024). As the name indicates, this field is dedicated to building and programming robots that mainly consist of soft materials. Unlike conventional robots, this characteristic can allow closer and safer interactions with humans, which is useful in multiple areas. For example, delicate tasks such as harvesting fruit can be performed by soft grippers, potentially reducing seasonal human labour (Elfferich et al. 2022). One of the fields with the highest demand for soft robotic development may be medicine. Modern medicine is constantly aiming to reduce the impact of surgical interventions. Minimally invasive surgery allows access to the region of intervention with little or no cutting, or by keeping the wound as small as possible. These procedures depend on very delicate tools, including sensors that help navigation inside the body (Tonutti et al. 2017). Soft robotics can contribute to the development of safer instruments for these applications (Iqbal et al. 2025, Qadrie et al. 2025).

In addition, in a world with an ageing society and reduced birth rates, soft robots may also assist in healthcare settings such as nursing homes, since their materials allow direct and safer interaction with patients (Ansari et al. 2017).

Ideally, the use of soft materials offers a wide range of movement patterns. However, what is arguably its biggest strength also comes with one of the main difficulties: control. Because soft structures can deform in many ways, it is challenging to predict and control their movements reliably. Taking a more focused view of tentacle-like soft robots, these systems represent a particularly relevant class of soft manipulators for complex and unstructured environments. Their continuum morphology allows them to bend along their entire length, conform to objects with irregular shapes, and establish distributed contact with the environment (Walker et al. 2005). This makes them ideal not only for grasping, but also for navigating confined spaces, interacting with delicate objects, and operating in environments where rigid robots may cause damage during collision or contact (Rus and Tolley 2015).

However, the same properties that make tentacle-like robots adaptable also create major challenges for modelling and control. Their bodies can deform in many possible ways, resulting in effectively infinite degrees of freedom. In addition, traditional external localisation may be unreliable in confined or visually occluded environments (Maloisel et al. 2021, Martini et al. 2026). Autonomous control offers a way to reduce this dependence on external tracking, but requires integrated proprioceptive sensing so that the robot can estimate its own body shape, posture, contact and strain during movement. This requires the integration of sensors, actuators and computational elements into structures that must remain bendable, stretchable and robust during deformation (Rus and Tolley 2015).

Several approaches have been developed to address these challenges. One strategy is to make use of the body itself, where the material properties and shape of the robot help it adapt to objects or surfaces and thereby reduce the control load, a principle often referred to as morphological computation. Other approaches use models to predict how the soft body will deform, or data-driven methods to learn complex movement patterns from experimental or simulated data. Although these approaches have advanced the field, challenges remain in sensor integration, actuator design, model accuracy and transfer to real-world environments (Della Santina et al. 2023).

Tentacle-like robots are commonly actuated by tendons, pneumatic chambers or combinations of different actuation strategies (Dou et al. 2021). These systems can generate highly adaptable movements, but their performance often depends on the number, placement and coordination of actuators and sensors. Because embedded components can change the mechanical properties of the soft body, it remains important to develop designs that provide functional control while minimising the number of integrated components required and preserving the robot’s compliance. This represents one of the major challenges in soft robotics and has encouraged an interdisciplinary approach: examining how comparable control problems are solved in biological soft structures. In nature, control is often not achieved by calculating every possible deformation centrally, but by combining local mechanical properties, distributed sensory feedback and stereotyped motor patterns. Many structures in the animal kingdom, including in humans, are capable of movement without a hardened internal or external skeleton, relying instead on hydrostatic structures. Soft

structures can be broadly divided into hydrostatic skeletons, in which liquid-filled chambers are compressed to form temporarily stiffened structures, such as in earthworms and leeches (see Figure 1 A, B), and muscular hydrostats, in which movement is generated by the precise interplay of muscles and connective tissue. Well-known examples of muscular hydrostats include tongues, lips, elephant trunks, and the limbs of cephalopods (Figure 1 C, D).

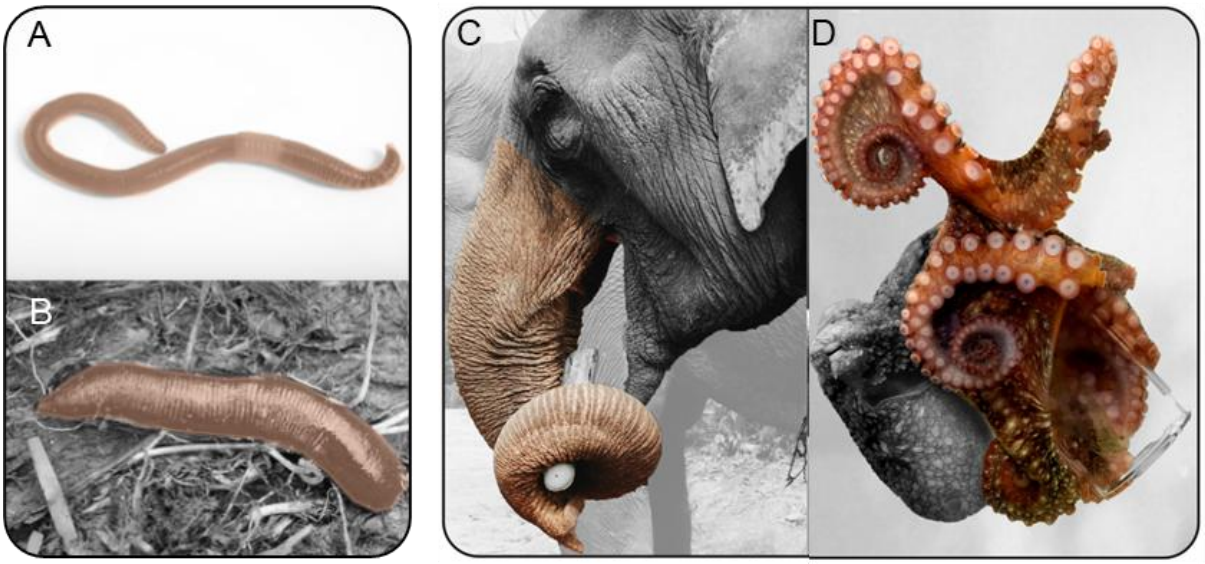

Figure 1 ***Examples of hydrostatic structures.*** *Hydrostatic skeletons represented by (A) an earthworm (photograph by Joel Sartore) and (B) a leech (photograph by Larry Doherty); muscular hydrostats represented by (C) an elephant trunk and (D) the arms of an octopus. Modified from Tekinalp et al. (2024).*

The behaviour of muscular hydrostats is shaped by local mechanical properties, neural circuits, and sensory feedback. For soft robotics, it is therefore essential to understand where and how sensory information is processed and how it contributes to movement control. One popular model organism in this context is the octopus. Octopuses do not rely on a vertebrate-like control architecture where body parts are represented somatotopically, suggesting that effective control can also be achieved through simplified control mechanisms that reduce load on the central nervous system (CNS) (Zullo et al. 2009).

In addition, octopus arms are equipped with chemo- and mechanoreceptors along their entire length, expressed in the over 300 suckers each arm and an extensible skin. This allows the animal to perceive information from the environment even when visual sensing is limited. Octopus suckers are particularly interesting because they can gently probe objects or clean the eggshells of offspring but also serve as highly

versatile attachment devices. While highly flexible arms already pose a major challenge to the nervous system, the ability to control large numbers of individual suckers makes the octopus an especially extraordinary model for understanding distributed control and embodied intelligence (Grasso and Basil 2009).

Therefore, it is of great interest for soft robotic control development to examine octopus arm motor control and environmental interaction. This includes the recruitment of muscle groups during stereotyped deformations, how sensory information from the suckers is integrated with CNS control to initiate stereotyped movements, and the strategies used by suckers to achieve loose attachment for surface exploration or strong attachment without tissue damage. By identifying these biological principles, this thesis provides an alternative and complementary perspective to purely model-based or data-driven soft robotic control approaches. Rather than controlling every degree of freedom centrally, octopus-inspired systems may benefit from local stiffness regulation, sensory thresholds, region-specific arm function and mechanically embedded attachment strategies.

1.2 Thesis focus and research questions

In this work, we employed the common octopus, *Octopus vulgaris* (Cuvier, 1797) and the two-spot octopus, *Octopus bimaculoides* (Pickford & McConnaughey, 1949), as model organisms. These two octopus species are very similar in term of behaviour, arm kinematics, anatomy of their arms and genetics, thus allowing us to perform parallel investigations in two very close animal species. The focus of this thesis is to understand how octopuses reduce the load on the CNS while still controlling eight highly flexible arms. A central aim is to determine how locally controlled stereotyped arm movements are generated and how sensory information from the suckers contributes to CNS-driven initiation of both arm and sucker stereotyped movements.

To address this, we focus on three levels of octopus arm motor control and sucker interaction:

1) Local motor control of stereotyped arm movements

Embedded within the nerve circuits in the peripheral nervous system (PNS) alone, stereotypical motions can be performed independently of the CNS. To do that, the arm has to reconfigure by activating two major arm muscle groups, the longitudinal and transverse muscles. In the experimental work, we specifically test how the major arm muscles contribute to feedforward extension movements and to resistance against pulling that may reflect withdrawal-like responses.

We want to understand whether these muscles co-activate to achieve particular kinematics and mechanical stability. Do arm and muscle deformations provide evidence for a cause-and-effect relationship between movement kinematics and muscle activation?

These questions serve as a basis to understand the level of arm autonomy through circuits in the PNS alone. In addition, we address CNS involvement and how sensory information is used to determine arm and sucker movement.

2) The role of sucker perception in stereotypical arm motion

To determine how sensory input at the sucker level influences the initiation and execution of stereotyped retrieval behaviours, we compare the response of arms in behaving animals with those of freshly separated arm samples.

In the *in vivo* experiment, we exposed the animals to food pieces of different sizes in a visually impaired setting. In a follow-up experiment, we presented the largest stimulus size with altered chemical cues, both to behaving animals and to an *ex vivo* arm preparation, where only local computing at the level of the arm and suckers was possible.

Here we asked how sucker sensory information drives the brain to set a certain level of muscle activation and how this influences the overall kinematics of the motion executed. In particular, we wanted to understand where in the control hierarchy decision-making occurs and whether larger food pieces, by providing stronger sensory input at the sucker contact site, lead to faster decisions and higher retrieval speeds.

3) Sucker stereotypical attachment and detachment patterns

Suckers contribute substantially to the octopus's perception of the environment. They provide sensory information that is continuously exchanged with the CNS. In addition, suckers are the first actors once a decision to manipulate an object is made, by initiating attachment with a single sucker or coordinated groups of suckers.

Here we asked what techniques a single sucker uses to form a seal to probe and attach to objects, and how the seal is released during detachment. Sucker performance was examined in a freely behaving octopus attaching to the front tank wall and to a platform equipped with multiple pressure sensors.

To frame these questions, the following section summarises the state of the art on stereotyped arm motor output, how sucker sensory input can recruit centrally coordinated behaviours, and how suckers generate stereotyped attachment and detachment.

1.3 State of the art

Principles of octopus arm motor control

Octopus arm control emerges from an interplay between muscle mechanics, connective tissue, and neural activity at both local and central levels. The octopus arm is a muscular hydrostat composed mainly of incompressible muscle tissue (Kier and Smith 1985, Smith and Kier 1989, Kier and Stella 2007, Feinstein et al. 2011, Fossati et al. 2011). Muscle fibres in muscular hydrostats are generally arranged perpendicular, parallel, or helical relative to the long axis (Kier and Smith 1985). Generally, muscular hydrostats follow the constant-volume muscle constraint (Wilson et al. 1991, Van Leeuwen and Kier 1997), meaning that any change in one dimension results in compensatory changes in at least one other dimension. This principle relies on coordinated activation of agonistic and antagonistic muscles and allows movements with theoretically infinite degrees of freedom.

Muscular hydrostats are widespread across the animal kingdom, with the elephant trunk being a well-known example (Kier and Smith 1985, Smith and Kier 1989, Longren et al. 2023). However, the octopus arm differs markedly from the trunk in its structure. Elephant trunks also include the nasal passages, making their internal anatomy more heterogeneous than the densely packed structure of octopus arms.

Octopus arms are composed of oblique muscles that run in a helical arrangement along the arm, as well as circular muscles, and the longitudinal and transverse muscle masses that form most of the arm's shape (Figure 2). They are composed of obliquely striated muscle cells (Kier and Smith 1985, Kier 2016). The longitudinal muscle comprises fibres running laterally, aborally and orally along the arm, parallel to the axial nerve cord (ANC). Transverse muscle fibres run around the nerve cord and are oriented perpendicular to the longitudinal axis (Graziadei 1964, 1971). Longitudinal muscles have been described as less stiff and more flexible, contributing more to graded responses. In contrast, transverse muscles are stiffer and show more resistance to deformation (Di Clemente et al. 2021) and they are thought to contribute more to posture and motion stabilisation (Flash and Zullo 2023).

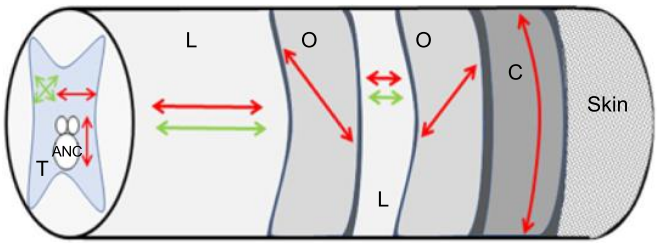

Figure 2 ***Octopus arm musculature.*** *Schematic of octopus arm anatomy showing the ANC, axial nerve cord and muscles including T, transverse muscle; L, longitudinal muscle; O, Oblique muscle; C, circular muscle with arrows indicating the muscles vector active (red) and passive (green) force. (Flash and Zullo 2023).*

The arm extraordinary repertoire of movements can therefore only be achieved through precise interplay between muscle physiological properties, morphological orientations, and anatomical positioning. Arm muscle framework proposes no obvious mechanical restrictions, thus making stereotypical movements such as shortening, elongation, bending and torsion to be performed at any location along the whole arm. However, in natural behaviour they occur relatively more frequently at specific arm locations and in selected arms (Levy and Hochner 2017, Kennedy et al. 2020, Nesher et al. 2020, Zullo et al. 2022, Flash and Zullo 2023, Bennice et al. 2025).

These movements can be achieved through the exploitation of both the extreme flexibility and graded control of specific muscles and the co-activation of antagonistic muscles, where no local volume change is generated, and connective tissue passively resists deformation (Kier and Smith 1985, Kier and Stella 2007, Hochner et al. 2023), thus bringing the arm to stiffen. In the latter case, portions of the arm are stabilised and temporary reconfigured in skeletal-like elements (Sumbre et al. 2006). Although, it is believed to be a key principle to maintain arm portions straight during stereotypical motions such as reaching, fetching and walking local stiffening in octopus has not been measured and fully quantified yet.

Hereafter I will describe the main stereotypical motions investigated in this work.

Arm extension

Arm extension is a movement used by the octopus to reach toward a target. It is generated through the formation of an initial bend at the base which is propagating along the arm till the arm tip (Gutfreund et al. 1996, Gutfreund 1998; Figure 3).

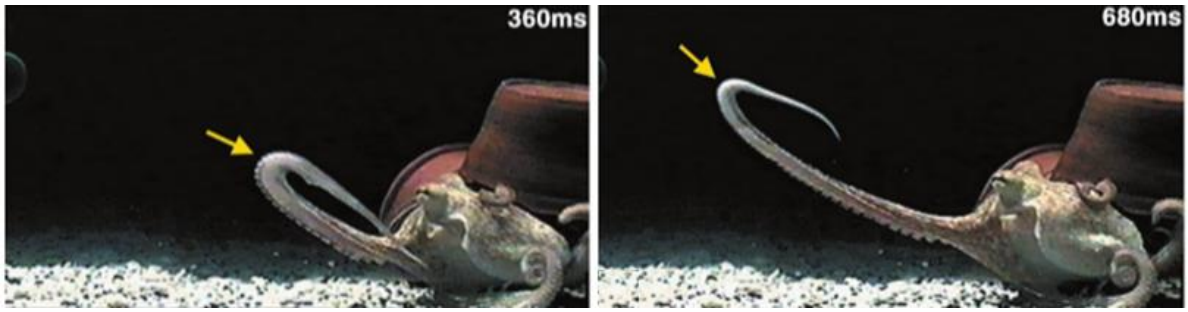

Figure 3 ***Octopus reaching movement.*** *A sequence of images showing arm reaching movement with a yellow arrow showing the site of bend propagating towards the arm tip. Modified from Sumbre et al. (2001).*

It requires local control of longitudinally organised muscles to contract and shorten on the side of the bend (Gutfreund et al. 1996, Gutfreund 1998), while transverse muscle activity may contribute to maintaining the deformation. Passive forces within the arm also support bend propagation, making the movement energetically efficient. The higher elasticity of the longitudinal muscles (Di Clemente et al. 2021) may facilitate yielding on the side opposite the bend, while the comparatively higher stiffness of transverse musculature can provide resistance, allowing the bend to propagate as contraction is released on the bend side. Consistent with precise motor control, electromyography (EMG) recordings indicate that muscle activation slightly precedes the bend that thus passively propagate from the base to the arm tip (Gutfreund 1998).

Arm elongation

To achieve arm elongation, Kier and Smith (Kier and Smith 1985) describe the involvement of muscle groups that actively decrease the cross-sectional area. In the octopus' arm, this includes transverse, oblique and radial muscle groups. During elongation, transverse and radial muscles contract while longitudinal muscles relax and passively elongate. Arm elongation generally occurs as part of other behaviours such as reaching in a constrained environment (Mazzolai et al. 2013, Hanassy et al. 2015) and during arm extension. Elongation occurs at a specific location along the arm and is supported by the different dimensions of the arm muscles along the proximal-distal axis (Kennedy et al. 2020, Zullo et al. 2022).

Arm withdrawal

A common and crucial reflex embedded in arm PNS circuits is the withdrawal reflex. Hague et al. (2013) described this reflex in *ex vivo* arm preparations positioned vertically or horizontally and elicited by mechanical or chemical stimulation (Figure 4 A, B). In vertically positioned arms, withdrawal consisted of proximal muscle contraction that produced rapid shortening and torsion, retracting the arm from a potentially harmful stimulus.

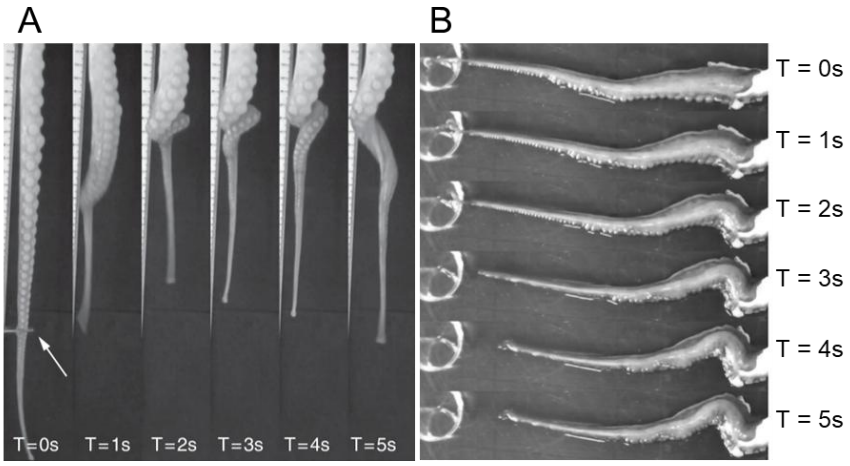

Figure 4 ***Octopus arm withdrawal.*** *(A) Mechanically induced withdrawal in a vertically mounted octopus' arm within a timeframe of 5 s. The white arrow indicates stimulus site. (B) Chemically induced withdrawal in a horizontally mounted octopus' arm within a timeframe of 5 s. (Hague et al. 2013).*

In the octopus' arms muscular hydrostat, shortening can be generated by longitudinal muscle contraction in the proximal region (Kier and Smith 1985, Kennedy et al. 2020), while co-activation of circular, oblique and transverse muscle groups may contribute to torsion and thereby support a rapid pull-away response. In horizontally positioned arm samples, withdrawal responses were again initiated in the proximal region and resulted in a local bend, driven by longitudinal muscle contraction on the side of the deformation (Hague et al. 2013).

Arm fetching

Some stereotypical arm movements require sensory information from the environment (visual, chemical, and/or tactile) to be integrated at the CNS level. A prominent example is the fetching movement described by Sumbre et al. (2006) in which three bend points function like temporary joints to bring prey to the mouth.

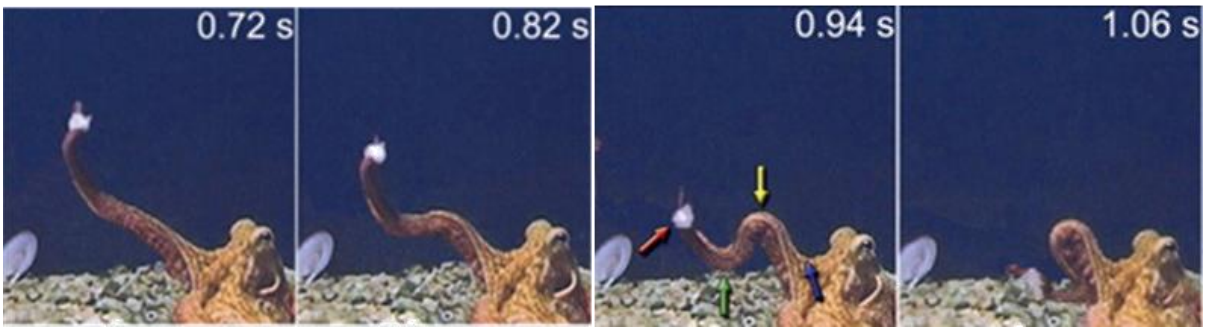

Figure 5 ***Octopus fetching movement.*** *A sequence of images showing the fetching movement. The red arrow shows the contact-point with the prey, the green, yellow and blue showing the distal, medial and proximal bending points. Modified from Sumbre et al. (2006).*

EMG recordings suggest that prey contact triggers a sensorimotor response that involves peripheral processing together with central coordination. This response produces two waves of muscle activation, one propagating from the base and the other from the tip, which converge to generate the medial bending point.

We have seen how the octopus arm muscle properties already help to elucidate the mechanisms that make it possible to control eight soft limbs with effectively indefinite degrees of freedom. Zullo et al. (2022) further proposed that passive constraints within arm musculature provide a predefined mechanical framework that reduces the need for complex feedforward commands, thereby reducing the load on the octopus CNS. To better understand how the octopus processes environmental information and translates neural activity and muscle activation into movement kinematics, the next section considers the organisation of the octopus nervous system.

Octopus nervous system

Octopuses are able to control eight arms using a highly complex nervous system. The nervous system of *O. vulgaris* consists of the CNS, including the brain and large optic lobes, and the PNS, composed of the arm nerve cords and ganglia (Young 1963, 1971; Figure 6).

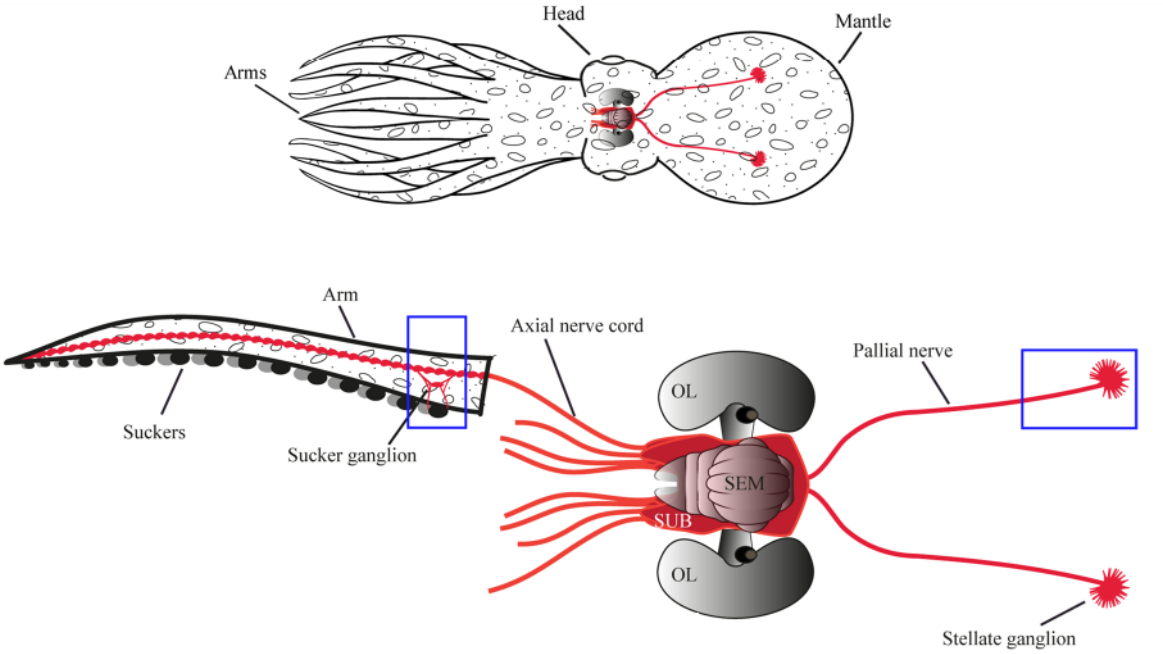

Figure 6 ***Nervous system of Octopus vulgaris.*** *Schematic of the octopus nervous system showing general anatomy (mantle, head, arms), the central nervous system, pallial nerves and stellate ganglions; OL, optic lobes; SEM, supraoesophageal mass; SUB, suboesophageal mass; and the peripheral nervous system, including the axial nerve cord and sucker ganglion, with their respective positions within the arm. Modified from Imperadore et al. (2019).*

Arm control is hierarchically organised, with higher-level control of arm movements located in the supraoesophageal lobes (Young 1971, Budelmann and Young 1985), intermediate-level control in the suboesophageal lobes, and lower- control within the PNS, including the nerve ring that links the ANCs and enables inter-arm communication (Chang and Hale 2023) as well as reflexes embedded within the arms' peripheral circuitry (Altman 1971).

Approximately two thirds of the octopus nervous system is located in the PNS (Young 1963). Most PNS neurons reside in the ANC, which carry both sensory information and motor output between the arms and the central brain (Rowell 1966,

Graziadei 1971, Sumbre et al. 2001). The ANC comprises a chain of ventral ganglia and two dorsal axonal tracts. Each ganglion has nerve projections that innervate two main arm regions: the intrinsic musculature and the sucker (via sucker nerves). Nerves innervating the intrinsic musculature originate on the dorsal and lateral sides of the ANC (Gutfreund et al. 2006), whereas sucker nerves exit ventrally and pass through the intrinsic muscle layers (Graziadei 1971). Each of the over 300 suckers is innervated by these nerves, which converge into a dedicated sucker ganglion (SG) or project into the sucker tissue.

This organisation of the octopus nervous system ensures sufficient control over such a highly redundant motor system. Although stereotypical, some movements such as fetching require sensory information from the prey contact site to be integrated in the CNS to ensure successful retrieval (Sumbre et al. 2006; Figure 7 B).

In contrast, the octopus also shows many examples of locally coordinated behaviour that does not require constant CNS involvement. For example, the motor programme for arm extension and withdrawal is embedded at a lower level of motor control within the arm itself (Sumbre et al. 2001, Hague et al. 2013). In this framework, higher motor centres are primarily involved in initiating the movement and setting parameters of the extension (Figure 7 A). Consistent with this, extension can be triggered in an arm isolated from the CNS through electrical stimulation of the ANC (Sumbre et al. 2001).

Another example are the suckers that can move independently from continuous CNS feedback (Altman 1971; Figure 7 C). Each sucker has a dedicated arm ganglion and a SG, located in the stalk of each sucker (Graziadei 1971, Young 1971, Neacsu and Crook 2024, Olson et al. 2025). Recent studies report that the SG contains markers of sensory and motor neurons, supporting circuitry for local reflexes without involvement of the ANC (Olson et al. 2025). Nerve fibres originating from the SG innervate local musculature and cells. In addition, they connect to the oral roots of the ANC, suggesting that information may be exchanged via the ANC. This is consistent with earlier hypotheses that sucker-to-sucker communication occurs through the ANC (Rowell 1963, Graziadei 1971, Olson et al. 2025).

Together, these examples illustrate how locally embedded motor programmes and peripheral processing contribute to flexible arm behaviour while reducing demands on the CNS. At the same time, it remains important to understand which sensory inputs trigger specific arm behaviours and under which conditions CNS feedback becomes necessary.

In an ideal environment, octopuses use a combination of vision, distance chemoreception, contact chemoreception, and mechano-tactile sensing. However, they regularly encounter conditions with limited visual feedback (e.g., at night or in low water clarity) and, despite being equipped with complex eyes with remarkable similarities to vertebrate eyes (Hanke and Kelber 2020), their dominant sensory modalities are chemo- and mechanotactile. These are largely mediated by receptors localised at the arm level and in particular within the sucker epithelium (Mather and O`Dor 1991, Budelmann 1996, Vincent et al. 1998, Villanueva et al. 2017).

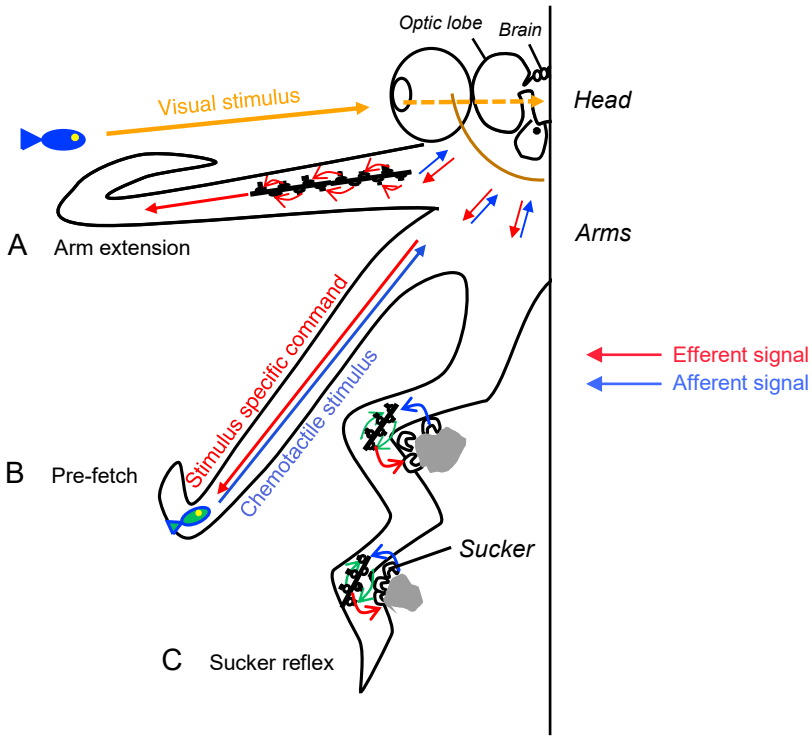

Figure 7 ***Octopus motor control.*** *Schematic of neural control of known stereotypical sucker and arm motion. (A) Visually induced arm extension; (B) Chemotactile induced (Pre-)fetch; (C) Chemo- and mechanotactile induced sucker reflex. Modified from Hochner et al. (2023).*

The next section therefore focuses on sucker sensory capabilities and the mechanics of sucker attachment and detachment.

Suckers as sensory and attachment organs

Given the extensive peripheral circuitry in the arms, suckers are not only effectors for manipulation and attachment but also major sensory organs that may contribute to local processing of chemical and mechanical information. The octopus sucker can be divided into four key parts (Figure 8). The inner chamber is called the acetabulum. In the centre of the acetabulum is a piston-like structure, the protuberance, that seals the chamber while the sucker attaches to a surface. The acetabular chamber is connected to the infundibular chamber via a narrow opening formed by a sphincter muscle, the so-called orifice. The infundibulum is the surface that is in direct contact with the environment and, together with the sucker rim, forms a tight seal during attachment (Girod 1884, Kier and Smith 1990). Each arm is equipped with more than 300 suckers which, in both species of interest (*O. vulgaris* and *O. bimaculoides*), are arranged in two alternating rows along the arm. In the common octopus, suckers decrease in histological complexity from base to tip (Graziadei and Gagne 1976).

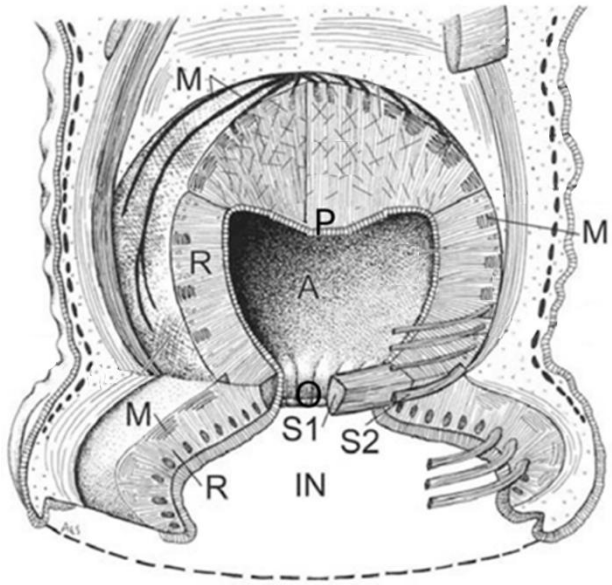

Figure 8 ***Schematic of an octopus sucker.*** *P, Protuberance; A, Acetabulum; S1, S2, Sphincter muscle; O, Orifice; IN, Infundibulum; M, meridional muscle; R, Radial muscle. Modified from (Kier and Smith 2002).*

Octopuses use their suckers to probe and manipulate objects in their surroundings. More specifically, they can recruit multiple suckers or control each individually to navigate, anchor to the substrate, investigate and manipulate objects, catch prey, transport food to the mouth and, in females, care for eggs by keeping them clean (Altman 1971, Grasso 2008, Hanlon and Messenger 2018, Buresch et al. 2022, Bidel et al. 2022).

Thousands of sensory neurons are associated with each sucker, with many receptors located in the rim (Graziadei 1962, 1964). This sensory organisation supports major foraging strategies in which octopuses insert their arms into crevices

in corals or stones to locate prey such as crustaceans (Yarnall 1969, Ambrose and Nelson 1983, Mather and O`Dor 1991, Forsythe and Hanlon 1997, Hanlon and Messenger 2018). They have also been observed performing speculative bottom searching by extensively probing the seafloor with their arms, potentially relying primarily on chemo- and mechanosensing (Hanlon and Messenger 2018). Buresch et al. (2022) further showed that, based on contact chemical cues alone, octopuses can distinguish prey-scented from non-prey-scented objects and can discriminate between different types of prey. They argue that, although evidence exists for distance chemosensing of prey and conspecifics (Walderon et al. 2011, Weertman et al. 2025), contact chemosensing may play a particularly important role in prey identification during foraging.

Based solely on mechanotactile information, octopuses can distinguish between smooth and rough textures (Wells and Wells 1957, Gutnick et al. 2020), between cubes vs. spheres, and balls vs. crosses (Wells 1964, Kawashima and Ikeda 2025), and between naturalistic three-dimensional shapes (Buresch et al. 2024). Mechanoreceptors in the sucker rim and infundibulum exhibit on/off responses (Graziadei and Gagne 1976), which may make them especially sensitive to moving prey. Mechanical information can already be extracted from the distortion of a single sucker (Wells 1964), which can elicit neuronal activity in neighbouring arm ganglia and lead to recruitment of additional suckers (Ten Cate 1928, Rowell 1966, Altman 1971, Wells 1978, Zullo et al. 2011). It has also been suggested that multiple suckers need to be engaged to gather sufficient mechanical information for reliable shape discrimination (Buresch et al. 2024).

As discussed above, suckers are also used to attach and anchor the animal to substrate. Based on the physical properties of water, muscle arrangement within the sucker (Kier and Smith 1990) and ultrasound imaging Tramacere et al. (2013) proposed a four-phase mechanism for sucker attachment (Figure 9). In the first phase (A), the infundibulum conforms to the surface to form a seal, after which radial muscles of the acetabulum contract (B) to increase chamber volume and reduce internal acetabular pressure (Pa). Subsequently, meridional muscles pull the acetabular protuberance down to interlock it in the orifice (C). After formation of a water torus, radial muscle contraction ceases and the protuberance is maintained in place (D) through friction of the ridges, cohesive forces of water, and elastic

energy stored in cross-connective tissue fibres. Suction can be released when circular muscles activate to disengage the protuberance. This energy-efficient attachment can generate pressure differences of up to 0.268 MPa in a single sucker (Smith 1991). Even though the mechanisms underlying suction and negative-pressure generation have been investigated, and sucker engagement and recruitment can be triggered by local reflexes independent of the CNS, stereotyped patterns of sucker attachment and detachment behaviour have not yet been described.

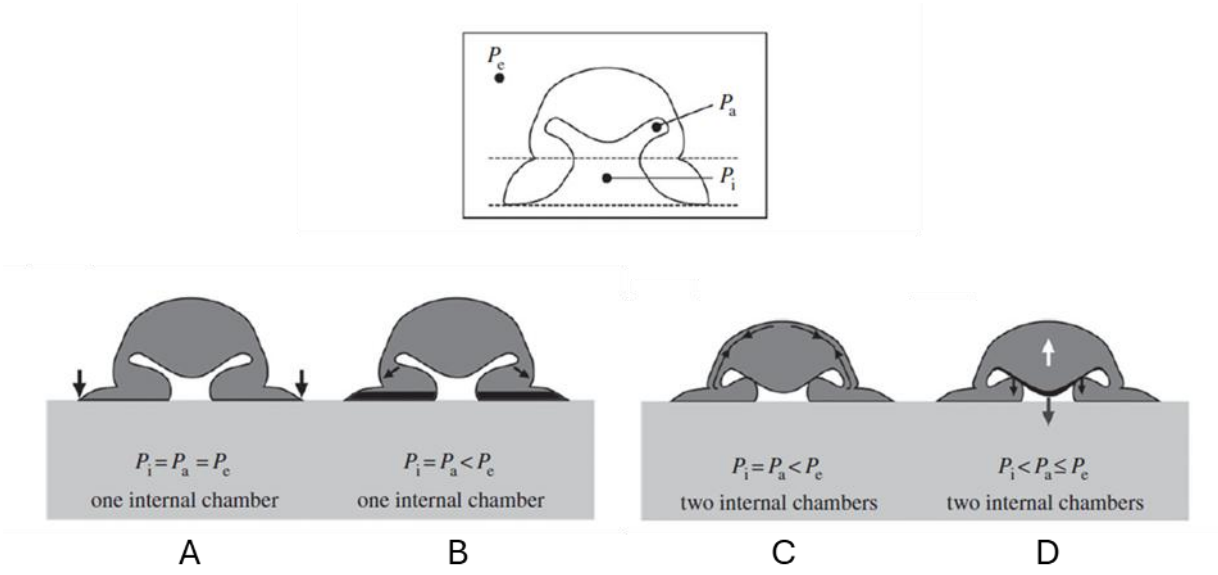

Figure 9 ***Proposed adhesion mechanism of an octopus sucker.*** *(A) The infundibulum contacts the surface and forms a seal. (B) Acetabular radial muscles contract, increasing chamber volume and drawing water into the acetabulum. (C) Meridional muscles contract and pull the protuberance down to interlock it within the orifice. (D) Muscle contraction ceases and passive forces maintain the protuberance in position. Pe, external pressure; Pa, acetabular pressure; Pi, infundibular pressure. (Tramacere et al. 2015).*

Based on this sensory and mechanical functionality, we next describe the experimental approaches used to link arm muscle activity and arm kinematics, to test how sensory information from the suckers is integrated with CNS control to initiate and fine-tune behaviour, and to quantify sucker stereotyped attachment and detachment.

1.4 Methodological and theoretical framework

To investigate how arm muscles are recruited during arm extension and withdrawal-like resistance solely on the level of the PNS, we used EMG in a whole-arm *ex vivo* preparation. Two electrodes were implanted within the same arm segment to record activity from the longitudinal and transverse muscles. Arm extension was elicited by electrical stimulation of the ANC following Gutfreund (1998), and EMG recordings were synchronised with video footage to segment the response into three kinematic phases. Withdrawal-like responses were induced by mechanically pulling the arm along the longitudinal deformation vector and holding it under stretch (~2 s), so that the analysed response reflects resistance under sustained elongation rather than a complete withdrawal. Video footage was used to identify pull onset and offset in the EMG trace. To assess whether the muscles co-activate, we compared overall muscle activity, temporal correlation, and co-contraction between the longitudinal and transverse EMG signals. The same videos were also used to quantify arm deformation using DeepLabCut-based marker tracking (Mathis et al. 2018).

To further characterise muscle behaviour during pulling-induced elongation and to test the contribution of local motor control, we used sonomicrometry. Five piezoelectric transducers were implanted on both sides of the lateral longitudinal muscles in *ex vivo* arm preparations. One set of arms was tested immediately after excision from an anaesthetised octopus, whereas a second set was tested several hours post-excision after confirming the absence of a response to arm-tip pinching. This design allowed comparison of responsive preparations with intact local activity versus non-responsive preparations, by quantifying muscle strain along the proximal–distal axis and changes in arm diameter during pulling.

We hypothesise that extension kinematics are closely linked to the timing and magnitude of activation in both longitudinal and transverse muscles. We further expect co-activation to increase arm stiffness and thereby provide a stable base for bend propagation towards the tip. Similarly, during resistance against pulling, we predict co-activation of both muscles to stabilise the arm base.

To examine how sensory information at the sucker level shapes CNS-driven action initiation and local arm motion, we conducted behavioural experiments *in vivo* and

ex vivo. *In vivo*, octopuses were presented with shrimp pieces of different sizes to test whether food size influences sucker perception and as a result might alter decision-making during food retrieval, including decision time, strategy choice, and retrieval velocity. In a follow-up experiment, agarose pieces matched to the largest shrimp size were presented either with shrimp extract or with seawater aiming to isolate the effect of chemical cues while keeping mechanical properties constant. To probe local sucker and arm reaction without CNS involvement, the same agarose stimuli were then presented to different locations along a separated arm to test whether sensitivity to chemical versus mechanical cues varies with arm location.

We hypothesise that, in the *in vivo* trials, larger and therefore more valuable food pieces provide stronger sensory input at the sucker level, leading to shorter decision times and faster retrieval than smaller food pieces. Similarly, agar pieces containing shrimp extract are expected to provide stronger chemotactile cues and are more likely to be picked up in the *in vivo* experiment.

To understand if chemical inputs from the suckers are mostly integrated and used at the brain level, we expect that removing the brain connection by using separated arms in an *ex vivo* setting and testing for their response to agar pieces with versus without prey extract will not show major differences in sucker and arm responses.

Finally, motivated by the importance of sucker contact for decision-making, we took a closer look at single-sucker behaviour. Suckers are both sensitive tools for exploring the environment and capable of forming a tight seal during attachment. To understand how octopuses achieve secure attachment while avoiding damage to the sucker surface, we quantified octopus sucker attachment and detachment, with particular emphasis on detachment strategies that release the seal by pressure control rather than by pulling. This was also intended to inform soft robotic designs in which silicone-based suckers and embedded sensors can degrade under repeated forceful pull-off. High-speed video was used to capture attachment/detachment sequences on the aquarium front glass. In addition, to measure seal pressure and relate attachment strategies to generated forces, we collaboratively developed a transparent platform incorporating pressure sensors. Pressure measurements and synchronised videos were collected as a freely

behaving octopus approached and attached to the platform mounted on the tank glass.

We hypothesise that octopuses use multiple attachment and detachment strategies. We further expect that the sensor platform will enable quantification of attachment strength and provide additional insight into the mechanics of seal formation and release.

1.5 Thesis structure

This thesis investigates how octopus control highly flexible arms by combining muscle mechanics with hierarchical neural processing and sensory feedback from suckers. Chapter 1 has outlined the motivation and aims of the thesis, reviewed the state of the art, and introduced the methodological roadmap and hypotheses. Chapter 2 then describes the experimental setups and analytical approaches used throughout the thesis. These include EMG recordings synchronised with kinematic tracking, sonomicrometry to quantify muscle strain during pulling, behavioural assays *in vivo* and *ex vivo* to probe sucker perception under controlled mechanical and chemical cues, and high-speed video and pressure measurements to analyse sucker attachment and detachment. Chapter 3 presents the results from these experimental components, moving from locally generated arm motor output in isolated preparations to behaviours that depend more strongly on sensory information from the suckers and CNS involvement, and finally to attachment and detachment stereotypical strategies at the level of single suckers. Chapter 4 synthesises these findings in the context of distributed motor control in muscular hydrostats and discusses their relevance for soft robotic design. Chapter 5 concludes by summarising the core contributions of the thesis and outlining future steps towards translating them into soft-robotic design.

2 Material and Methods

2.1 Animal maintenance

Octopus vulgaris

27 *O. vulgaris* specimens were used in this study. Animals of both sexes (body mass 200–300 g) were collected from local fishers on the Ligurian coast of Italy between October and May. This research conformed to the ethical principles of the three Rs (Replacement, Reduction and Refinement) and to minimising animal suffering, in accordance with Directive 2010/63/EU (Italian Legislative Decree D. Lgs. no. 26/2014) and the guidelines of Fiorito et al. (2014, 2015). All experimental procedures were approved by the institutional board and the Italian Ministry of Health (authorisation no. 465/2017-PR).

After capture, the animals were housed in aquarium tanks (80 × 50 × 45 cm) filled with artificial seawater (Tropic Marin, Wartenberg, Germany) and enriched with a sand substrate and clay-pot dens. The temperature was maintained at a constant 17 °C, corresponding to the average temperature at the collection site, and the water was continuously circulated through a biological filter system. Oxygenation was ensured using a dedicated aeration system, and all relevant physicochemical water parameters were checked daily. Animals were allowed to acclimatise for at least 10 days before the experiments. They were inspected daily and fed shrimp three times per week.

Octopus bimaculoides

13 *O. bimaculoides* of both sexes (body mass 100–200 g) were collected off the coast of southern California. After capture, the animals were housed in 190 L aquarium tanks supplied with flowing natural seawater and enriched with clay-pot dens for shelter, as well as rocks, artificial plants and children’s toys. Temperature was maintained at a constant 16 °C. Animals were allowed to acclimatise for at least 10 days before the experiments. They were inspected daily and fed frozen pieces of penaeid shrimp, as in the experiments. Feeding was withheld on days when individuals participated in the experiment.

This research conformed to the ethical principles of the three Rs (Replacement, Reduction and Refinement) and to minimising animal suffering, in accordance with the Marine Biological Laboratory's Cephalopod Care policy and the guidelines of Fiorito et al. (2014, 2015). All experimental procedures were approved by the MBL IACUC committee.

Anaesthesia

For *ex vivo* arm preparation, animals were anaesthetised in a 3.5% magnesium chloride ($MgCl_2$; Sigma-Aldrich Company Ltd, Gillingham, UK) solution prepared in fresh seawater. Anaesthetic depth was assessed by applying a mechanical stimulus to the arm tip (pinch). Animals were considered adequately anaesthetised when pinching did not elicit an arm withdrawal response. Once anaesthesia was confirmed, one arm was excised using a scalpel. Each animal was anaesthetised two times and up to three arms were dissected in total.

2.2 Electromyography

To characterise muscle activity, electromyography (EMG) was used. Electrodes were customised following the method described by Gutfreund (1998) (see Figure 10). The recording and reference electrodes were made from Teflon-coated stainless-steel wire (0.0045 inch; A-M Systems Inc., Sequim, USA). For each recording electrode, a plastic bead was fixed to the wire, leaving a free end. Subsequently, 2 mm of insulation was removed from the free end at an appropriate distance from the bead to expose the wire within the target muscle. The free end was threaded laterally through the arm using a syringe needle, and a second bead was attached to secure the electrode at the implantation site.

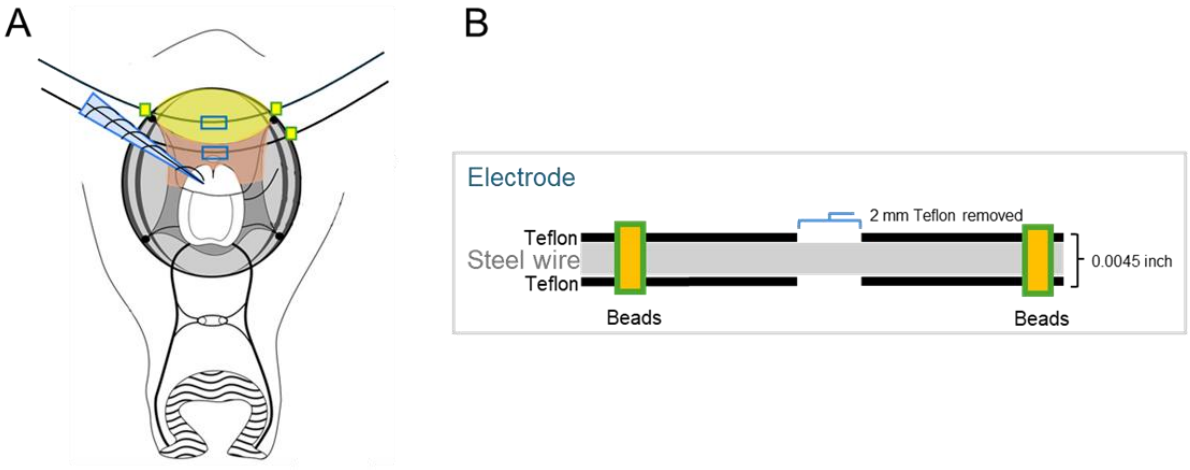

Figure 10 ***Electrodes for EMG.*** *(A) Transverse arm section showing the electrode implantation site and location of electrical stimulation using a suction electrode. Aboral longitudinal muscle in yellow. Aboral transverse muscle section in red. Site of removed Teflon coating is framed in blue. (B) Schematic of the Teflon-coated reference electrode (steel wire).*

The experimental setup consisted of a tank filled with artificial seawater and an incorporated platform occupying approximately one third of the tank. An isolated *ex vivo* arm preparation was fixed at the base to stabilise the exposed ANC, which was accessed through a small incision on the aboral side. The remainder of the arm hung freely over the platform edge.

Two customised recording electrodes were implanted into the arm: one into the aboral longitudinal muscle and a second into the same region but positioned to record from the deeper transverse muscle. The free ends of the reference electrodes were placed in the water bath.

Arms were either electrically stimulated using a suction electrode on the ANC thus inducing arm extension or mechanically pulled and held under stretch to elicit a withdrawal-like resistance response.

The EMG signal was recorded at 10 kHz, amplified (×10,000), and band-pass filtered (300 Hz–3 kHz), digitised, and saved using Clampex (ALA Scientific Instruments Inc., Farmingdale, USA). Arm motion was recorded with a camera (Huawei Nova 5T; Huawei, Shenzhen, China) positioned above the recording chamber. Kinematics of the motion were quantified off-line from video recordings, which were processed in CapCut (ByteDance, Haidan, China) and synchronised using a light cue marking the onset of electrical stimulation.

Raw EMG data were rectified (rEMG), smoothed (sEMG, moving window of 10 ms), and integrated into 50 ms time bins to obtain integrated EMG (iEMG; see Figure 11). To remove background noise, for each trial a threshold was set at mean + 3 standard deviations of the first 100 ms of the smoothed baseline signal, and values below this threshold were treated as background activity and removed prior to further quantification. Signal processing was performed using the biosignalEMG package (Guerrero & Macías-Díaz, 2019).

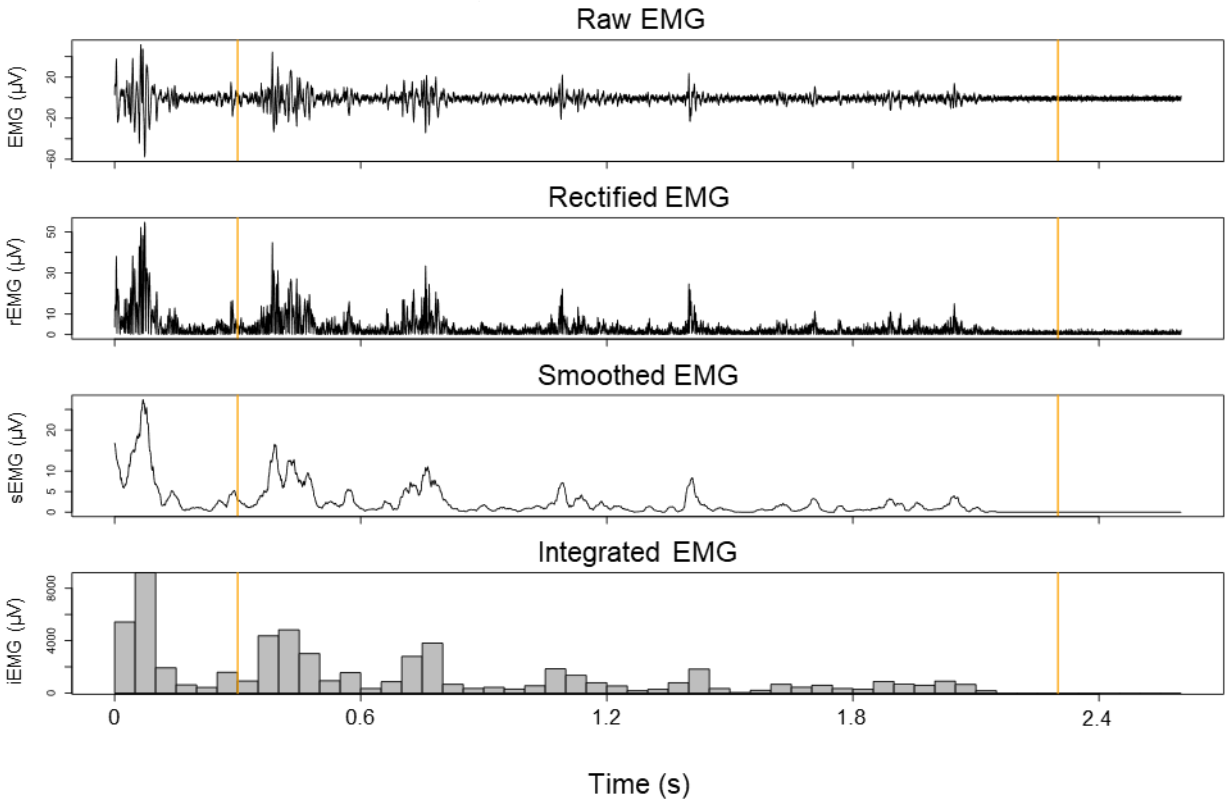

Figure 11 ***Exemplary EMG signal and data processing.*** *Raw, rectified, smoothed and integrated EMG signal during an arm pull. The analysed interval is indicated by the yellow margins. EMG, Electromyography; rEMG, rectified EMG; sEMG, smoothed EMG; iEMG, integrated EMG.*

Electrode positions were confirmed by histological analysis after EMG recordings.

Arm extension

In the first experiment, the arm was folded onto the platform and extension was induced by electrical stimulation of the ANC delivered via a suction electrode using a stimulus isolation unit (ISO-Flex; A.M.P.I., Jerusalem, Israel). Stimulation consisted of a 50 Hz train of 100 pulses at 40–90 V with a 5 ms positive voltage step

(Master-8-cp; A.M.P. I., Jerusalem, Israel). The entire stimulus artefact was excluded from the analysis and an additional 0.01 s after stimulation offset was removed to avoid residual stimulus artefacts. During the electrical stimulation, the arm unfolded rapidly and extended.

Based on changes in motion pattern, the evoked extension response was divided into three phases (Figure 12): phase 1 began immediately after stimulation offset, resulting in finalisation and maintenance of arm extension; phase 2, a subsequent arm turn followed by a second smaller elongation; and phase 3, another change of direction and a final shortening or relaxation, in some cases accompanied by curling towards the base. Phase onset and offset times were identified for each trial and used to compute phase-specific EMG metrics.

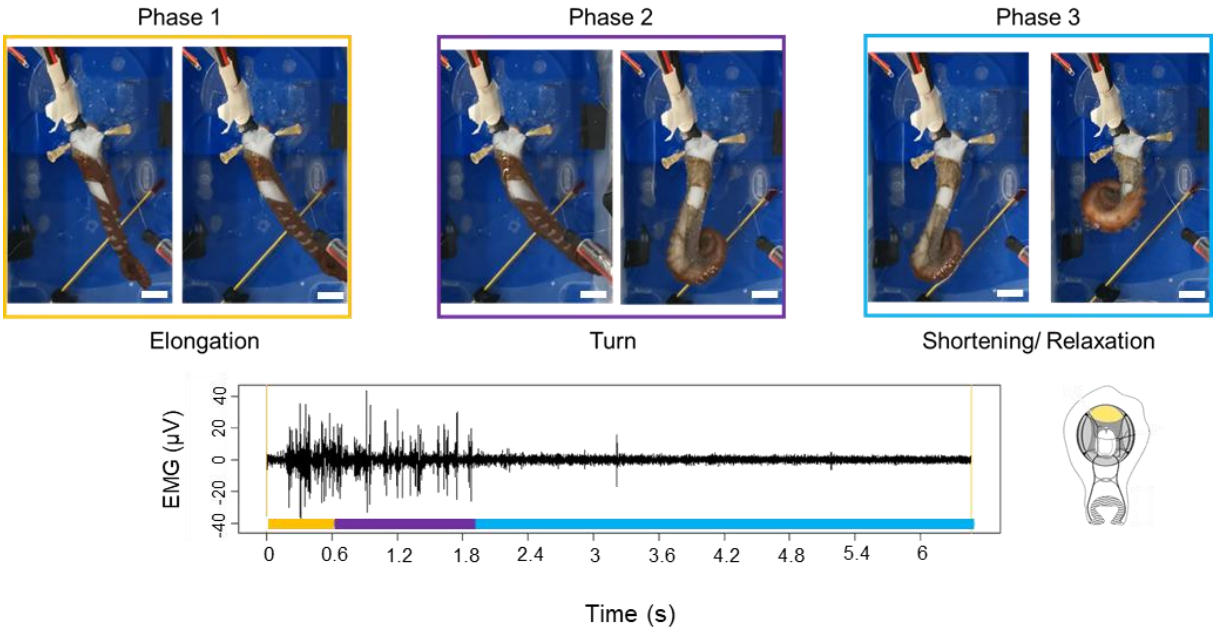

Figure 12 ***Three phases of arm extension.*** *Electrical stimulation elicits a three-phase arm response: extension (yellow), turning (purple), and shortening (blue) shown with representative video frames (top), scalebar 20 mm (white), and the synchronised raw longitudinal-muscle EMG trace (bottom). EMG, Electromyography.*

To quantify overall activity, the sEMG signal was normalised to its maximum within each trial. Phase activity was then quantified by summing the 50 ms integrated values within each phase and dividing by phase duration to account for variable phase length, yielding a time-normalised measure of activity (Int/s).

To assess temporal co-activation, the correlation coefficient between the two muscles was computed within each phase using Pearson correlation (implemented with cor.test in R) on the phase-specific sEMG signals. Correlation strength was interpreted using conventional thresholds (correlation coefficient < 0.3, weak; 0.3–0.7, moderate; > 0.7 strong). In addition, co-contraction was quantified using the co-contraction index (CCI; Figure 13), computed pointwise as

$$CCI(t) = \frac{2 \cdot min(L(t), T(t))}{L(t) + T(t)}$$

where $L(t)$ and $T(t)$ are the sEMG values of the longitudinal and transverse muscles at time t. The phase-specific CCI was then calculated as the mean of $CCI(t)$ across all samples in that phase (excluding time points where $L(t) + T(t) = 0$). CCI values range from 0 to 1, where 0 indicates no overlap in activation and 1 indicates equal activation of both muscles. For descriptive interpretation, we used the following operational thresholds: CCI < 0.3 low overlap, 0.3–0.6 moderate overlap, and > 0.6 high overlap.

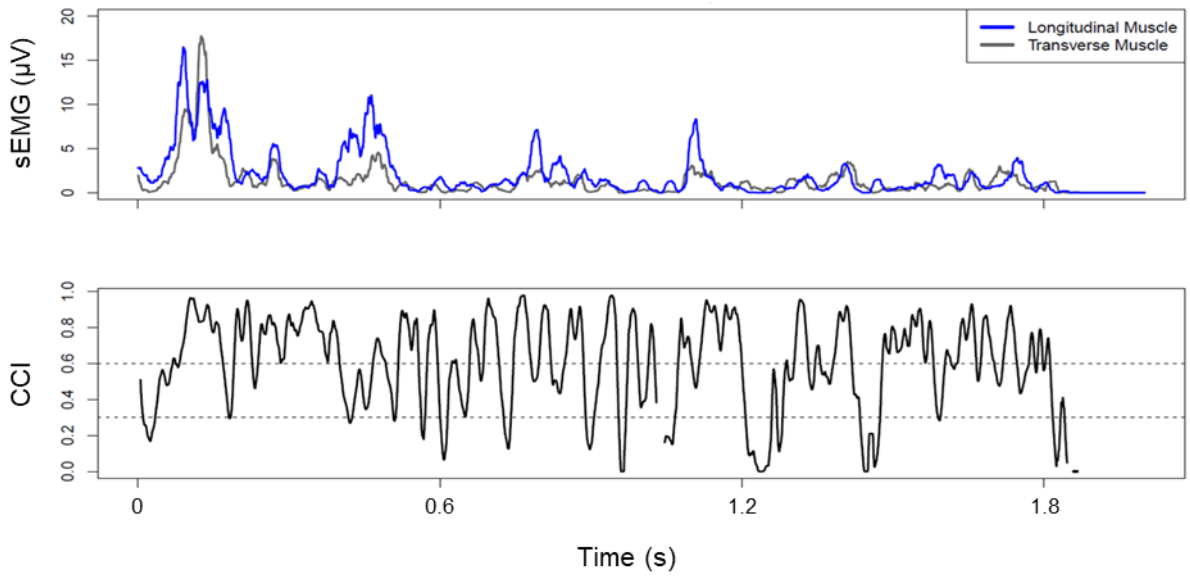

Figure 13 ***Example EMG signals and corresponding co-contraction index (CCI).*** *Top: sEMG signals of the longitudinal muscle (blue) and transverse muscle (black) used to determine the correlation coefficient. Bottom: co-contraction index over time. sEMG, smoothed electromyography.*

Statistical analysis

Int/s values were square-root transformed to improve distributional properties. Then the data were fitted using a linear mixed-effects model (lme) as a function of phase, muscle, and the phase × muscle interaction (nlme package). To account for non-independence of observations, random intercepts were included for each sample, with trial nested within sample. As variability differed across phases, heteroscedasticity was modelled using a phase-specific variance structure. Models were fitted using restricted maximum likelihood, with optimisation settings adjusted to ensure convergence.

Correlation coefficients and CCI were Fisher z-transformed prior to analysis to improve normality and stabilise variance. Transformed values were analysed using an lme model with phase as a fixed effect and a random intercept for trial (restricted maximum likelihood).

Arm withdrawal

In the second experiment, the arm was mechanically pulled against the fixation point to stretch the arm. This pull would normally induce the arm to withdraw, however in the current setting the arm was held for approximately 2 s and the analysis was restricted to the time the arm was kept under a stretch condition.

Pull onset was determined from video footage as the first frame in which the arm began to elongate (Figure 14). Trials were divided into consecutive fixed time windows of 0.66 s each, starting at pull onset. The sEMG signal was normalised to its maximum within each trial, and phase activity (Int) was computed by summing the 50 ms integrated values within each time window. Because all windows had equal duration, Int values were directly comparable across phases. For each phase, Int, the correlation coefficient, and the co-contraction index (CCI) were quantified.

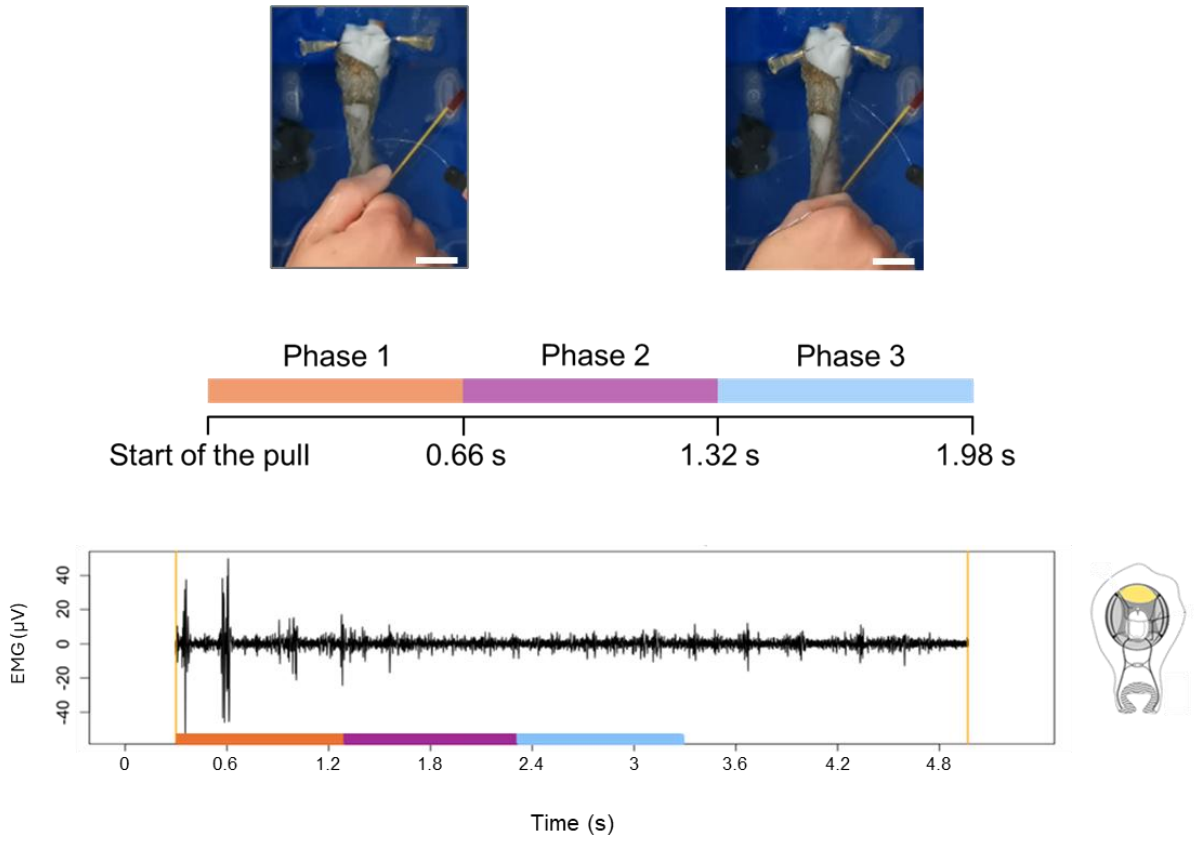

Figure 14 ***Three time-defined phases of arm withdrawal response.*** *Responses are divided into Phase 1 (0–0.66 s; orange), Phase 2 (0.66–1.32 s; purple), and Phase 3 (1.32–1.98 s; blue). Top: representative video frames, scalebar 20 mm (white), Bottom: synchronised raw longitudinal muscle EMG trace (µV). Coloured bars indicate phase boundaries. EMG, electromyography.*

Statistical analysis

The resulting Int values were log-transformed to improve distributional properties. The transformed Int data were modelled as a function of phase, muscle, and the phase × muscle interaction using an lme model. To account for non-independence of observations, random intercepts were included for each trial, with an additional intercept for phase nested within trial. As variability differed across phases, heteroscedasticity was modelled using a phase-specific variance structure. Models were fitted using restricted maximum likelihood, with optimisation settings adjusted to ensure convergence.

Correlation coefficients and CCI were Fisher z-transformed prior to analysis and analysed using an lme model with phase as a fixed effect and a random intercept for trial (restricted maximum likelihood).

For both models, fit was evaluated using AIC and visual inspection of residual diagnostics (Q–Q plots and residuals versus fitted values).

2.3 Motion kinematic analysis

Arm deformation: DeepLabCut

For a proof-of-concept analysis and to further characterise arm motor output, arm kinematics were reconstructed from two video recordings acquired during the mechanical pull experiment. Three digital markers were tracked along the arm using DeepLabCut (Mathis et al. 2018) to mark the arm base, the electrode location, and the hand (Figure 15). Marker positions were extracted at 20 frames per second throughout the pulling movement to match the EMG integration bin size (50 ms) and to capture passive arm elongation with sufficient temporal resolution. Changes in distance between markers were calculated and synchronised with the corresponding EMG signals using the same synchronisation procedure as described for the EMG recordings.

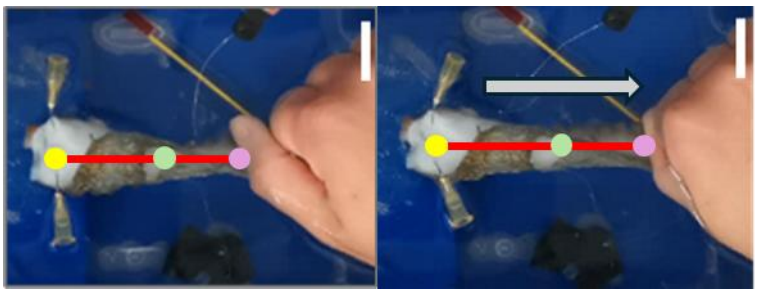

Figure 15 ***Marker placement.*** *Representative video frames showing digital marker placement at the base (yellow), electrode location (light green), and point of pull/hand (light purple). The red line indicates the distance of interest, and the grey arrow shows the passive elongation vector, scalebar 20 mm (white).*

Muscle deformation: Sonomicrometry

To assess how neural activity within the arm influences muscle deformation during pulling, we used sonomicrometry in responsive and unresponsive *ex vivo* arm preparations. Preparations were classified as responsive when pulling elicited an overt active movement response and measurements were performed immediately after excision. Preparations were classified as unresponsive when no overt response to pulling was observed and measurements were performed only after the arm had been separated for a longer period.

Sonomicrometry uses piezoelectric crystals to transmit and receive ultrasonic pulses (Figure 16 A). Each crystal acts as both a transmitter and a receiver. Distances between crystals were calculated from the acoustic transit time between crystal pairs and an assumed speed of sound in the tissue; changes in inter-crystal distance were used to quantify deformation.

Five crystals (Sonometrics Corporation, Ontario, Canada) were implanted into each *ex vivo* arm preparation. Two crystals were implanted into each of the two lateral longitudinal muscle masses on opposite lateral sides of the arm to form two longitudinal crystal pairs (see Figure 16 B, C). A fifth crystal was implanted into the lateral longitudinal muscle on one side of the arm, adjacent to one of the distal crystals, to provide an additional reference for distance calculations and overall deformation during passive pulling.

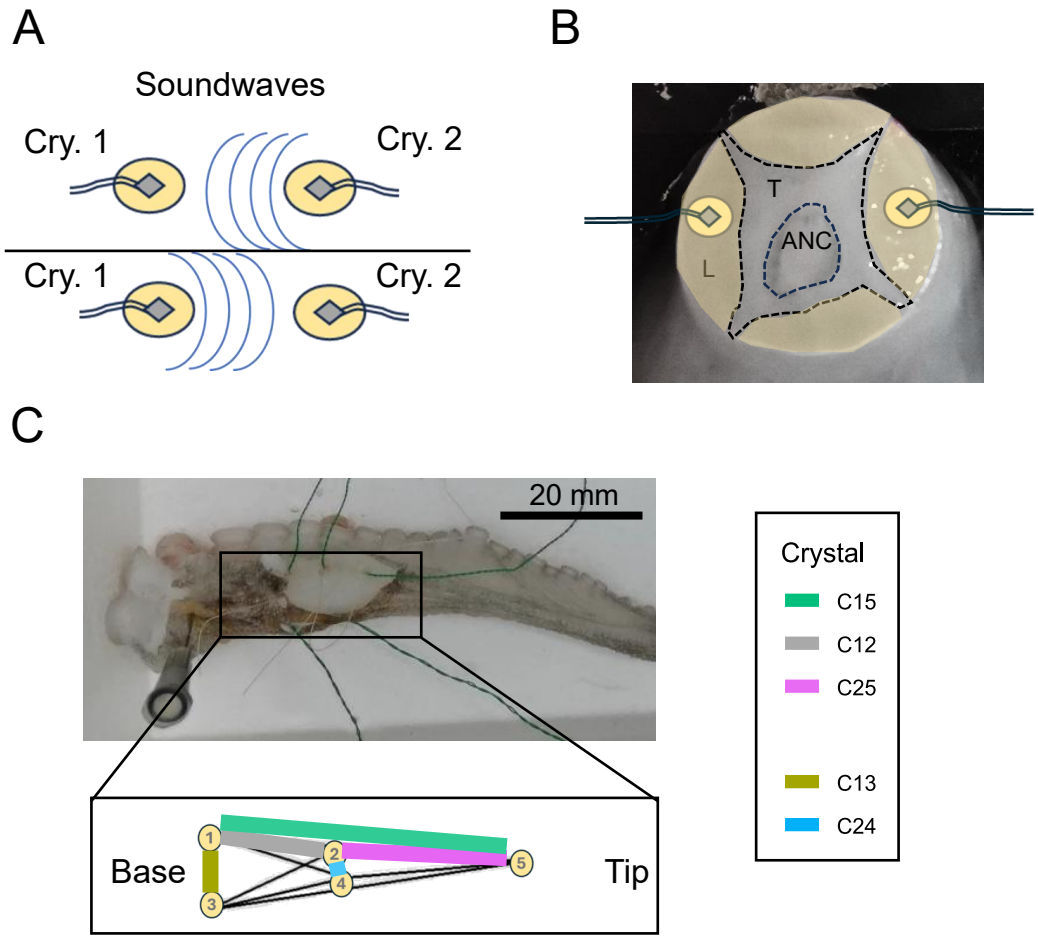

Figure 16 ***Sonomicrometry setup and crystal placement****. (A) Schematic of crystal pairing. (B) Transverse section indicating approximate crystal placement within the arm. (C) Example preparation showing implantation site (boxed) and the analysed crystal pairs (C15 in green; C12 in grey; C25 in purple; C13 in olive green; C24 in blue). Cry., Crystal; L (light yellow), longitudinal muscle; T, transverse muscle; O, oblique muscle; ANC, axial nerve cord.*

Longitudinal deformation was recorded continuously during a 2 s passive elongation. Data were collected and processed using SonoLabDS3 and SonoSoft (Sonometrics Corporation, Ontario, Canada).

To compare muscle deformation between sample types, distances were normalised to the pre-pull distance for each crystal pair (L/L0), such that the pre-pull baseline was set to 1 in all plots. Maximum deformation (MaxDef) was defined as the L/L0 value at the start of the visually identified post-pull plateau (i.e., immediately after the pull ramp ended; see Figure 17). MaxDef along the pull axis was quantified using crystal pairs 1–5 (C15), 1–2 (C12) and 2–5 (C25), and changes in arm diameter were quantified using crystal pairs 1–3 (C13) and 2–4 (C24).

In addition, deformation curves from the start of the pull until MaxDef for crystal pair C12 were examined. Specifically, the C12 deformation trace contained repeated episodes of transient slowing during the pull. To quantify these events, we analysed the time-varying slope of the deformation curve. Specifically, we estimated the local slope by fitting a linear regression within a sliding window of 10 samples, generating a rolling slope signal over time. Local maxima in the rolling slope were detected using findpeaks (pracma package) in R with a minimum peak distance of 5 samples and a minimum peak height ≥ 0. For each detected slope maximum (Slope_max), we identified the subsequent minimum (Slope_min) defined as the first turning-point minimum before the slope began to increase again (Figure 17). All automatically detected events were visually inspected and, where necessary, corrected manually. For each max–min pair, the slope drop magnitude (Slope_diff) was calculated as

$$Slope\_diff = Slope\_max - Slope\_min$$

Events with Slope_diff < 0.05 were excluded to remove low-amplitude fluctuations. To avoid overweighting pulls with more detected events, Slope_diff values were summarised per pull using the median for visualisation.

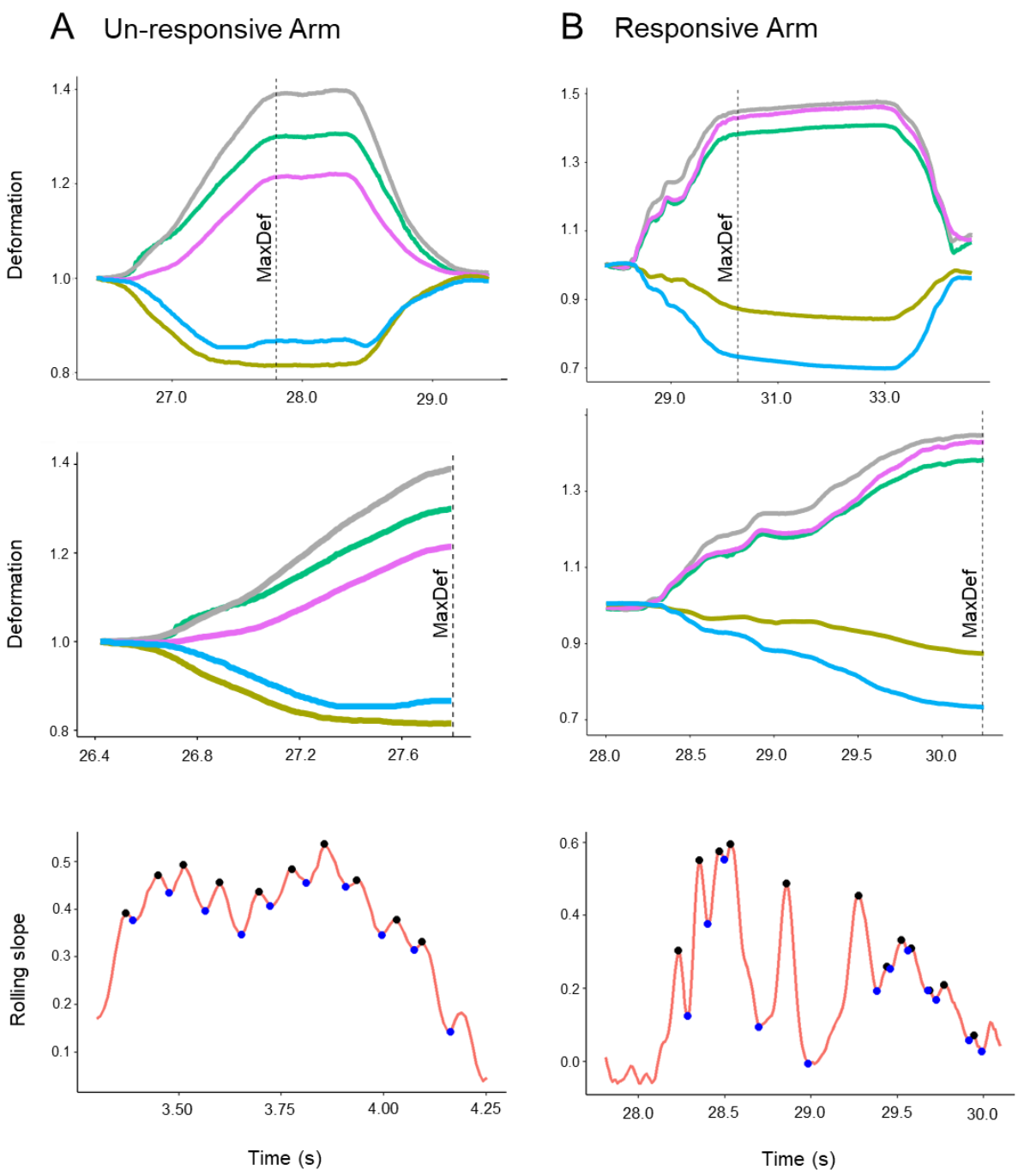

Figure 17 ***Example of muscle deformation curve analysis.*** *Muscle deformation represented by five crystal pairs (C15 in green; C12 in grey; C25 in purple; C13 in olive green; C24 in blue) and rolling slope of C12 over time in an (A) unresponsive arm and a (B) responsive arm. MaxDef, Maximum deformation.*

Statistical analysis

For each dataset, MaxDef (L/L0) was modelled as a function of crystal pair (Crystal) using an lme model. To account for non-independence arising from repeated pulls within the same preparation, random intercepts were included for SampleID, with

an additional random intercept for PullID nested within SampleID. Because variability differed among Crystal, heteroscedasticity was modelled using a crystal-specific variance structure. Models were fitted using restricted maximum likelihood. Model fit was evaluated using AIC and visual inspection of residual diagnostics (Q–Q plots and residuals versus fitted values).

2.4 Behavioural experiments

The behavioural experiments were conducted at the MBL in Woods Hole, MA, USA using the local species *O. bimaculoides*. Behavioural tests were run in a dedicated experimental tank filled daily with fresh seawater and equipped with marine gravel of different sizes and colours, which allowed for the 'goal object' to be masked on the tank bottom. Goal objects consisted of food pieces (Experiment I) and agar cylinders that were either embedded with shrimp juice or seawater (Experiment II). Experiment III used an *ex vivo* arm preparation to test local arm responses using the same agar stimuli. More details are given for each experimental methodology.

The tank was illuminated using an LED lamp (Godox™ WL8P LED; Godox, Shenzhen, China). Data were collected from video footage recorded from two iPhone 14s (Apple Inc, Cupertino, USA) positioned at the front and lateral side of the tank (Experiment I). The recording area was isolated using black curtains thus preventing the animals from being visually distracted by the operator.

Experiment I – Effect of food size on behaviour

This experiment was designed to test whether food size influenced an octopus' behaviour and retrieval strategies. A total of five octopuses were used in this experiment.

Food pieces of different sizes were cut from frozen penaeid shrimp using biopsy punches to produce cylindrical pieces of 2, 4 and 10 mm diameter, with heights matched to the punch diameter (i.e., 2, 4 and 10 mm, respectively). One octopus per session was moved to the experimental tank. After an acclimatisation period of 30 minutes, it was lured to the back of the tank using an artificial crab, and a vertical opaque barrier was placed in the tank mid portion to prevent the animal from seeing

the food placement on the tank floor. One food item was positioned on the bottom of the tank for each trial, close to the front wall, to facilitate camera tracking.

Recording started prior to lifting the barrier and the animal was given 5 minutes to find the food. If the food was retrieved, a new trial would start 3 minutes after eating. If the food was not retrieved, the octopus was encouraged to explore the bottom of the tank by luring it with visual stimuli (e. g. an artificial crab) moved outside the tank. Each octopus was presented with all three food sizes at least three times per day (9 trials per animal per day) in a randomised order. Trials ended when the octopus retrieved the food or when it touched each food piece at least three times, regardless of whether it retrieved it or not. Octopuses were rewarded with half a shrimp at the end of each experimental day to ensure cooperation.

Animal behaviour was analysed using Behavioural Observation Research Interactive Software (BORIS; Friard et al. 2016). An ethogram was created in BORIS comprising predefined state events, which were used to quantify the time animals spent interacting with the food and the velocity of food retrieval.

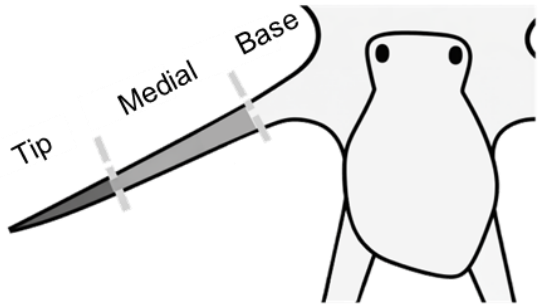

Figure 18 ***Arm division.*** *Visualisation of the three arm locations (Base, Medial, Tip) used in the analysis. Modified from Kennedy et al. (2020).*

In addition, point events were defined to document the retrieval strategy and the arm region interacting with the food. Arm location was categorised by virtually dividing the arm into three segments as illustrated in Figure 18. A total of 268 interactions were quantified and categorised into five different behaviours: Explore, Fetch, Clamp, Parachute and Sucker to Sucker (Figure 19). For interactions that did not result in retrieval, the duration of the animal touching the food was documented (Explore; Figure 19 A).

Four different strategies were used to retrieve the food. The most frequent strategy was Fetch (Figure 19 B). Following the description by Sumbre et al. (2006), fetch is achieved if pseudo-joints form at three locations to bend the arm and transport the food to the mouth. Two state events were quantified: 1) the time from first touching the food piece to the decision to retrieve it (Touch-to-Fetch) and 2) the velocity of

the fetching (Fetch-to-Mouth). The second most frequent strategy was Clamp (Figure 19 C) where the octopus touched the food and used two arms to bring it to its mouth. Two state events were quantified: the duration of the touch (Touch-to-Clamp) and retrieval (Clamp-to-Mouth). Another less frequent strategy we observed was Parachute (Figure 19 D). The octopus jumped onto the food piece. Subsequently, an arm picked up the piece and brought it towards the mouth. We measured the duration of the touch (Touch-to-Parachute), the duration between completing the parachute and initiating the fetch (Parachute-to-Fetch), and the duration of the fetch (Parachute-Fetch-to-Mouth).

Only once out of 143 observed retrievals did we encounter Sucker to Sucker transport (Altman 1971; Figure 19 E). During this behaviour, the arm touched a small food piece and passed it from one sucker to the neighbouring sucker to transport it closer to the mouth. We measured the duration of the touch (Sucker-to-Sucker), and the time until the food reached the mouth (Sucker-to-Sucker-Fetch-to-Mouth).

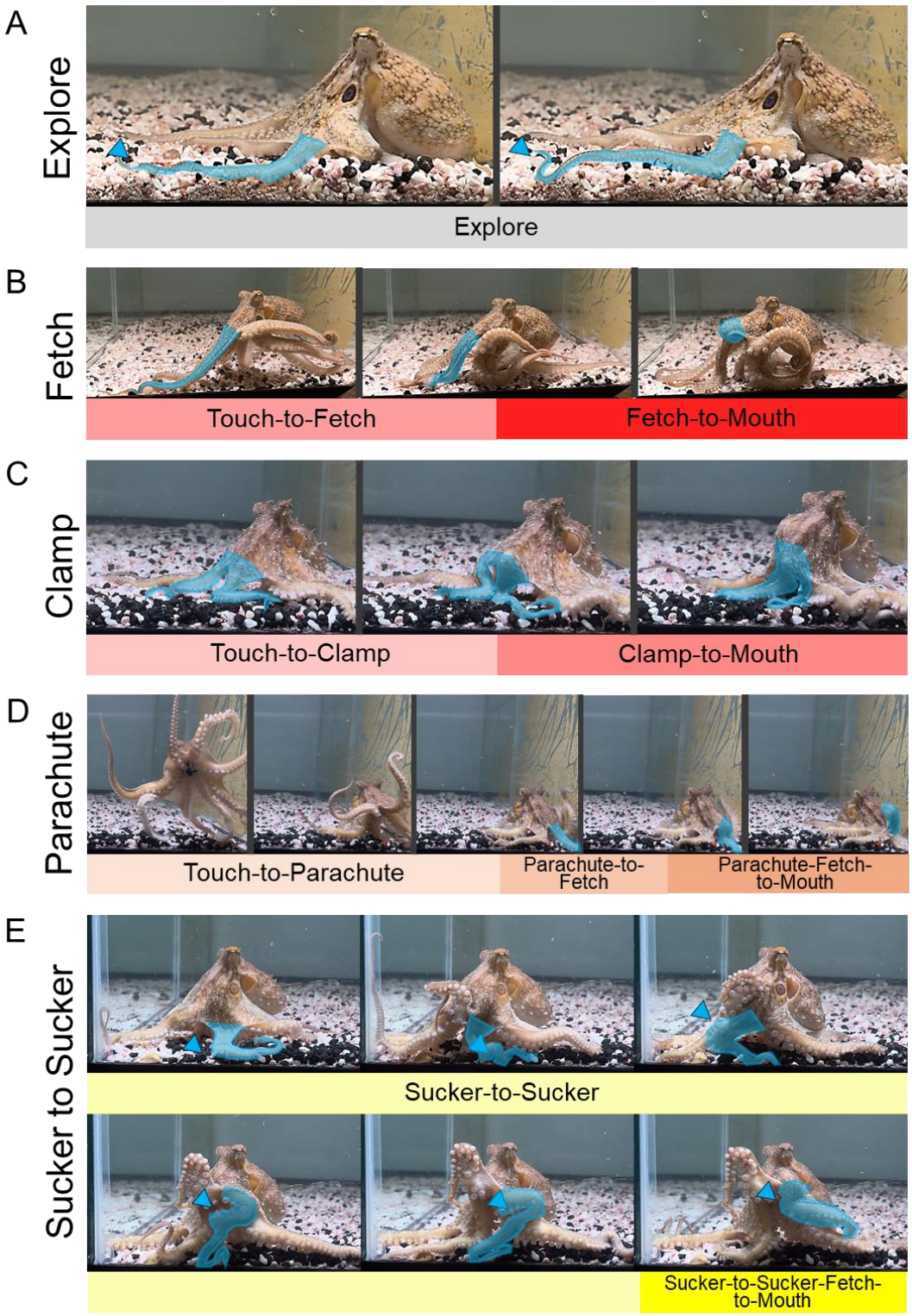

Figure 19 ***Ethogram of behaviours while interacting with food pieces*** *Example video frames illustrating the behavioural state events used for timing and distance measurements during food interactions. (A) Explore. (B) Fetch: Touch-to-Fetch and Fetch-to-Mouth. (C) Clamp: Touch-to-Clamp and Clamp-to-Mouth. (D) Parachute: Touch-to-Parachute, Parachute-to-Fetch, and Parachute–Fetch-to-Mouth. (E) Sucker to Sucker: Sucker-to-Sucker and Sucker-to-Sucker–Fetch-to-Mouth. The focal arms are highlighted in light blue. Blue arrows (panel A and E) indicate the position of the food item.*

Statistical analysis

To statistically analyse the retrieval strategies, we fitted a negative binomial regression (Glm.nb) with a log link to model counts as a function of arm location, food size, and their interaction using the MASS package. Model fit was evaluated using standard residual diagnostics, including inspection of residuals versus fitted values and an assessment of dispersion based on Pearson residuals.

To analyse the effects of food size and arm location on interaction duration and retrieval velocity, we fitted two generalised linear mixed-effects models (GLMMs) using the glmmTMB package. Interaction duration (model 1) and velocity (model 2) were modelled using a Gamma error distribution with a log link, with arm location, food size, and their interaction included as fixed effects. To account for repeated measurements within individuals, Subject was included as a random intercept. Residual dispersion was allowed to vary as a function of food size and arm location. Model fit was assessed using residual diagnostics, including plots of residuals against fitted values and simulation-based checks using the DHARMa package.

Experiment II – Effect of chemical cues on behaviour

To understand whether arm reactions and behaviour were influenced by chemical or mechanical cues, we conducted a second set of experiments using 10 mm agarose cylinders (10 mm diameter × 10 mm height) prepared with either seawater or shrimp extract. Scented agarose pieces were prepared by dissolving 1.2 g low-melting-point agarose powder (Sigma-Aldrich Company Ltd, Gillingham, UK) in 23 mL seawater from the aquarium system in a beaker on a heated hot plate with a magnetic stirrer (medium heat) until the solution became clear. The agarose was then cooled to 35 °C and 3 mL shrimp juice was added (shrimp juice test; SJ). For the control condition, the same agarose mixture was prepared without shrimp juice (seawater control; SW). Agar was poured into a Petri dish and one small stone was placed into each piece to prevent it from floating in the tank. After solidification, the biopsy punch used in the previous experiment was used to cut agar pieces of the same 10 mm size.

Agar pieces were presented to six octopus' specimens (SJ: 24 trials; SW: 22 trials) following the same procedure as for Experiment I. Agarose SW control and SJ-treated agar pieces were given in a randomised order and placed at the bottom of the tank. To strengthen chemical cues, SJ-treated pieces were additionally soaked in shrimp juice shortly before the trial.

We documented the type of interaction with the agar piece for each trial.

Statistical analysis

Behaviour was analysed using a GLMM fitted using the glmmTMB package. We modelled the probability of a retrieval outcome (binary response) as a function of Treatment (SW vs. SJ) as a fixed effect, with Subject included as a random intercept to account for repeated trials within individuals. Because residual diagnostics indicated extra-binomial variation, the model was fitted using a beta-binomial error distribution with a logit link. Model fit was evaluated using simulation-based residual diagnostics in the DHARMa package.

Experiment III – Effect of chemical cues on separated arm behaviour

To further investigate neural control mechanisms underlying arm responses to chemical cues, we tested the response of *ex vivo* arm preparations (N = 8 different arms from 3 different animals) with SJ and SW agar. In this experimental setting recordings were taken from two cameras. One was placed on the top, and the other was placed at the front of the tank.

Arms were removed from anaesthetised octopus and fixed at the base on a silicone platform submerged in the experimental tank. The arm was given 10 minutes to recover from anaesthesia. Forceps were used to place one agar piece on the base, medial or tip location of the arm. Each arm location was presented with an agar piece three times for each treatment (SJ and SW), with a 3-minute interval between presentations. Across a total of 168 trials, we documented the arm reaction type for each treatment and arm location.

Statistical analysis

To test whether treatment influenced the probability of a reaction, and whether this effect differed across arm locations, we fitted a binomial GLMM with reaction (Reaction01; yes/no) as the response, treatment (SJ vs SW), arm location (Base, Medial, Tip), and their interaction as fixed effects, and arm identity as a random intercept. Model fit was assessed using the DHARMa package.

2.5 Quantifying sucker attachment and detachment

High-speed video recording

To investigate which strategies octopus suckers use to attach and detach, high-speed video footage was recorded (120 frames/s, Huawei Nova 5T; Huawei, Shenzhen, China) from one specimen interacting with the front tank wall. Videos were analysed using the interactive zoom and frame-by-frame function of the software VLC player (VideoLAN Project, Paris, France). For comparative reasons, only suckers from the middle section of the arm length were analysed.

Sucker diameter, attachment and detachment strategy, and qualitative attachment strength were analysed from three sequences of the same individual's arm motion. Attachment strength was not measured directly but was assessed qualitatively based on visual inspection of the video sequences. Attachments were classified into three categories: Strong, Medium, and Loose. Attachments that resisted arm movement were classified as Strong. Attachments that were released during arm movement were classified as Medium. Attachments that were released without any obvious arm movement were classified as Loose.

Statistical analysis

To test the relationship between sucker diameter and the pattern of attachment and detachment observed, a Kruskal-Wallis test was used, with pairwise Wilcoxon tests performed for post hoc comparisons.

Platform with integrated pressure sensors

To quantify pressure changes associated with single-sucker attachment and potentially to characterise multi-sucker use, we designed and built a vertical platform that could be fixed to the inside of the tank's front glass wall. The platform (8 × 23 × 2 cm) was made from Plexiglas to allow visual documentation of sucker placement and attachment behaviour (see Figure 20 A). Embedded in the side of the platform are six pressure sensors (Honeywell International Inc., Charlotte, USA) which are able to detect positive and negative pressure of ± 400 kPa, covering the -0.168 MPa measured in octopus single sucker attachment before (Smith 1991). The sensors are each connected to a water-filled 1 mm drilled channel ending at the centre of the platform. Sensors and their respective cables were sealed with silicone and connected to a motherboard. The platform was connected with a computer through a USB connection and a customised software allowing to collect real-time pressure changes at 100 Hz (Figure 20 B).

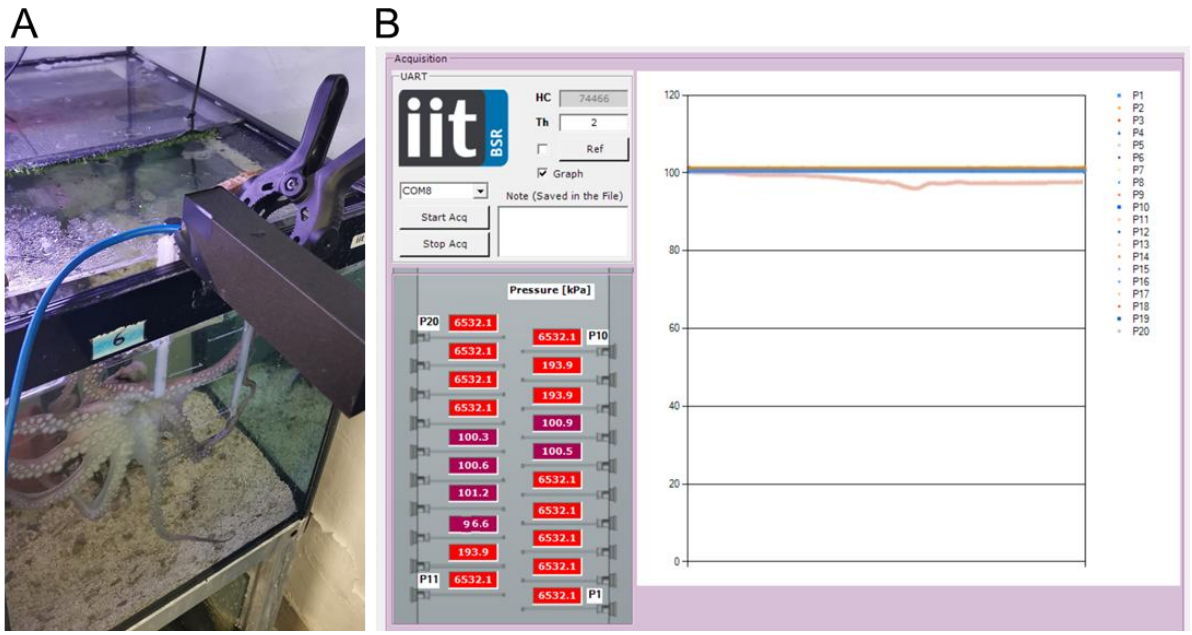

Figure 20 ***Platform setup.*** *(A) Image showing the platform hardware and (B) the software that allows pressure measurements at 100 Hz.*

All pressure channel outlets were spaced within 2.5 cm of each other to maximise the chance of measuring pressure changes generated by multiple suckers at the same time, preferably from the same arm. Real-time pressure measurements were

synchronised with video footage to relate pressure dynamics to the animal's behaviour.

2.6 Data analysis

Data collected during the experiments were processed, visualised and statistically analysed using R Version 2025.09.1 (Version 2025.09.1, R Core Team 2021).

3 Results

In this result section medians are reported descriptively, whereas 95% confidence intervals (CI) are reported for model-based estimates (estimated marginal means and contrasts).

3.1 Local motor control of stereotyped arm movements

EMG recordings were attempted in 10 *ex vivo* preparations; 2 yielded stable, analysable recordings and were included below. The remaining datasets were excluded based on pre-defined quality criteria (unstable signals and/or incorrect electrode placement, verified histologically). Because analysable EMG data were obtained from two preparations, statistical inference is driven by repeated trials within preparations and should be interpreted cautiously as evidence at the preparation level rather than as population-level estimates.

Arm extension

Arm extension and the corresponding EMG induced by electrical stimulation of the ANC were analysed in six trials (n = 6) from two *ex vivo* preparations (N = 2).

The analysis of the EMG recordings showed that across phases, Int/s did not differ significantly between the longitudinal and transverse muscles, indicating no main effect of muscle (lme model, $p > 0.05$; Figure 21 A; Table 1). Collapsed across muscles, in contrast, the results indicated an effect of phase on Int/s. Activity in phase 1 (median = 0.25) was significantly higher than in phase 2 (median = 0.082; lme model, $p < 0.001$) and phase 3 (median = 0.069; lme model, $p < 0.001$; Figure 21 B), whereas phases 2 and 3 showed similar Int/s values.

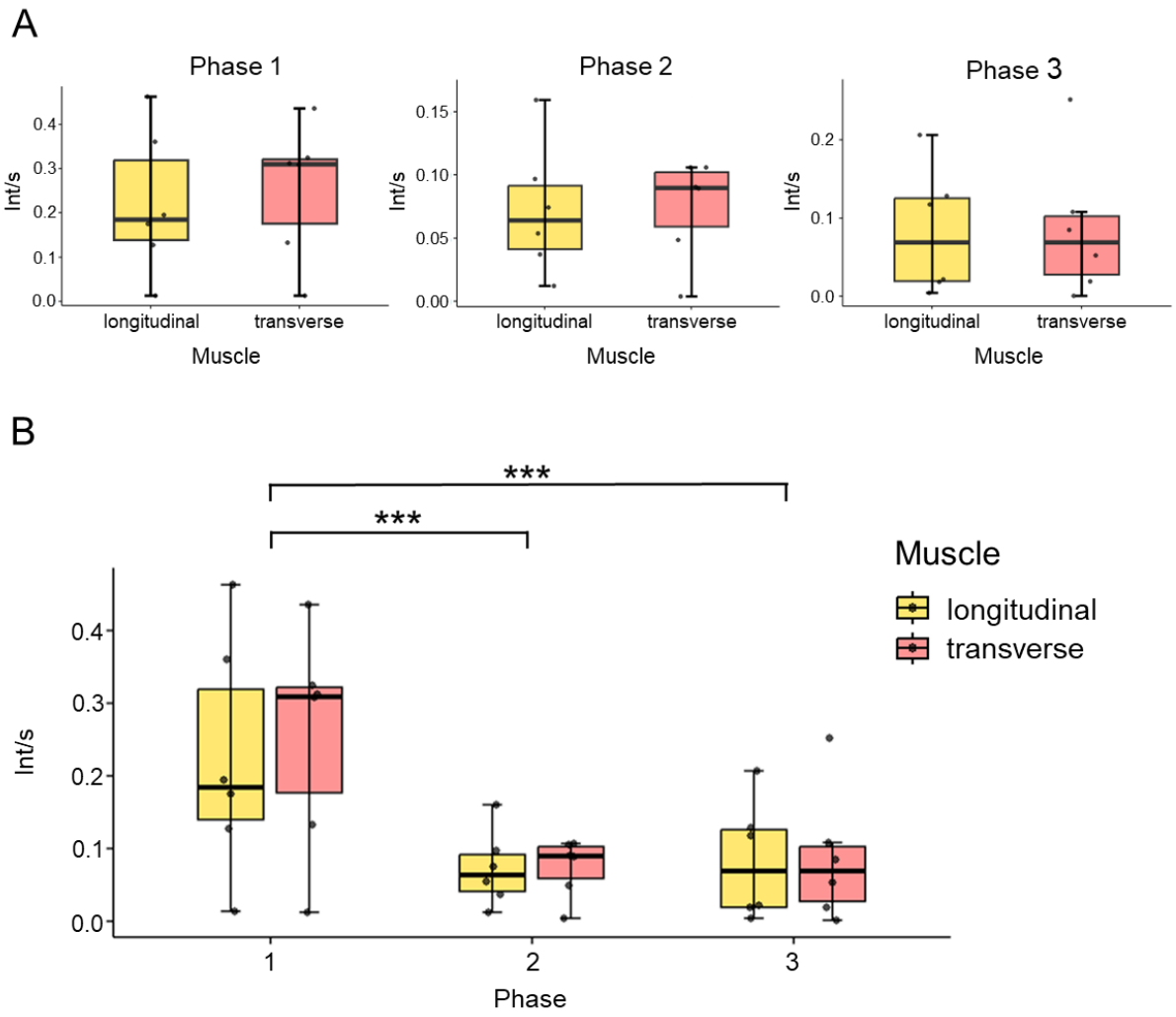

Figure 21 ***Muscle activity of both arm muscles across extension phases.*** *(A) Int/s shown separately for the longitudinal (yellow) and transverse (light red) muscles within each phase (n = 6, N = 2, lme model, muscle effect: all p > 0.05) (B) Int/s shown grouped by phase to facilitate comparison across phases for both muscles (n = 6, N = 2, lme model, phase 1 vs. 2, p < 0.001; phase 1 vs. 3, p < 0.001; phase 2 vs. 3, p > 0.05); Boxplots show median and IQR; points are individual extensions. Int/s, Phase muscle activity/time.*

Table 1 ***Phase effects on Int (square-root) during extension***

lme Model: Int (sqare-root) ~ Phase × Muscle + (1 | Sample/Trial) N = 2; n = 6				
Phase	***Estimated marginal means**	**SE**	**95% CI**	**Tukey post hoc**
1	0.45	0.06	0.34 – 0.56	1 vs. 2: p < 0.001
2	0.26	0.05	0.16 – 0.35	2 vs. 3: p = 0.996
3	0.25	0.05	0.15 – 0.35	1 vs. 3: p < 0.001

* Estimated marginal means are averaged over Muscle (equal weights)

The results showed an effect of phase on the correlation coefficient (Figure 22 A; Table 2). Correlation was significantly stronger in phase 2 (median = 0.78) than in phase 1 (median = 0.47), where a moderate correlation was revealed (lme model, p = 0.01). Correlation in phase 3 was also strong (median = 0.73) but did not differ significantly from the other phases.

The results also showed an effect of phase on CCI (Figure 22 B; Table 3). CCI was highest in phase 1 (median = 0.58), indicating moderate overlap in activation, and was significantly higher than in phase 2 (median = 0.32) and phase 3 (median = 0.32; lme model, both p < 0.001). Phase 2 and phase 3 did not differ with respect to CCI.

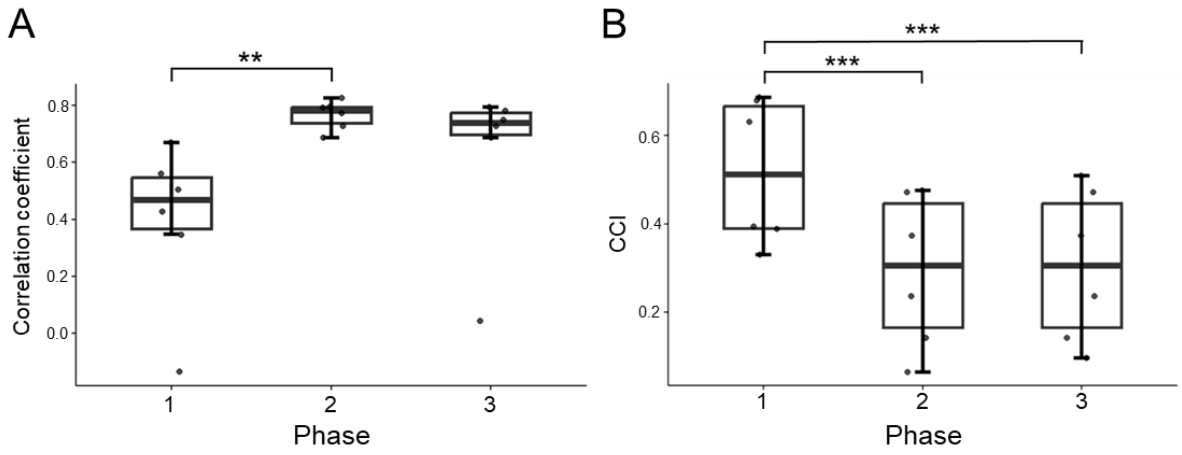

Figure 22 ***Activation patterns of longitudinal and transverse arm muscles during arm extension.*** *(A) Correlation coefficient (n = 6, N = 2, lme model, phase 1 vs. 2, p < 0.01; phase 1 vs. 3 and phase 2 vs. 3, p > 0.05) and (B) CCI calculated between longitudinal and transverse muscle activity for each movement phase (n = 6, N = 2, lme model, phase 1 vs. 2, p < 0.001; phase 1 vs. 3, p < 0.001; phase 2 vs. 3, p > 0.05); Boxplots show median and IQR; points are individual extensions. CCI, co-contraction index.*

Table 2 ***Phase effects on Correlation coefficient during extension***

lme Model: Correlation coefficient ~ Phase + (1 | Sample/Trial) N = 2; n = 6				
Phase	**Estimated marginal means**	**SE**	**95% CI**	**Tukey post hoc**
1	0.42	0.18	0.06 – 0.78	1 vs. 2: p < 0.01
2	0.99	0.09	0.81 – 1.18	2 vs. 3: p = 0.461
3	0.79	0.19	0.42 – 1.17	1 vs. 3: p = 0.240

Table 3 ***Phase effects on CCI during extension***

lme Model: CCI ~ Phase + (1 | Sample/Trial) N = 2; n = 6				
Phase	**Estimated marginal means**	**SE**	**95% CI**	**Tukey post hoc**
1	0.59	0.10	0.40 – 0.78	1 vs. 2: $p < 0.001$
2	0.31	0.09	0.14 – 0.48	2 vs. 3: $p = 0.267$
3	0.32	0.09	0.15 – 0.49	1 vs. 3: $p < 0.001$

Arm withdrawal-like resistance

A total of 19 EMG recordings (n = 19) from two *ex vivo* samples (N = 2) were analysed.

The EMG analysis showed that during arm stretch, Int did not differ significantly between the longitudinal and transverse muscles, indicating no main effect of muscle (lme model, $p > 0.05$; Figure 23 A; Table 4). Collapsed across muscles, in contrast, the results showed an effect of phase on Int. Activity in phase 1 (median = 671.1) was significantly higher than in phase 2 (median = 224.29; lme model, $p < 0.001$) and phase 3 (median = 176.56; lme model, $p < 0.001$; Figure 23 B), whereas phases 2 and 3 showed similar Int values (lme model, $p > 0.05$).

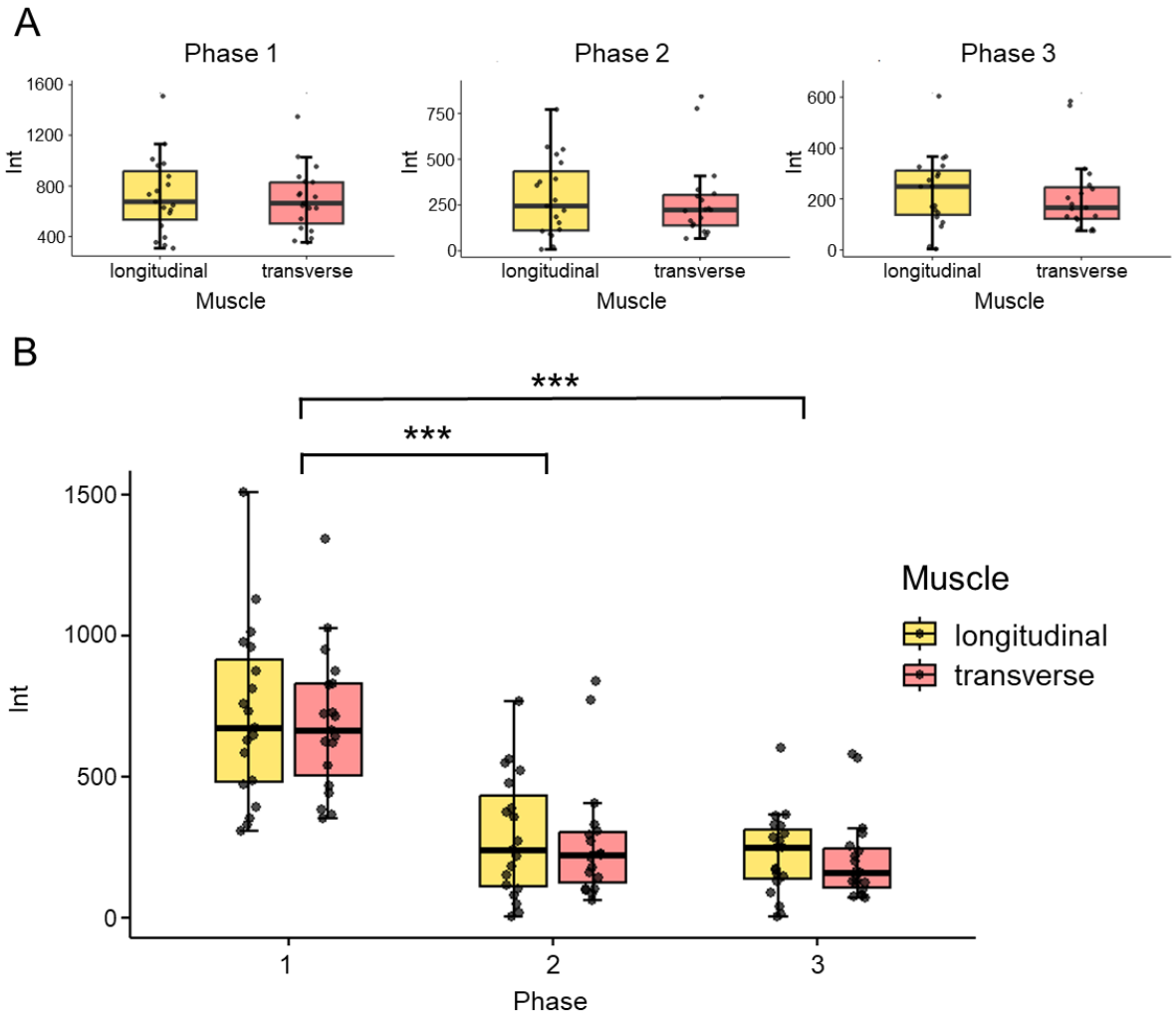

Figure 23 ***Muscle activity of both arm muscles across withdrawal phases.*** *A) Int shown separately for the longitudinal (yellow) and transverse (light red) muscles within each phase (n = 19, N = 2, lme model, main effect of muscle: p > 0.05) (B) Int shown grouped by phase to facilitate comparison across phases for both muscles (n = 19, N = 2, lme model, phase 1 vs. 2, p < 0.001; phase 1 vs. 3, p < 0.001; phase 2 vs. 3, p > 0.05); Boxplots show median and IQR; points are individual pulls. Int, Phase muscle activity.*

Table 4 ***Phase effects on Int (log) during withdrawal-like stretch***

lme Model: Int (log) ~ Phase × Muscle + (1 | Sample/Trial) N = 2; n = 19				
Phase	***Estimated marginal means**	**SE**	**95% CI**	**Tukey post hoc**
1	6.48	0.185	6.11 – 6.84	1 vs. 2: p < 0.001
2	5.28	0.222	4.84 – 5.71	2 vs. 3: p = 0.529
3	5.07	0.223	4.64 – 5.51	1 vs. 3: p < 0.001

* Estimated marginal means are averaged over Muscle (equal weights)

The results showed an effect of phase on the correlation coefficient (Figure 24 A; Table 5). Correlation was highest in phase 1 (median = 0.85), indicating a strong correlation, and was significantly higher than in phase 2 (median = 0.49) and phase 3 (median = 0.31; lme model, both $p < 0.001$). Correlation in phase 2 and phase 3 did not differ significantly (lme model, $p > 0.05$).

The results did not show an effect of phase on CCI (lme model, $p > 0.05$; Figure 24 B; Table 6). CCI values indicated moderate overlap in activation across phases, with no significant differences between phase 1 (median = 0.58), phase 2 (median = 0.41), and phase 3 (median = 0.53).

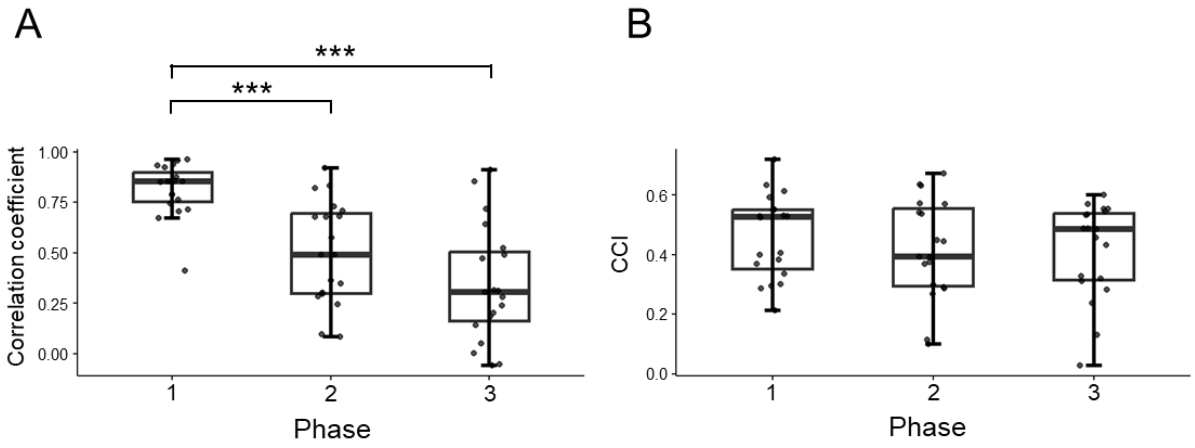

Figure 24 ***Activation patterns of longitudinal and transverse arm muscles during arm withdrawal.*** *(A) Correlation coefficient (n = 19, N = 2, lme model, phase 1 vs. 2, p < 0.001; phase 1 vs. 3, p < 0.001; phase 2 vs. 3, p > 0.05) and (B) CCI calculated between longitudinal and transverse muscle activity for each movement phase; (n = 19, N = 2, lme model, main effect of phase:, p > 0.05); Boxplots show median and IQR; points are individual pulls. CCI, co-contraction index.*

Table 5 ***Phase effects on Correlation coefficient during withdrawal-like stretch***

lme Model: Correlation coefficient ~ Phase + (1 | Sample/Trial) N = 2; n = 19				
Phase	**Estimated marginal means**	**SE**	**95% CI**	**Tukey post hoc**
1	1.25	0.13	1.00 – 1.50	1 vs. 2: p < 0.001
2	0.64	0.11	0.42 – 0.85	2 vs. 3: p = 0.054
3	0.43	0.11	0.21 – 0.65	1 vs. 3: p < 0.001

Table 6 ***Phase effects on CCI during withdrawal-like stretch***

lme Model: CCI ~ Phase + (1 | Sample/Trial) N = 2; n = 19				
Phase	**Estimated marginal means**	**SE**	**95% CI**	**Tukey post hoc**
1	0.51	0.06	0.40 – 0.63	1 vs. 2: p = 0.349
2	0.46	0.06	0.35 – 0.57	2 vs. 3: p = 0.231
3	0.45	0.06	0.34 – 0.56	1 vs. 3: p = 0.968

Overall, both EMG experiments showed no difference in integrated activity between the longitudinal and transverse muscles, but a clear phase dependence, with highest activity in phase 1 and lower activity in phases 2–3. Across phases, the two muscles showed at least moderate, and in some cases strong, temporal correlation and co-contraction.

3.2 Arm kinematics during withdrawal-like resistance

Using DeepLabCut, two pull-EMG datasets were synchronised with overall arm kinematics (Figure 25 A, B). Both trials showed arm elongation, reflected by an approximately linear increase in marker distance over time. In both examples, deformation of the proximal arm segment (Base to electrode marker; BE) and the distal segment (Electrode to hand marker; EH) followed similar patterns and contributed comparably to the overall deformation (Base to hand; BH).

In the first trial, the marked increase in overall muscle activity coincided with a temporary reduction in marker distance (Figure 25 A). Beyond this period, no clear relationship between EMG activity and arm deformation was observed.

In the second trial, longitudinal muscle activity was initially high and was followed shortly by a peak in transverse muscle activity (Figure 25 B). Overall EMG activity was highest before and during the temporary reduction in marker distance. Subsequent changes in muscle activity did not appear to affect the deformation trajectory. Beyond these periods of distance reduction, no clear relationship between EMG activity and arm deformation was observed in either trial.

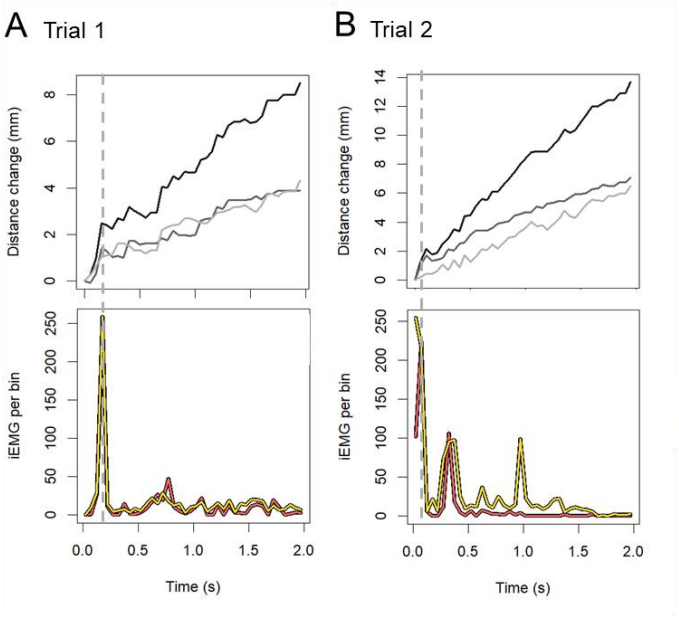

Figure 25 ***Motion kinematic analysis during pull.*** *Arm deformation between markers and real-time corresponding iEMG signal of (A) Trial 1 and (B) Trial 2 n = 2, N = 1; BH = Base to hand marker, black line; BE = Base to electrode marker, dark-grey line; EH = Electrode to hand marker, light-grey line. Longitudinal muscle signal in light red. Transverse muscle signal in yellow. iEMG, integrated electromyography.*

Overall, both trials showed comparable deformation of the proximal and distal arm segments over time. Early EMG peaks coincided with a brief reduction in marker distance at pull onset, while no clear correspondence was observed later in the pull.

3.3 Local muscle deformation during withdrawal-like resistance

Sonomicrometry was attempted in 13 arms; out of these, 5 arm samples provided 32 complete, analysable signals for the required crystal pairs and were included. Because analysable sonomicrometry data were obtained from five arms (N = 5) with repeated pulls per arm, statistical inference is driven by within-preparation replication and should be interpreted cautiously as evidence at the preparation level rather than as population-level estimate. Included samples comprised three responsive and two unresponsive arms (N = 3, n = 15 and N = 2, n = 17, respectively).

The results of the sonomicrometry measurements indicate that deformation along the pull axis was not uniform in the unresponsive arm preparation (Figure 26 A; Table 7). The results showed an effect of crystal pair on MaxDef along the pull axis. MaxDef was greatest for crystal pair C12 (median = 1.37), which was significantly higher than for C25 (median = 1.25; lme model, $p = 0.02$) and for the overall pull-axis deformation represented by C15 (median = 1.27; lme model, $p < 0.001$).

Changes in arm diameter did not differ between the two transverse crystal pairs: C13 (median = 0.82) and C24 (median = 0.86) showed similar MaxDef values (lme model, p > 0.05; Figure 26 B).

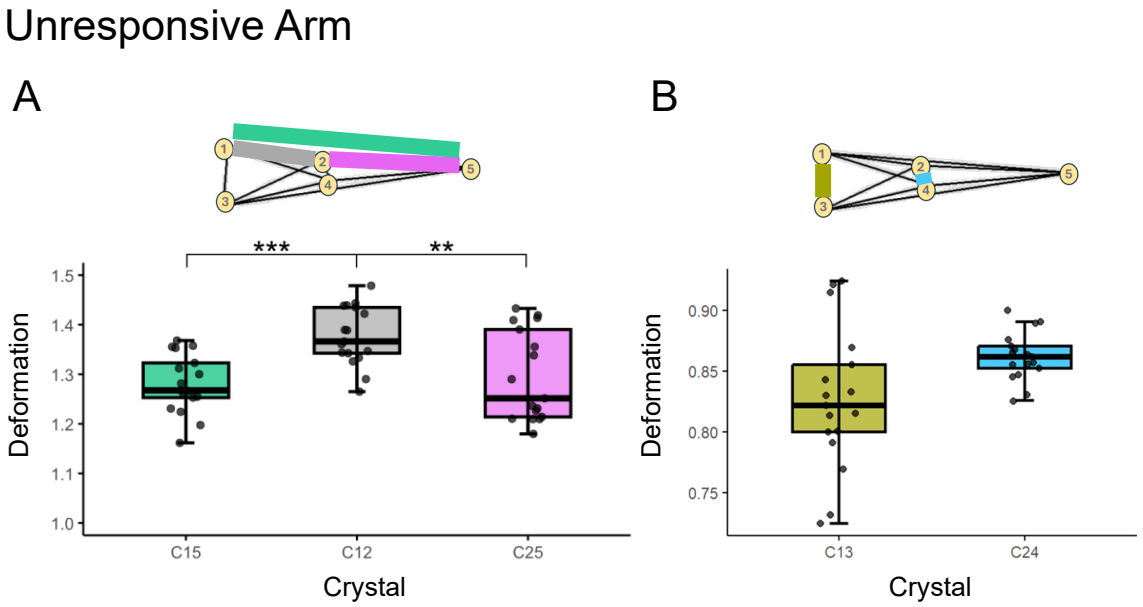

Figure 26 ***Unresponsive arm deformation.*** *(A) Maximum normalised deformation (L/L0) along the pull axis (C15, C12, C25) (n = 18, N = 2, lme model, C15 vs. C12, p < 0.001; C15 vs. C25, p > 0.05; C12 vs. C25, p < 0.01) (B) Change in arm diameter (C13, C24) (n = 18, N = 2, lme model, C13 vs. C24, p > 0.05); Boxplots show median and IQR; points are individual pulls. C followed by a number indicates the crystal pair.*

Table 7 ***MaxDef among crystal pairs in unresponsive arms***

lme Model: MaxDef ~ Crystal + (1 | Sample/Trial) N = 2; n = 17				
Crystal	**Estimated marginal means**	**SE**	**95% CI**	**Tukey post hoc**
C15	1.28	0.01	1.10 – 1.46	C15 vs. C12: p < 0.001
C12	1.38	0.01	1.19 – 1.56	C12 vs. C25: p < 0.01
C25	1.30	0.02	1.02 – 1.57	C15 vs. C25: p = 0.979
C13	0.83	0.01	0.65 – 1.00	C13 vs.C24: p = 0.110
C24	0.86	0.01	0.80 – 0.93	

In contrast, the responsive *ex vivo* arm preparation showed no evidence of differences in MaxDef among crystal pairs, either along the pull axis (C12, C25, C15) or in arm diameter (C13, C24) (lme model, all, $p > 0.05$; Figure 27 A, B; Table 8).

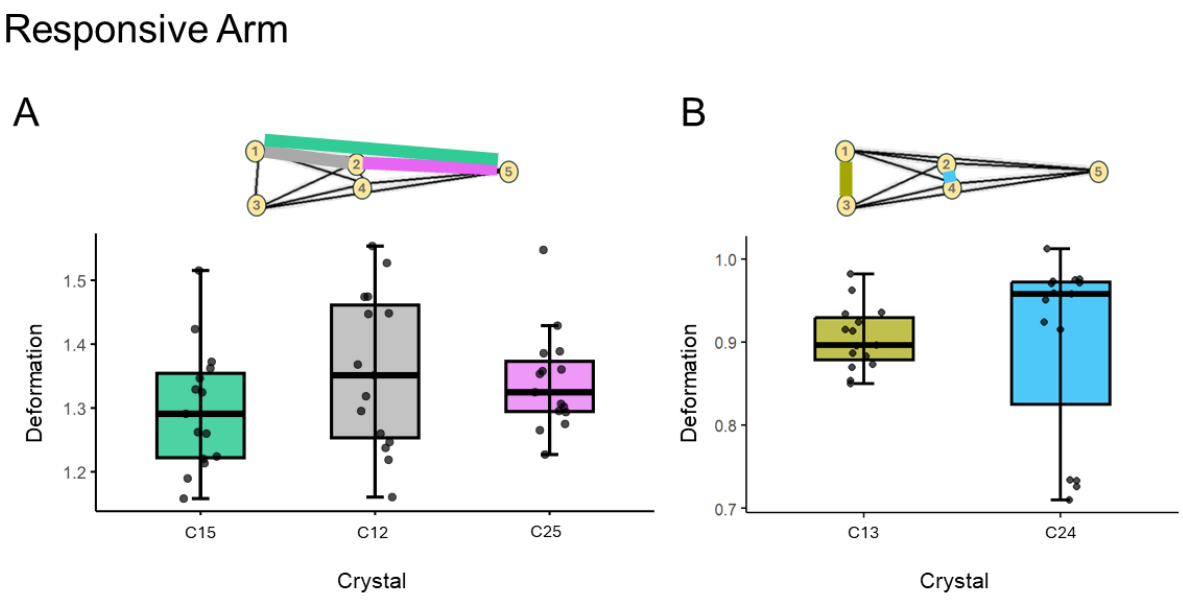

Figure 27 ***Responsive arm deformation.*** *(A) Maximum normalised deformation (L/L0) along the pull axis (C15, C12, C25) (n = 17, N = 3, lme model, C15 vs. C12, p > 0.05; C15 vs. C25, p > 0.05; C12 vs. C25, p > 0.05) (B) Change in arm diameter (C13, C24) (n = 17, N = 3, lme model, C13 vs. C24, p > 0.05); Boxplots show median and IQR; points are individual pulls. C followed by a number indicates the crystal pair.*

Table 8 ***MaxDef among crystal pairs in responsive arms***

lme Model: MaxDef ~ Crystal + (1 | Sample/Trial) N = 3; n = 15				
Crystal	**Estimated marginal means**	**SE**	**95% CI**	**Tukey post hoc**
C15	1.30	0.03	1.19 – 1.41	C15 vs. C12: p = 0.497
C12	1.36	0.03	1.23 – 1.50	C12 vs. C25: p = 0.985
C25	1.34	0.03	1.24 – 1.44	C15 vs. C25: p = 0.640
C13	0.91	0.02	0.84 – 0.97	C13 vs.C24: p = 1.000
C24	0.90	0.03	0.76 – 1.04	

The MaxDef analysis showed that the unresponsive arm exhibited substantially higher deformation in the segment represented by crystal pair C12. As this

difference was not present in the responsive *ex vivo* preparation, we examined the shape of the C12 deformation curve in both sample types.

In both sample types, most Slope_diff events were of small magnitude (Figure 28 A). However, responsive arms showed a broader distribution with occasional larger Slope_diff values (a heavier right tail), whereas unresponsive arms were more strongly concentrated at low amplitudes. Overall, Slope_diff values were similar between groups, with only a trend towards higher Slope_diff in responsive arms (median = 0.075) compared with unresponsive arms (median = 0.055; Figure 28 B).

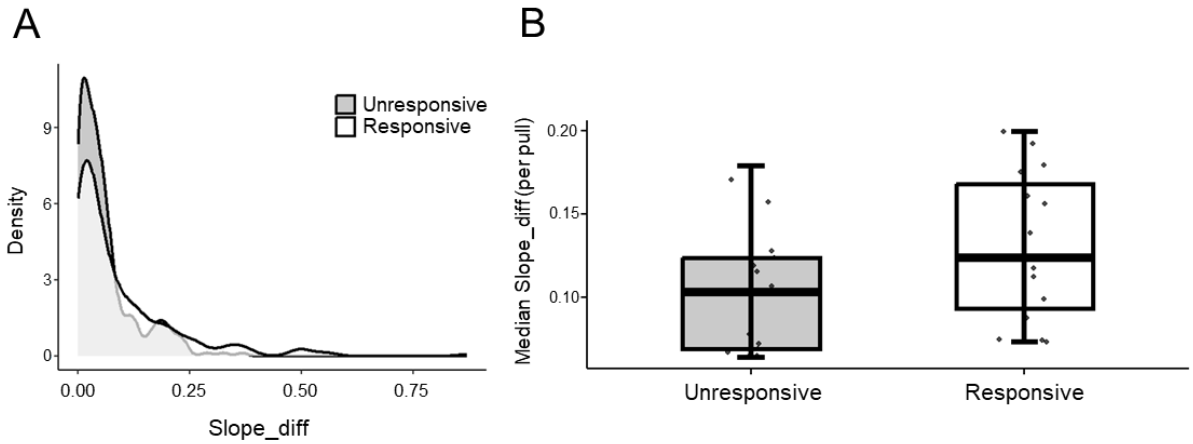

Figure 28 ***Deformation curve analysis*** *(A) Density distribution of Slope_diff values for unresponsive and responsive arm samples. (B) Per-pull median Slope_diff values for unresponsive vs. responsive samples Boxplots show median and IQR; points are individual pulls. Slope_diff, slope drop magnitude.*

Overall, MaxDef did not differ across crystal pairs in responsive arms, whereas in unresponsive arms the proximal segment (C12) showed greater deformation than more distal segments. Slope-drop magnitudes were broadly similar between groups, with only a trend towards larger events in responsive arms.

3.4 Sucker perception and CNS-driven retrieval

Experiment I – Effect of food size on behaviour

Octopus – food interaction

Using the ethogram, we documented the frequency of each behaviour for each food size (Figure 29 A). Octopuses interacted with the food pieces a total of 268 times across five individual octopuses, with at least 15 trials per animal. The 2 mm pieces were interacted with most frequently (115 interactions) and were mostly explored (78/115) while fetched only 36/115 times. In one case, a Sucker to Sucker retrieval was observed.

The second highest number of interactions was observed with the 4 mm pieces (100 interactions). In contrast to the 2 mm food size, 63/100 interactions resulted in a fetch; 36/100 were exploration only, and the Clamp strategy was used a single time to retrieve the food.

Interactions occurred least frequently with the 10 mm food piece (53 interactions) as most of the time the food piece was retrieved immediately without further exploration. In particular, 36/53 interactions resulted in a fetch, 11/53 were exploration only, 4/53 were retrieved using the Clamp, and 2/53 using the Parachute strategy.

Due to the overall distribution of strategies and the very low frequency of Clamp (n = 4), Parachute (n = 3) and Sucker to Sucker strategies (n = 1), we focused our analysis on Explore and Fetch.

Frequency of Explore and Fetch

To examine whether the arm location in contact with the food during exploration and fetching was associated with strategy and timing, we divided the behaviours based on predefined arm locations: Base, Medial, and Tip (n = 260). Food pieces were explored or fetched most frequently with the medial location (Medial: 148). The tip was used 102 times, and the base was used only 10 times (Figure 29 B). Due to the

limited use of the base for the 4 mm and 10 mm pieces, statistical comparisons involving the base were restricted to the 2 mm data.

The results showed an effect of arm location on the frequency of Explore and Fetch (Table 9). Within food-size groups, results showed that the base was used less often than the medial location (Glm.nb, $p < 0.001$) and the tip (Glm.nb, $p < 0.01$) to explore or fetch the 2 mm piece. In contrast, there was no difference between the use of medial and tip for the other food sizes (Glm.nb, all $p > 0.05$).

Additionally, an effect of food size on the frequency of Explore and Fetch was found. Within arm locations, differences in behaviours to food size were detected only for the tip: the tip was used more often to explore or fetch a 4 mm piece than a 10 mm piece (Glm.nb, $p < 0.05$). All other comparisons within arm location groups were non-significant (Glm.nb, all $p > 0.05$).

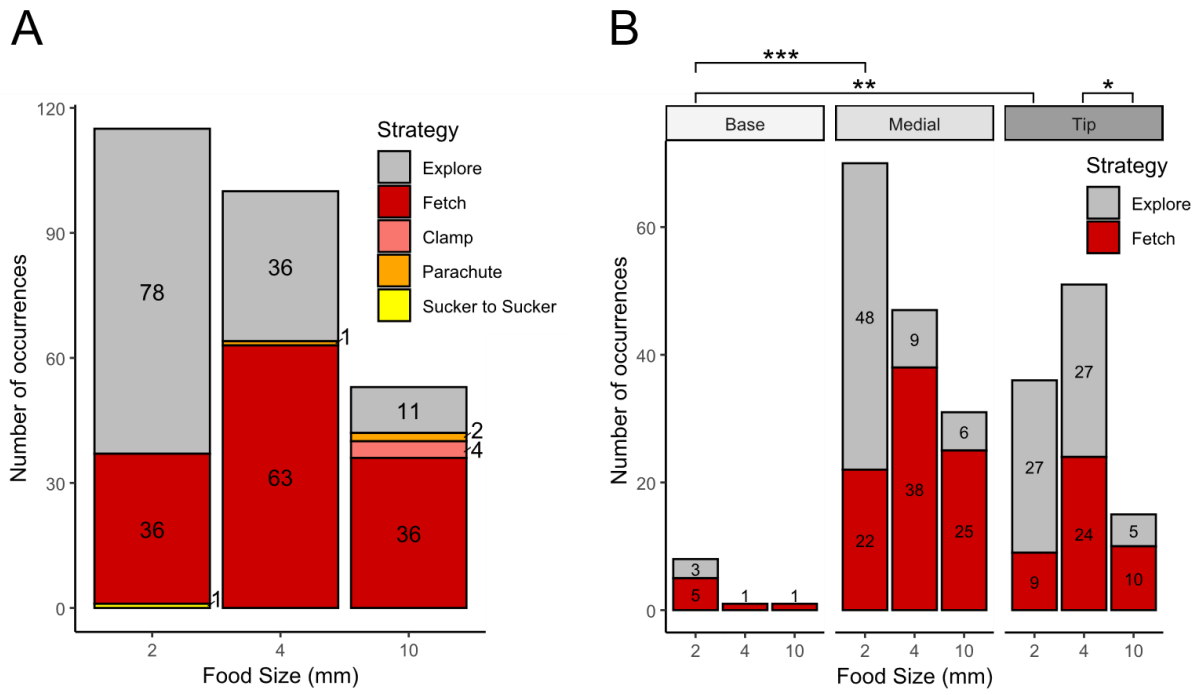

Figure 29 ***Behavioural strategies.*** *(A) Number of strategies used per food size. (B) Number of Explore and Fetch events across arm locations and food sizes. (N = 5, n shown in the figure; Glm.nb: 2 mm, Base vs Medial, $p < 0.001$; Base vs Tip, $p < 0.01$; Tip, 4 mm vs 10 mm, $p < 0.05$).*

Table 9 ***Effects of arm location and food size on Explore and Fetch counts***

glm.nb Model: Count ~ Arm location * Food size N = 5; n = 260					
Arm location	**Food size**	**Estimated marginal means**	**SE**	**95% CI**	**Tukey post hoc**
Base	2	4.00	1.81	1.65 – 9.70	Base vs. Medial: p < 0.001 Base vs. Tip: p < 0.01
Medial	2	35.00	10.7	19.23 – 63.72	2 vs. 4: p = 0.366
	4	23.5	7.45	12.63 – 43.74	4 vs. 10: p = 0.366
	10	15.5	5.17	8.06 – 29.82	10 vs. 2: p = 0.07
Tip					*All* Medial vs. Tip: p > 0.05
	2	18.0	5.89	9.48 – 34.17	2 vs. 4: p = 0.443
	4	25.5	8.01	13.77 – 47.21	4 vs. 10: p < 0.05
	10	7.5	2.86	3.55 – 15.85	10 vs. 2: p = 0.081

Duration of Touch-to-Fetch

For the Fetch strategy, we measured the duration of the Touch-to-Fetch state event, here referred to as touch duration.

Due to the low sample size for Base in the 4 mm and 10 mm groups (Base: n = 1 in each), these results were not included in the statistical comparisons (Table 10). An effect of food size on touch duration within the medial arm location was found (Figure 30 B). The time spent investigating the shrimp was significantly longer for 2 mm pieces (median = 12.34 s) than for 4 mm (median = 4.94 s; GLMM, $p < 0.001$) and 10 mm pieces (median = 2.01 s; GLMM, $p < 0.001$). In addition, the 4 mm touch duration was significantly longer than the 10 mm touch duration (GLMM, $p < 0.001$).

Similarly, an effect of food size on touch duration at the tip location was found (Figure 30 C). The touch duration was longer for the 2 mm piece (median = 9.50 s) than the 4 mm (median = 4.29 s; GLMM, $p = 0.003$) and 10 mm pieces (median = 1.69 s; GLMM, $p < 0.001$). There was also a longer touch duration for 4 mm pieces than to the 10 mm pieces (GLMM, $p < 0.001$).

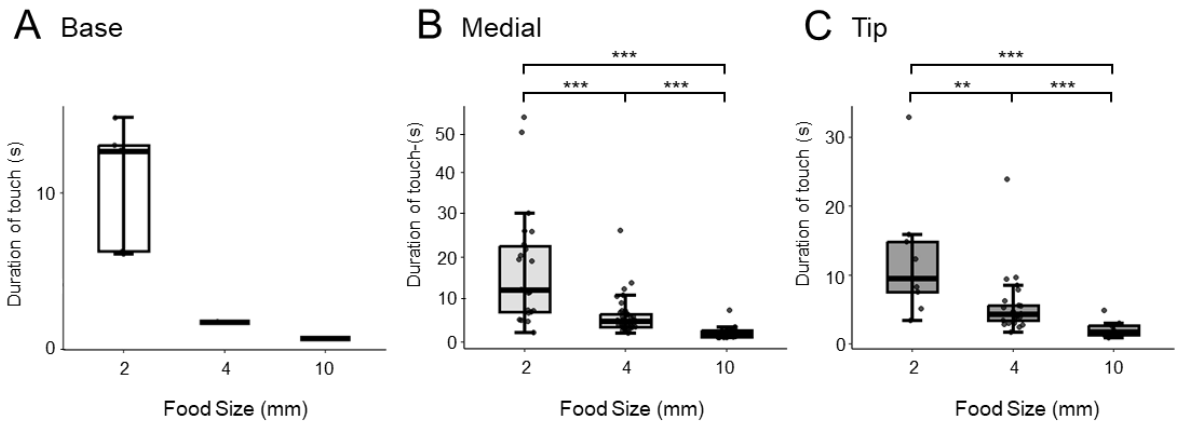

Figure 30 ***Food size vs. Duration of touch.*** *Effect of food size on the duration of the Touch-to-Fetch state event. Within arm location groups of (A) Base (N = 5, n = 7), (B) Medial (N = 5, n = 85; GLMM: all, p < 0.001) and (C) Tip (N = 5, n = 43; GLMM: all, p < 0.01); Boxplots show median and IQR; points are individual interactions resulting in a fetch.*

Table 10 ***Effects of arm location and food size on Duration of touch***

GLMM: Duration ~ Arm location * Food size + (1 | Subject) N = 5; n = 135					
Arm location	**Food size**	**Estimated marginal means**	**SE**	**95% CI**	**Tukey post hoc**
Medial					*All* Medial vs. Tip: p > 0.05
	2	1.99	0.4	1.34 – 2.94	2 vs. 4: p < 0.001
	4	2.86	0.63	1.85 – 4.41	4 vs. 10: p < 0.001
	10	10.37	1.29	8.12 – 13.24	10 vs. 2: p < 0.001
Tip	2	2.24	0.23	1.83 – 2.75	2 vs. 4: p < 0.01
	4	6.13	0.58	5.09 – 7.38	4 vs. 10: p < 0.01
	10	17.49	2.7	12.93 – 23.68	10 vs. 2: p < 0.01

In contrast, there was no effect of arm location on touch duration within any food size group (GLMM, all, p > 0.05).

Velocity of Fetch

For the Fetch strategy, we measured the velocity of the Fetch-to-Mouth state event, here referred to as fetch velocity.

An effect of food size on fetch velocity was found at the medial arm location (Figure 31 B). In particular, the fetch velocity was higher for the 10 mm shrimp pieces (median = 6.59 mm/s) than for the 4 mm food pieces (median = 3.75 mm/s; GLMM, $p < 0.001$) and the 2 mm (median = 3.00 mm/s; GLMM, $p < 0.001$). There was no difference in the fetch velocity between the 2 mm and 4 mm food sizes (GLMM, $p > 0.05$).

An effect of food size at the tip arm location was found (Figure 31 C; Table 11). When the tip was used to perform the Fetch, the fetch velocity was higher for the 10 mm pieces (median = 9.59 mm/s) than the 4 mm pieces (median = 6.92 mm/s; GLMM, $p < 0.001$) and the 2 mm pieces (median = 6.86 mm/s; GLMM, $p < 0.001$). There was no difference in the fetch velocity between the 2 mm and 4 mm food sizes (GLMM, $p > 0.05$).

Regarding the effect of arm location within each food size group, we found an effect of arm location on fetch velocity, such that in all three groups (Figure 32 A–C) shrimp pieces were fetched significantly faster using the tip than those fetched using the medial arm location (GLMM, all $p < 0.001$).

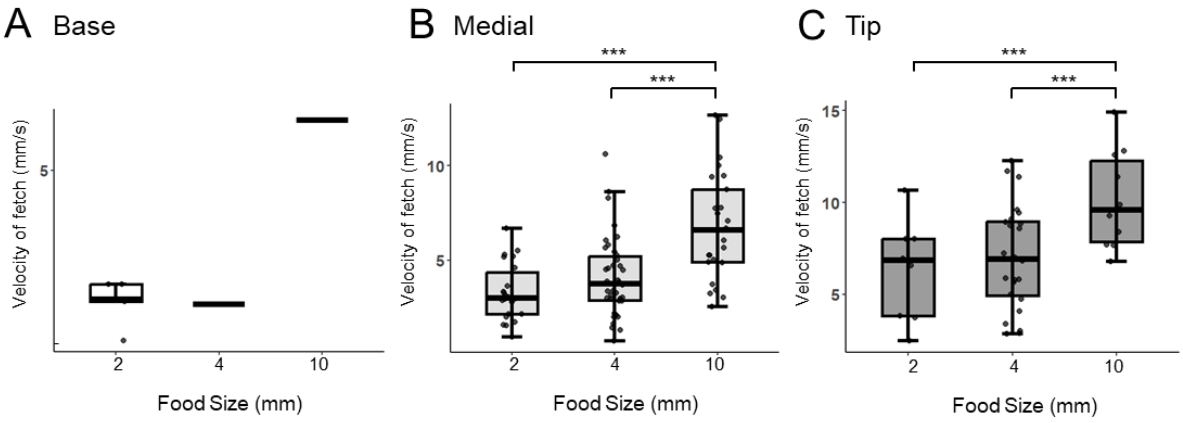

Figure 31 ***Food size vs. Velocity of fetch****. Within arm location groups of (A) Base (N = 5, n = 7), (B) Medial (N = 5, n = 85; GLMM: 2 mm vs 4 mm, $p < 0.001$; 2 mm vs 10 mm, $p < 0.001$) and (C) Tip (N = 5, n = 43; GLMM: 2 mm vs 4 mm, $p < 0.001$; 2 mm vs 10 mm, $p < 0.001$); Boxplots show median and IQR; points are individual interactions resulting in a fetch.*

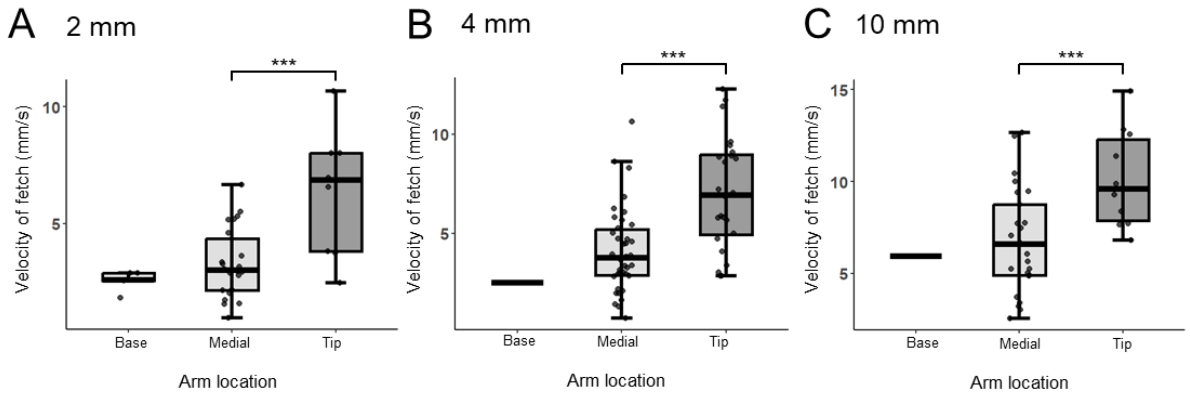

Figure 32 ***Arm location vs. Velocity of fetch*** *Within food size groups of (A) 2 mm (N = 5, n = 36), (B) 4 mm (N = 5, n = 63) and (C) 10 mm. (N = 5, n = 36; GLMM: all sizes, Medial vs. Tip, p < 0.001); Boxplots show median and IQR; points are individual interactions resulting in a fetch.*

Table 11 ***Effects of arm location and food size on Fetch Velocity***

GLMM: Velocity ~ Arm location * Food size + (1 | Subject) N = 5; n = 135					
Arm location	**Food size**	**Estimated marginal means**	**SE**	**95% CI**	**Tukey post hoc**
Medial					*All* Medial vs. Tip: p < 0.001
	2	3.11	0.37	2.46 – 3.93	2 vs. 4: p = 0.059
	4	4.02	0.39	3.32 – 4.87	4 vs. 10: p < 0.001
	10	6.73	0.59	5.67 – 7.99	10 vs. 2: p < 0.001
Tip	2	5.99	0.80	4.61 – 7.77	2 vs. 4: p = 0.273
	4	7.04	0.65	5.87 – 8.44	4 vs. 10: p < 0.001
	10	10.76	1.12	8.78 – 13.20	10 vs. 2: p < 0.001

Overall, the results show that Fetch was the most frequently used strategy. Touch-to-Fetch duration was longer for smaller food pieces, but once Fetch was initiated, larger pieces were retrieved faster, especially when the tip region of the arm was used.

Experiment II - Effect of chemical cues on *in vivo* behaviour

In vivo: SW vs. SJ

To further understand what type of sensory information triggers a fetch, we tested whether chemical cues increased the likelihood of food retrieval by presenting six octopuses with 10 mm agar pieces treated with shrimp juice (SJ) or control seawater (SW). Two types of behaviour were observed: Fetch or Explore.

The results show an effect of presence versus absence of chemical cues on the behaviour (Fetch vs Explore; Figure 33; Table 12).

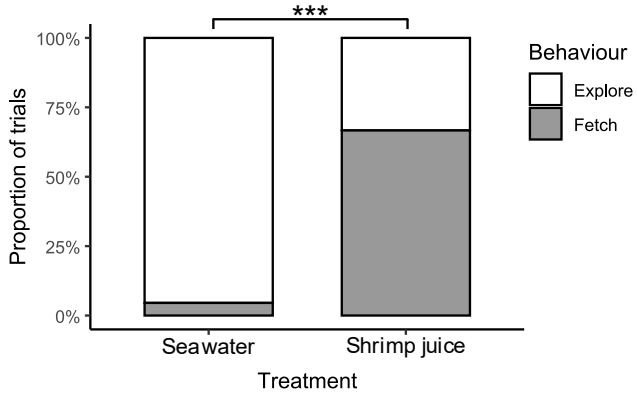

Figure 33 ***Results of in vivo behaviour.*** *Effect of shrimp-juice–treated agar pieces (SJ) compared to seawater control agar pieces (SW) on octopus in vivo interaction behaviour (Fetch vs Explore) (N = 6, n = 46; GLMM; SW vs. SJ, p < 0.001).*

In particular, both agar pieces elicited an explore behaviour, however SW exploration resulted in a fetch only one time (1/22 trials; 4.54%) while exploration of SJ elicited a fetch most of the time (16/24 trials, 66.70%) (GLMM, p < 0.001).

The results show that agar pieces treated with shrimp extract were retrieved more often than agar pieces without extract.

Table 12 ***Effects agar treatment on Behaviour***

GLMM: Fetch ~ Agar + (1 | Subject) N = 6; n = 46				
Agar	**Estimated marginal means**	**SE**	**95% CI**	**Tukey post hoc**
SW	0.05	0.04	0.01 – 0.26	SW vs. SJ: p < 0.001
SJ	0.67	0.1	0.46 – 0.82	

Experiment III– Effect of chemical cues on *ex vivo* arm behaviour

To understand if the signal which triggers the Fetch can be computed locally, we ran a similar test as in Experiment II on *ex vivo* arm preparations (N = 8). We used 10 mm agar pieces treated with SJ or SW and placed each on three different locations along the arm (tip, middle and basal portion).

We found no difference in the frequency of reaction following SJ or SW exposure of the *ex vivo* arm sample in any of the three arm segments (GLMM, $p > 0.05$; Figure 34 A; Table 13).

We then categorised the arm reaction based on the elicited behaviour. Five different behaviours were observed: 1) no reaction (NR), 2) sucker reaction by orienting towards the agar (SR), 3) Sucker reaction and arm reaction by bending or lifting (SR + AR), 4) Sucker reaction in combination with the suckers attachment to the piece followed by a sucker-to-sucker transport (SR + StS), or 5) a combination of SR, StS and AR (SR + StS + AR).

Reaction patterns differed across arm locations within each treatment condition (Figure 34 B–C).

Effect of SW control agar on arm behaviours at different locations

When a SW control agar piece was placed at the base (Figure 34 B), all five reaction categories were observed. In particular, SR + AR was observed in 10/27 trials and a SR only in 9/27 trials. A combination of all three reaction types (SR + StS + AR) was observed in 2/27 trials.

When a SW control agar piece was placed on the medial location, three reaction categories were observed, with one dominating the distribution. Specifically, a SR occurred in 23/30 trials, a SR + AR in 6/30, and NR in 1/30 trial.

The tip showed only two reaction categories. In particular it showed NR towards SW control agar pieces in most trials (18/27) and a SR occurred in 9/27 trials.

Our results collectively show that arm location influenced the reaction probability under the SW control condition, such that the tip was significantly less likely to react than the medial location and the base (GLMM, both $p < 0.001$). The medial location

showed the highest probability of reacting and was significantly more likely to react than the base (GLMM, $p = 0.025$).

Effect of SJ-treated agar on arm reactions at different locations

For SJ–treated agar pieces all five reaction categories were observed at the base (Figure 34 C). In particular, we observed a SR in 9/27 trials, a SR + AR in 7/27, a combination of all three reactions (SR + StS + AR) in 4/27, a SR + StS in 1/27, and NR in 6/27 trials.

At the medial location, as in the SW control condition, three reaction categories were observed. Responses were again dominated by SR (20/31 trials). A SR + AR occurred in 8/31 trials, and NR in 3/31 trials.

At the tip, three reaction categories were observed: SR in 8/26 trials, SR and AR in 3/26 trials, and NR in 15/26 trials.

These results show that there is an effect of arm location on reaction probability under the SJ condition, such that the tip was least likely to react to the SJ–treated agar piece, showing significantly lower reactivity than both the base and medial locations (GLMM, both $p < 0.001$). In contrast to the SW control condition, the probability of reacting did not differ between the base and medial locations for SJ–treated agar pieces (GLMM, $p > 0.05$).

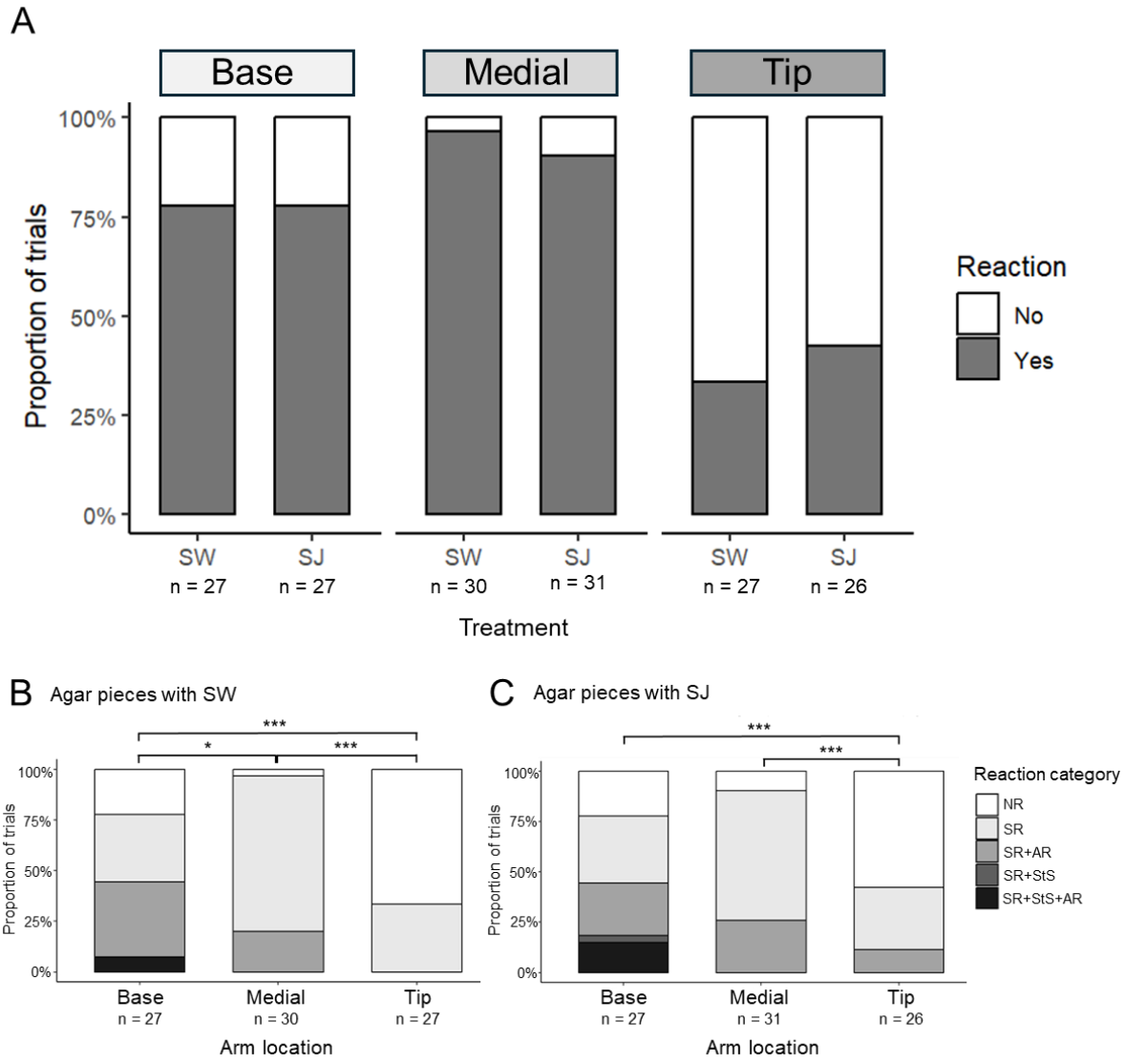

Figure 34 ***Results of ex vivo arm behaviour.*** *(A) Effect of shrimp-juice–treated 10 mm agar pieces (SJ) compared with seawater control agar pieces (SW) on ex vivo arm reaction (Fetch vs Explore) by arm location (Base, Medial, Tip) (N = 8; n shown in the figure; GLMM: all, p > 0.05). (B) Distribution of reaction categories by arm location for SW-control agar pieces (N = 8; n shown in the figure; GLMM: Base vs Medial, p < 0.05; Base vs Tip, p < 0.001; Medial vs Tip, p < 0.001) and (C) for SJ-treated agar pieces (N = 8; n shown in the figure; GLMM: Base vs Tip, p < 0.001; Medial vs Tip, p < 0.001). NR = no reaction; SR = sucker reaction; AR = arm reaction; StS = sucker-to-sucker transport.*

Table 13 ***Effects agar treatment and arm location on Reaction***

GLMM: Reaction ~ Agar * Arm location + (1 | Subject) N = 8; n = 168					
Agar	**Arm location**	**Estimated marginal means**	**SE**	**95% CI**	**Tukey post hoc**
SW					*All* SW vs. SJ: p > 0.05
	Base	0.99	0.04	0.65 – 1.00	Base vs. Medial: p < 0.05
	Medial	0.99	0.01	0.90 – 1.00	Medial vs. Tip: p <0.001
	Tip	0.37	0.30	0.04 – 0.88	Tip vs. Base: p <0.001
SJ	Base	0.97	0.04	0.67 – 1.00	Base vs. Medial: p = 0.087
	Medial	1	0.003	0.95 – 1.00	Medial vs. Tip: p <0.001
	Tip	0.25	0.24	0.02 – 0.81	Tip vs. Base: p <0.001

Collectively, the results show that, unlike *in vivo*, the isolated arm showed no differences in either the frequency or type of response following exposure to SJ or SW pieces.

3.5 Sucker stereotyped attachment and detachment

Attachment and detachment patterns

A total of 52 events (18 attachment events and 34 detachment events) from 16 different suckers were quantified to assess the stereotyped strategies of attachment and detachment, as well as attachment-strength category.

Attachment

From video footage, we identified two stereotyped patterns that resulted in sucker attachment: ‘Whole-Cup Attachment’ and ‘Wave-Like Attachment’ (WLA).

In Whole-Cup Attachment, the entire rim of the sucker contacts the surface at once. Whole-cup attachments were further subdivided into ‘Contraction Attachment’ (CA) and ‘Orientation–Contraction Attachment’ (OCA; Figure 35). In CA, the sucker cup already faces the glass surface, allowing immediate whole-cup attachment. In OCA, the focal sucker and neighbouring suckers do not initially face the glass. They start turning, either simultaneously or one by one, towards the glass surface and adjust their position with a small forward movement, enabling immediate whole-cup attachment.

WLA is achieved when the sucker touches the glass surface with one edge of the sucker rim and then places the complete cup stepwise. This produces a wave-like motion of the rim as it seals progressively across the glass (Figure 35).

The most frequent attachment strategy was OCA (11/18 cases), followed by CA (4/18 cases) and WLA (3/18 cases).

Regarding attachment strength, 5/11 OCA cases resulted in a loose attachment, 2/11 in a medium attachment, and 4/11 in a strong attachment. Regarding neighbouring suckers, in most cases (5/11) no neighbouring sucker was attached. In 4/11 cases one sucker was attached and in 2/11 cases both suckers were attached. In all cases, the arm was steady.

In 2/3 cases, WLA resulted in a medium attachment, and in 1/3 cases in a strong attachment. In all WLA cases, no attachment of neighbouring suckers was observed, and, prior to attachment, the arm was in motion.

In 1/4 cases, CA resulted in a loose attachment and in 3/4 cases in a strong attachment. In half of the cases, no neighbouring suckers were attached. In the other half, either one or both neighbouring suckers were attached. In all but one observation, the arm was moving prior to attachment.

Detachment

Two stereotyped detachment strategies were identified: ‘Wave-Like Detachment’ (WLD) and ‘Contraction Detachment’ (CD; Figure 35). In WLD, the sucker cup either detaches step-by-step from the surface or detaches all at once. In both cases, detachment is initiated by the rim lifting from the glass at a single point, followed by full detachment, allowing pressure release. In CD, the sucker rim contracts and detaches immediately from the glass surface.

WLD was observed in 26/34 cases and CD in 8/34 cases.

Across attachment-strength categories, WLD was used in 7/26 cases from a loose attachment, in 11/26 cases from a medium attachment, and in 8/26 cases from a strong attachment. Half of the time (13/26), one neighbouring sucker was also attached. In 10/26 cases, no neighbouring sucker was attached, and in 3/26 cases both neighbouring suckers were attached. In 18/26 cases, the arm was moving and WLD was induced by overall arm motion (Pull–Release behaviour). In 6/26 cases, the arm was steady, and in 2/26 cases we observed a Pull–Stop–Release sequence, in which the arm first pulled the sucker and, upon resistance, stopped and then moved again, releasing the sucker from attachment.

The remaining detachments were achieved through CD, either from a loose (3/8) or a strong (5/8) attachment. In most cases (5/8) a single neighbouring sucker was attached, and in the remaining cases (3/8) no neighbouring sucker was attached. In the majority of cases (3/8), the arm was moving while the sucker detached (Pull–Release behaviour). In 2/8 cases, we observed the Pull–Stop–Release pattern described above. In a single case, the sucker contracted and released immediately before the arm moved. In 2/8 cases, the sucker detached without the arm moving before or shortly afterwards.

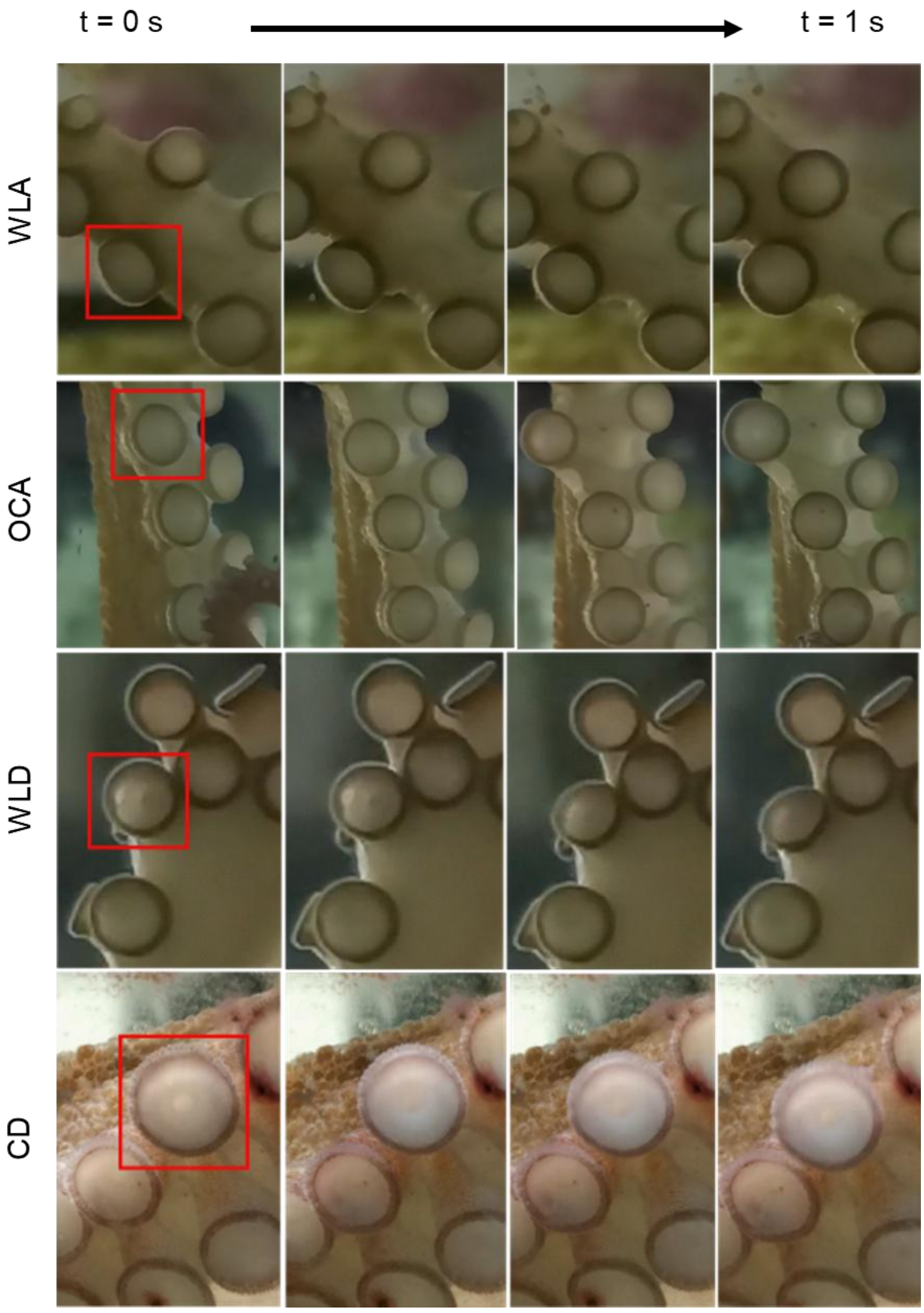

Figure 35 ***Sucker strategies.*** *'Wave-Like Attachment' (WLA), 'Orientation-Contraction Attachment' (OCA), 'Wave-Like Detachment' (WLD) and 'Contraction Detachment' (CD) within a timeframe of 1 s. The focal suckers are framed in red.*

No significant differences were detected between sucker diameter and attachment strategy, detachment strategy, or attachment strength (Kruskal–Wallis tests, all $p > 0.05$). However, additional observations across a wider range of sucker sizes and arm positions are needed to confirm this pattern.

Here, we show that suckers, like the arm, can produce stereotyped movement patterns. We identified three attachment patterns (WLA, CA, OCA) and two detachment patterns (WLD, CD), and additionally classified each event by attachment strength, based on the behaviour of the arm itself and neighbouring suckers.

Time profile of internal sucker pressure during attachment

Pressure-platform recordings were attempted in 3 sessions; 1 yielded analysable single-sucker events with synchronised video. These pressure results are therefore presented as proof-of-concept. A set of four sucker attachment and detachment events from one octopus were synchronised with real-time measurements of pressure difference.

In one case, WLA and WLD were observed, resulting in a loose attachment (Figure 36 A). The pressure trace showed a steep decrease of 2.7 kPa followed by a short plateau (1), which then transitioned into a gradual return towards baseline until (2) a small step increase of 1 kPa marked release of the attachment. Video footage indicated that pressure was released slowly as neighbouring suckers detached and the arm moved laterally.

The second attachment lasted approximately six times longer than the other attachments, which were around 0.5 s. Attachment strategy was categorised as CA and detachment as CD (Figure 36 B). The pressure trace indicated a two-step decrease: an initial drop of 3.3 kPa (1) followed by a second steep decrease of 6.2 kPa (2). Upon detachment, pressure increased almost immediately back to baseline levels (3). Based on the total pressure drop of 9.5 kPa, this attachment was categorised as strong. This was supported by the observation that the animal moved the platform during the period when suction increased (i.e., during the pressure

decrease). Video footage showed that the sucker was released nearly simultaneously with all neighbouring suckers.

The third attachment also used CA and was detached using CD (Figure 36 C), resulting in a medium-strength attachment. Upon contact, pressure decreased by 4.8 kPa. The initial decrease was steep, similar to the previous traces, but slowed before reaching the minimum pressure (1). Detachment caused a sharp increase in pressure back to baseline levels (2). During attachment, no neighbouring suckers attached, and the arm moved slowly, with minimal interaction with the platform.

The fourth attachment was achieved using CA, whereas detachment followed a WLD strategy (Figure 36 D). Pressure decreased slowly by 1.8 kPa at first, reaching a plateau (1). This was followed by a steep drop of 2.4 kPa (2) and a sudden increase back to baseline levels upon detachment (3). During the initial attachment (1) neighbouring suckers did not attach. Only when the focal sucker further reduced pressure did neighbouring suckers attach to the platform and remain attached during the focal sucker's detachment (3). With a total pressure change of 4.5 kPa, this attachment was classified as medium-strong.

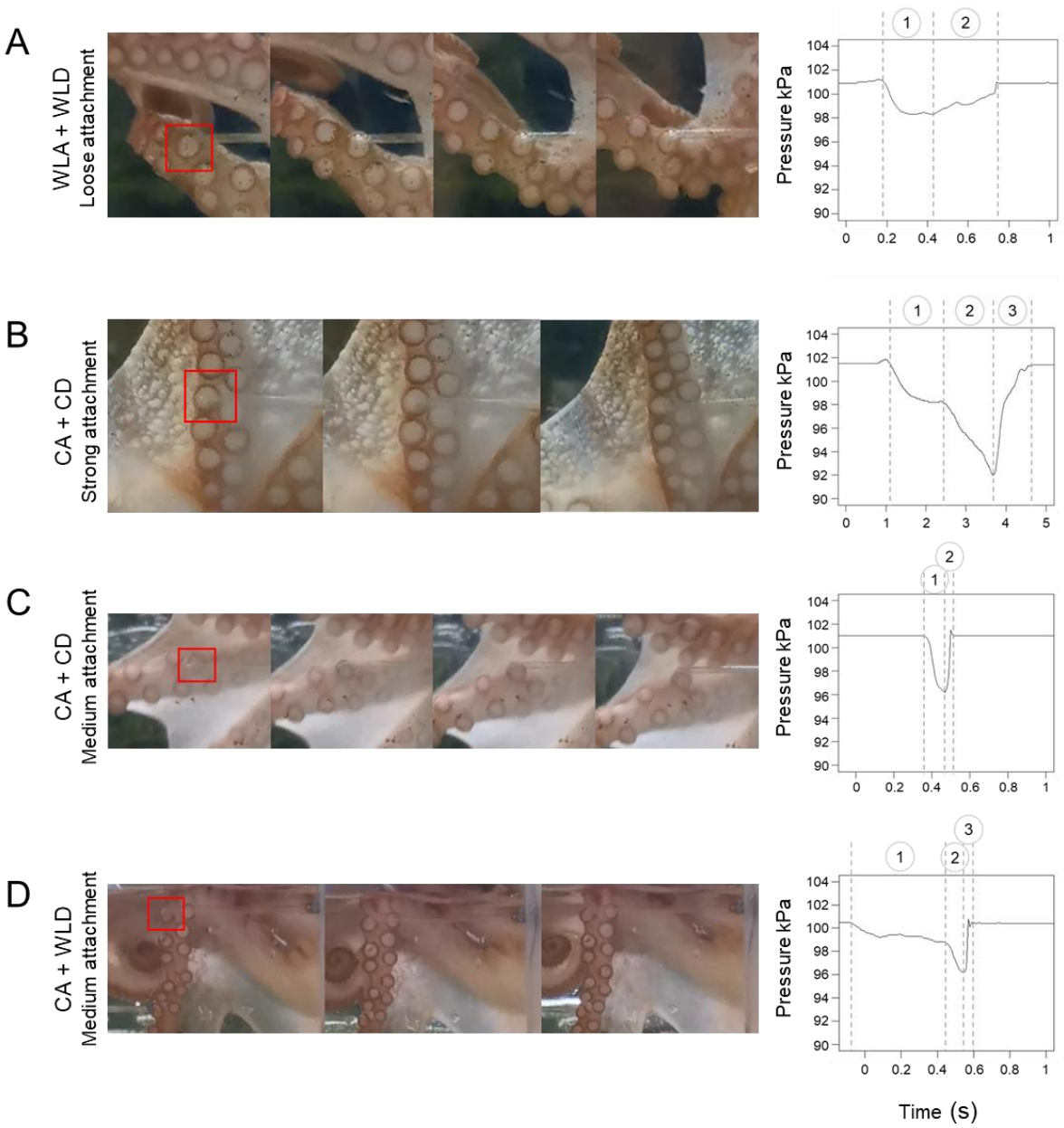

Figure 36 ***Sucker attachment strategies and real-time pressure measurements.*** *(A) WLA and WLD resulting in a loose attachment; the pressure trace shows (1) attachment and (2) detachment. (B) CA and CD resulting in a strong attachment; the pressure trace shows (1) initial attachment, (2) reinforced attachment, and (3) detachment. (C) CA and CD resulting in a medium attachment; the pressure trace shows (1) attachment and (2) detachment. (D) CA and WLD resulting in a medium attachment; the pressure trace shows (1) initial attachment, (2) reinforced attachment, and (3) detachment. The focal suckers are framed in red. WLA, 'Wave-Like Attachment'; WLD, 'Wave-Like Detachment'; CA, 'Contraction Attachment'; CD, 'Contraction Detachment'.*

Overall, the pressure traces show dynamic, strategy-dependent changes in internal sucker pressure, including stepwise reinforcement, plateaus, and gradual versus abrupt release.

4. Discussion

Octopuses display remarkable motor control abilities that allow them to handle eight limbs with potentially infinite degrees of freedom in movement patterns. A somatotopic organisation like the one we see in vertebrate brains does not exist in octopuses. Octopuses therefore rely on a different solution and use a hierarchical control system that is distributed from the CNS throughout the PNS. Although the lack of skeletal structures imposes few restrictions on movement patterns, octopuses nonetheless show stereotyped arm motions for specific tasks, such as reaching towards prey (Hanassy et al. 2015). These motor programmes are embedded locally within the arm nervous system and require a command from the CNS to be activated (Gutfreund 1998).

Another example of local control can be found in the suckers that run along the entire length of the octopus' arm. These structures can move independently and exchange sensory information via the ANC (Olson et al. 2025). Suckers are used both for probing the environment and for attachment. Although octopuses have a highly developed visual system (Hanke and Kelber 2020), suckers are a vital tool for foraging in visually impaired environments (Hanlon and Messenger 2018). Isolated arms readily attach to many surfaces but can show limited capability to coordinate detachment (Altman 1971). Brain-surgery studies suggest that it is likely that the supraoesophageal mass in the CNS is responsible for sending commands that promote sucker release (Rowell 1966). Consequently, some sucker behaviours require CNS involvement.

Even though we have thorough knowledge of arm muscle arrangement and properties, and of longitudinal muscle activation during stereotyped movements, important questions remain about how muscle recruitment, local processing of sucker perception and CNS involvement are integrated. In addition, we are still refining our understanding of how suckers perceive mechanical and chemical input, and how this information can be translated into pressure changes and movements at single- and multi-sucker level. These gaps in octopus motor control are addressed in this thesis.

Beyond improving our understanding of distributed control in a muscular hydrostat, our results also highlight principles that may be useful for soft robotics, where compliant bodies and suction-based attachments face similar challenges in control, sensing and reliable detachment.

With this framework in mind, we first discuss muscle recruitment during electrically evoked extension and mechanically induced withdrawal-like resistance, before turning to arm and muscle kinematics, behaviour shaped by sucker perception, and stereotypical sucker attachment motion and dynamics.

4.1 Local motor control of stereotyped arm movements

First, we asked how the aboral longitudinal and transverse muscles are recruited locally to generate PNS-embedded arm extension and withdrawal-like resistance. Across EMG, kinematic tracking of arm and muscles, our data are consistent with the idea that the proximal arm segment contributes primarily to stabilisation during both extension and sustained stretch, potentially through increased local stiffness. At our proximal recording site, the aboral longitudinal and transverse muscles were co-activated in both stereotyped motions.

Arm elongation and shortening are known to occur preferentially in the proximal arm region (Huffard et al., 2005; Levy et al., 2015; Kennedy et al., 2020). Arm extension is commonly described as a combination of bend propagation and local elongation (Sumbre et al. 2001, Hanassy et al. 2015). During elongation, the longitudinal musculature is expected to relax while the transverse musculature contracts, reducing local diameter and, via the constant-volume constraint, producing elongation. Conversely, shortening is expected to involve longitudinal contraction with transverse relaxation, increasing cross-sectional area locally. In contrast to these simple antagonist patterns, our recordings showed co-activation of longitudinal and transverse muscles. Rather than facilitating elongation-related diameter reduction, simultaneous activation would be expected to resist deformation and instead increase local stiffness (Kier and Smith 1985, Hochner et al. 2023). Although we did not directly measure diameter at the recording site, the observed

co-activation is compatible with increased stiffness and supports a stabilising role of this proximal region.

In the extension experiment, this interpretation aligns with Gutfreund's (1998) proposal that once a bend has passed a region, sustained activity can reflect stiffening to keep that region straight and stable. In our data, the phase structure is consistent with a shift in motor strategy: from stabilisation after the initial extension to later posture maintenance through finer muscle adjustment. Phase 1 showed the highest overall activity, moderate temporal correlation, and substantial overlap in activation between the two muscles (as reflected in the CCI values). This pattern suggests that maintaining the straight posture and damping residual motion after the extension movement requires substantial co-activation, while still allowing one muscle to be modulated as the other remains active. Phases 2 and 3 showed lower overall activity and tighter temporal coordination, with reduced CCI, consistent with a shift towards smaller, more energy-efficient adjustments once the proximal region is stabilised.

For the withdrawal-like condition, our setup imposed a sustained stretch: the arm was pulled and held, which would normally evoke a withdrawal response, but here prevented completion of the full movement. Hague et al. (2013) describe withdrawal in horizontally mounted arms as a proximal bend, and in vertically mounted arms as proximal shortening accompanied by torsion. In our constraint condition, the proximal co-activation may therefore reflect an attempt to stabilise the proximal region under load, either to resist passive elongation and limit tissue strain, or to provide a mechanically stable base while withdrawal-related output is expressed elsewhere along the arm. As in the extension EMG analysis, the withdrawal-like condition also showed a phase-dependent shift in motor strategy. In phase 1 (first 0.66 s), muscle activity and temporal correlation were highest and CCI indicated moderate overlap, consistent with a tightly coordinated onset response that rapidly increases resistance. In phases 2 and 3, overall activity decreased and temporal correlation became less tightly coupled, while CCI remained moderate. This combination is consistent with maintained co-activation for posture/resistance but

more flexible timing during sustained loading. The reduction in activity could also reflect desensitisation of sensory perception to the ongoing mechanical stimulation, although additional trials would be required to test this directly.

Additional evidence for a stabilising role of the proximal region comes from the deformation and kinematic analyses. In sonomicrometry, responsive preparations showed broadly similar MaxDef across the measured segments, whereas unresponsive preparations showed greater deformation in the most proximal segment than in more distal segments and in the overall pull-axis deformation (Figure 26, Figure 27). One interpretation is that residual local neural activity in responsive arms limits localised stretching under load and promotes more uniform strain distribution, but differences in tissue condition between responsive and unresponsive preparations (e.g., time post-excision) may also contribute. Importantly, Slope_diff values did not differ between groups, so we cannot ascribe the responsive pattern to discrete contraction events from these data alone. In the DeepLabCut proof-of-concept trials, overall arm deformation of the proximal and distal segments contributed comparably to overall deformation (Figure 25), which may be expected if stabilisation is spatially restricted and therefore averaged out over the relatively long BE segment. Notably, both trials showed a brief deviation at pull onset (a transient reduction in marker distance) that coincided with peaks in integrated EMG, consistent with an early active resistance component, whereas later kinematic variations were not clearly linked to proximal EMG activity. Together, these results are compatible with local, short-range stabilisation under load, but a direct test will require simultaneous EMG and kinematics using DeepLabCut and sonomicrometry to link local activation to local deformation and whole-arm motion.

The existence of a mechanism to coordinate the activation level of the two antagonistic muscles is interesting from the perspective of central brain control. Indeed, it points to the existence of a central setting of motor programs that are then distributed at the level of the arm PNS to reach a timely coordinated activation of the muscles.

4.2 Sucker perception and CNS-driven retrieval

Having examined local motor output and mechanical responses in isolated preparations, we next asked how sensory input at the sucker contact site shapes action selection during foraging, and under which conditions this sensory information is sufficient to shift behaviour from exploration to retrieval. Our *in vivo* experiments indicate that the initiation and execution of fetch retrieval can be fine-tuned by the CNS based on sensory information received by the suckers. In contrast, *ex vivo* trials suggest that prey extract alone does not alter local sucker and arm reactivity in the absence of central input.

In particular, *in vivo* experiments testing three food sizes, the most frequent behaviours were Explore and Fetch. Because food pieces did not stand out from the gravel on the tank floor (limited visibility), the animals shifted from the usual visually triggered parachute strategy (Bidel et al. 2022) to a retrieval strategy that is consistent with the probing behaviour described by Hanlon and Messenger (2018).

Our results show that the 2 mm food piece was explored more often than it was fetched. In more than 50% of encounters, exploration of a food piece of this size did not result in retrieval, whereas encounters with the 4 mm and 10 mm pieces more often resulted in retrieval. Shape characterisation is highly developed in octopus, and they can discriminate between objects of different shapes and roughness through tactile sensing alone (Wells 1964, Gutnick et al. 2020, Buresch et al. 2024). Attachment itself is supported by local sensorimotor processing within the arm nervous system, with CNS involvement depending on context (Nesher et al. 2014), indicating that contact and initial attachment can be initiated peripherally. Since previous studies show that octopus suckers become more persistent in attachment when central control is removed, active release is likely to depend on CNS input. This suggests that the transition from exploration to retrieval depends on integration of contact cues at the CNS level.

The amount of mechanical and chemical information available from a 2 mm piece is much less than from the 4 mm and 10 mm pieces. The 2 mm piece has a smaller surface area and likely stimulates fewer tactile and chemical receptors than the larger pieces. In addition, it may be mechanically more difficult to grasp the piece securely: less surface provides fewer attachment sites and fewer suckers that can

be recruited through local bending. Consistent with this, Touch-to-Fetch duration was longest for 2 mm pieces, intermediate for 4 mm pieces, and shortest for 10 mm pieces. This suggests that initiating retrieval of smaller pieces required longer sensory sampling and grasping time than for larger pieces. Additionally, medial and tip locations showed similar Touch-to-Fetch durations within size groups.

Once fetch was initiated, 10 mm pieces were fetched faster than 2 mm and 4 mm pieces. This result is very relevant if we consider that, consistent with previous work (Gutfreund et al. 1996), the velocity of motion execution is determined by muscle activation level, which is set centrally at the CNS level. Fetching behaviour is initiated by the sensory stimuli provided by the grasped object and, once initiated, Fetch can be organised through arm biomechanical constraints with limited central specification (Sumbre et al. 2001). This suggests that the CNS may tune the fetching velocity based on the size of the food, which likely changes the amount of chemotactile information travelling from the suckers to the brain motor control centres. However, this tuning may be threshold-like, as there was no velocity difference between 2 mm and 4 mm pieces. We also found an effect of arm location on velocity across all size groups, with faster retrieval when the tip region was used. This fits with the idea that the tip provides more effective wrapping and attachment sites and, because Fetch relies on a pseudo-joint structure, potentially allowing a more efficient movement when a longer arm section is available. A distal bias in grasping and bend expression has also been reported in freely behaving octopuses (Kennedy et al. 2020, Bennice et al. 2025). In line with this, Bennice et al. (2025) found that the tip is preferentially used for grasping compared to more proximal arm regions and suggested that this functional partitioning may be supported by proximal–distal differences in longitudinal muscle dimensions. If pseudo-joints are formed by local bending, such a distal mechanical specialisation could facilitate faster or more reliable bend formation during Fetch, especially when the object is grasped at the tip.

To further isolate the role of sucker chemosensory cues in retrieval initiation, we presented 10 mm agar pieces treated with seawater (SW) or shrimp juice (SJ). Consistent with earlier work showing that octopuses are able to discriminate agar

stimuli based on prey extract (Buresch et al. 2022), we tested the retrieval strategies used by animals in a context where only the chemical cues were modified but size and mechanical properties of the grasping object were kept constant. With a single exception, octopuses fetched exclusively SJ–treated agar pieces. This indicates that food chemosensory cues perceived at the sucker level are essential to the initiation of a fetching behaviour.

To test whether processing of the sucker-perceived prey cues can occur locally within the arm PNS or requires CNS involvement, we presented the same agar stimuli to isolated arms. We hypothesised that if the behavioural bias driven by prey extract is primarily computed centrally, then removing the brain would eliminate that treatment-dependent modulation of the response. In that case, isolated arms would still express local, mechanically driven reaction patterns consistent with early observations (Uexküll 1893, Ten Cate 1928) and may retain local chemotactile detection, but would not reliably differentiate between the two agar treatments at the level of overall reactivity. As the agar pieces were identical in all respects except for the chemical cues, this would result in a similar reactivity of the arm to both conditions. Interestingly, our hypothesis was confirmed as no effect of agar piece treatment on arm reactivity was observed. Hence, the presence or absence of prey-related chemical cues alone does not modify the local arm reaction loop. These findings and previous studies support the idea that the type of chemical cue may be fundamental to action selection. Indeed, it has been shown that octopus sucker attachment can be inhibited at the peripheral level by specific chemical cues; for example, Nesher et al. (2014) showed that chemicals in octopus skin inhibit attachment, likely to avoid entanglement.

Taken together, these data support the interpretation that chemical cues bias action selection primarily when central processing is available, rather than through PNS-only circuitry.

As in the previous experiment, we were also interested in the possible presence of arm-specific reaction. However, arm location influenced reaction probability for both agar types, with the medial region showing the strongest responses. In Experiment I, arm location did not affect Touch-to-Fetch latency for 10 mm pieces, whereas the

ex vivo agar experiment showed clear location-dependent reactivity. This contrast suggests that CNS involvement may modulate peripheral reactivity during intact foraging, potentially preventing indiscriminate attachment during probing while still enabling rapid retrieval when prey-like cues are present.

Together, these results support a threshold-like model in which stimuli perceived by suckers and processed centrally drive retrieval decisions and retrieval kinematics *in vivo*, whereas isolated arms express local, location-dependent reactivity without a corresponding shift in action selection.

4.3 Sucker stereotyped attachment and detachment

After examining how suckers collect sensory information that shape arm behaviour and CNS decision-making, we next took a closer look at sucker motion patterns during attachment and detachment. We observed that suction attachment/release and arm movement can be coordinated in different ways depending on behavioural context, potentially involving contributions from both peripheral and central control.

This is particularly evident when looking at the different mechanisms of sucker attachment (Figure 35). The most frequently used strategy was the so-called ‘Orientation–Contraction Attachment’ (OCA) which often resulted in a loose attachment. In most cases, attachment was restricted to a single sucker without support from neighbouring suckers. As a result, the sucker could attach and detach quickly and follow the overall arm movement. This strategy may be used in exploratory behaviour, where the animal collects information about the probed surface, potentially to recruit additional suckers or to continue probing with a single sucker if no relevant sensory stimuli are perceived. Similarly, in ‘Wave-Like Attachment’ (WLA), the most frequent attachment method observed when arms were in motion, no neighbouring suckers were attached. This stereotypical attachment may also help the cup establish contact in the direction of arm movement without interfering with it and support exploratory probing.

The second most frequent strategy was ‘Contraction Attachment’ (CA). CA was often accompanied by relatively steady arm posture and generally resulted in strong

attachment, suggesting it may be used to mechanically support the arm and the animal's attachment to surfaces, but possibly also in object holding and active probing.

Attachments were divided into three strength categories: loose, medium and strong. In loose attachment, only the sucker rim, the region richest in sensory receptors (Graziadei and Gagne 1976), appeared to be in contact with the surface. In medium and strong attachments, a larger portion of the sucker's inner surface (the infundibulum) was in contact with the front tank wall and the protuberance of the acetabulum was pressed over the sphincter. In this configuration, internal negative pressure increases and attachment strength rises (Packard 1988, Tramacere et al. 2013, 2015). Loose attachments may therefore be used during exploratory actions when strong attachment is not required, whereas stronger attachment may be initiated once a 'potentially interesting' target is sensed.

Similarly, various strategies to detach from surfaces were detected. In most of the cases, detachment appeared to be induced indirectly by arm movement that pulled the sucker away from the surface generating a Wave-Like Detachment' (WLD). In this case, detachment is initiated by the rim lifting from the glass at a single point, followed by full detachment, allowing pressure release. Whether this is driven purely by mechanical pull-off or assisted by a neural signal that induces cup contraction/relaxation and concomitant release will need further investigation. A second mechanism was the so-called 'Contraction Detachment' (CD) in which the sucker rim contracts and detaches immediately from the glass surface.

In addition, we also report evidence for a possible modulation of the dynamic pressure changes within the suction cup during attachment and detachment. We show that the different strategies are associated with distinct pressure profiles and are consistent with the possibility that suction is dynamically modulated over time depending on behavioural context. We show that across all four events, negative pressure developed only after the sucker had visibly sealed, consistent with the four-phase sequence proposed by (Tramacere et al. 2013). The pressure traces further indicate ongoing suction adjustment during attachment, including stepwise reinforcement followed by gradual release. Within the framework proposed by Tramacere et al. (2013), one possible explanation is that the sucker does not simply

progress once through the four phases, but can return to an earlier attachment state to increase suction again. In that case, reinforcement could involve re-engaging the mechanism that increases chamber volume while the protuberance is briefly disengaged and then relocked. The protuberance could therefore act as a valve, allowing suction to be strengthened without the negative pressure being fully lost, which would fit with our traces not showing a return to baseline between reinforcement steps. Our data therefore suggest that the four-phase framework could be extended to include continuous suction modulation during the attached state. These patterns could reflect local control mechanisms within the arm PNS, including coordination with neighbouring suckers, and/or higher-level control (Bagheri et al. 2020, Hochner et al. 2023).

The results also highlight the strength of our custom-built setup, developed in direct collaboration with engineers from the Bioinspired Soft Robotics group, which enables precise pressure profiling during voluntary sucker attachments in a freely moving octopus. However, because of the spacing between pressure-channel outlets, we could not reliably quantify simultaneous multi-sucker recruitment or resolve pressure contributions from multiple suckers acting at once. Additionally, because we recorded the video only from the front, we could not detect out-of-plane movements of the sucker or arm. Adding a side-view camera would help capture changes in infundibulum shape in depth, but this may still not fully resolve subtle deformations. In future work, combining multi-view video with DeepLabCut motion capture or other tracking approaches could help determine whether the infundibulum is being forcefully deformed during attachment. These limitations should be addressed in the next platform prototype by reducing outlet spacing and/or increasing spatial sensor density.

4.4 Implications for soft robotic control

To summarise the broader relevance of the experimental findings, Table 14 links the main biological principles identified in this thesis to current challenges in tentacle-like soft robotics. Rather than proposing direct robotic implementations, the table highlights how specific octopus arm and sucker behaviours may inspire design principles for soft robotic control, sensing, stiffness regulation and attachment.

Table 14 ***Biological principles identified in this thesis and their potential relevance for tentacle -like soft robotics***

Experiment	Treatment	Tested factor	Time to initiate fetch	Velocity of fetch	Biological effect	Biological function	Robotic challenge	Possible implementation
Octopus food retrieval using fetch 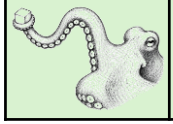	Single food piece: 2, 4 or 10 mm	Food size	2 mm +++ 4 mm ++ 10 mm + ↓	2 mm ++ 4 mm ++ 10 mm +++ ↓	**Larger food** items **reduce** decision time and **increase** retrieval speed	Sensory information modulates action selection and motor output	How to adapt robot behaviour to sensory relevance?	Sensory-weighed decision threshold and adaptive speed control
		Arm location used	Medial + Tip +	Medial ++ Tip +++ ↓	**Tip** use is associated with **higher** retrieval velocity	Arm shows functional partitioning	How to implement segment specialisation in continuum arms?	Segment-specific material stiffness and local actuator/sensor modules

Experiment	Movement	Muscle	Active	Activity over phases	Correlation over phases	CCI over phases	Biological effect	Biological function	Robotic challenge	Possible implementation
Octopus arm base antagonistic muscle activity 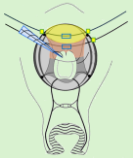	Extension	Aboral longitudinal	✓	Phase 1 +++ Phase 2 ++ Phase 3 ++ ↓	Phase 1 + Phase 2 +++ ↑ = Phase 3	Phase 1 +++ Phase 2 ++ Phase 3 ++ ↓	**Both** muscles contract and show initial **increase** in both **activity** and **co-contraction**	Stabilisation of the arm base to terminate movement and dampen residual motion Low-cost posture maintenance	How to stabilise a continuum arm locally without restricting distal motion?	Variable stiffness control using antagonistically arranged actuators and region-specific material stiffness
		Transverse	✓							
	Withdrawal-like	Aboral longitudinal	✓	Phase 1 +++ Phase 2 ++ Phase 3 ++ ↓	Phase 1 +++ Phase 2 ++ Phase 3 ++ ↓	Phase 1 ++ Phase 2 ++ Phase 3 ++	**Both** muscles contract and show initial **increase** in both **activity** and **temporal correlation**	Stabilisation of the arm base to resist passive deformation	How to stabilise and hold a continuum arm under constant load?	Local proprioceptive feedback/sensing coupled with antagonistically arranged actuators and variable-stiffness locking
		Transverse	✓							

Experiment	Technique	Pressure modulation	Biological effect	Biological function	Robotic challenge	Possible implementation
Sucker attachment/ detachment strategies 	Wave-like	✓	The **sucker** attaches/detaches **gradually** and adjusts attachment pressure	Stepwise adjustment to the surface to explore, improve seal and to reduce strain Dynamic strategy transition between exploring and anchoring to a surface	How to adapt artificial sucker behaviour for exploration, anchoring and dynamic pressure control?	Sensorised suction cups Stepwise vacuum build-up/release Actuated rim-peeling for controlled detachment
		✓				
	Cup-contraction	✓	The **whole sucker** attaches/detaches **immediately** and adjusts attachment pressure	Rapid attachment for immediate anchoring Dynamic strategy transition between exploring and anchoring to a surface		
		✓				

Symbols indicate relative changes in the measured variables; arrows indicate the direction of the observed effect.

Together, these examples suggest that octopus-inspired soft robotic control may benefit from combining centralised task-level commands with local mechanical and sensory rules distributed along the arm. In particular, region-specific arm function, sensory thresholds for action initiation, local stiffness modulation and controlled attachment/detachment may provide complementary strategies to purely model-based or data-driven control approaches.

5. Conclusion

This thesis aimed to uncover octopus arm and sucker control mechanisms that may offer biological strategies for reducing control complexity in muscular hydrostats and, ultimately, inform soft-robotic design. To address this, we linked local arm muscle recruitment, sucker sensory-driven action selection, and sucker attachment dynamics.

Octopuses are a prime example of embodied intelligence. Motor programmes embedded within the arm PNS allow stereotypical movements to be induced in isolated arms through simple electrical or mechanical stimulation. Taking a closer look at the biomechanics revealed evidence of regional arm specialisation, where the proximal arm region primarily serves a stabilising role. We induced arm extension and withdrawal-like resistance and recorded at a proximal site in an *ex vivo* arm preparation. Our analysis showed consistent co-activation of antagonistic muscles and reduced local deformation under load. This is consistent with behavioural studies reported in the literature, which show that deformations requiring greater flexibility, such as torsion, are expressed primarily in medial–distal arm segments. Arm segment specialisation also appears in our foraging experiments. We found that food pieces are retrieved most often with the medial and distal portions of the arm. Moreover, food pieces grasped by the arm tip are fetched faster than when grasped at the medial segment. In this case, the differences in mechanical constraint along the arm seem to play a role in the overall velocity of the resulting deformations. In addition, the CNS also appears to be involved in tuning fetch velocity based on the food size and therefore its possible ‘value’.

We show that the three steps leading to the execution of an action (action selection, initiation, and modulation) are strongly driven by a feedback system between the suckers’ sensory system and the brain. Decision-making processes in the CNS are based on selectively evaluating the type and amount of sensory information received at the sucker level. Our *in vivo* experiments demonstrated that sucker chemo- and mechanotactile input supported food-size discrimination and was associated with faster initiation and higher fetch velocities for larger food items. Chemical cues, in particular, seem to play a role in CNS decision-making. We

observed that prey-related chemical cues strongly biased retrieval when information was processed in the CNS, but this effect disappeared in isolated arms. This information exchange from the suckers to the CNS is enabled by thousands of chemotactile and mechanotactile receptors in the sucker rim.

Suckers can transition from probing, with rim contact only, to forming a full seal that increases both sensory stimulation and attachment force. The attachment and detachment pattern is carefully chosen for its purpose to minimise tissue damage while also providing strong attachment, depending on context. We consistently observed three attachment and two detachment patterns, with proof-of-concept evidence that suction can be adjusted dynamically during attachment, consistent with context-dependent modulation of seal strength.

Overall, our findings highlight how octopuses manage the control demands of highly redundant limbs through embodied intelligence and hierarchical organisation. This includes arm segment specialisation during stereotyped movements, sucker-to-brain sensory feedback that supports action initiation and tuning, and stereotyped sucker attachment strategies adapted to behavioural context.

For soft robotics, these results underline the value of combining distributed sensing with local, predefined control circuits. Mimicking sucker-like attachment could further enable robust, damage-minimising manipulation, particularly in tight, visually constrained environments where large movements and vision-driven control are limited. By translating these biological control principles into engineered systems, we can help make soft robots safer, more capable, and more useful in the environments where they matter most.

Future work

In future steps we will complement our EMG data by incorporating proximal arm recordings from additional longitudinal muscle groups (e.g., lateral and oral longitudinal musculature) to better resolve the muscle recruitment underlying stabilisation. To directly link activation to deformation, EMG measurements will be combined with simultaneous sonomicrometry and DeepLabCut motion tracking within the same trials. Finally, the dataset of the pressure-platform will be extended to increase the number of recordings with improvements that will allow more robust comparisons and enable analyses of multi-sucker recruitment.

6. References

Altman, J. S. 1971. Control of Accept and Reject Reflexes in the Octopus. Nature 229:204–206.

Ambrose, R. F., and B. V. Nelson. 1983. Predation by Octopus vulgaris in the Mediterranean. Marine Ecology 4:251–261.

Ansari, Y., M. Manti, E. Falotico, Y. Mollard, M. Cianchetti, and C. Laschi. 2017. Towards the development of a soft manipulator as an assistive robot for personal care of elderly people. International Journal of Advanced Robotic Systems 14:1–17.

Bagheri, H., A. Hu, S. Cummings, C. Roy, R. Casleton, A. Wan, N. Erjavic, S. Berman, M. M. Peet, D. M. Aukes, X. He, S. C. Pratt, R. E. Fisher, and H. Marvi. 2020. New Insights on the Control and Function of Octopus Suckers. Advanced Intelligent Systems 2:1900154.

Bennice, C. O., K. C. Buresch, J. H. Grossman, T. D. Morano, and R. T. Hanlon. 2025. Octopus arm flexibility facilitates complex behaviors in diverse natural environments. Scientific Reports 15:31875.

Bidel, F., N. C. Bennett, and T. J. Wardill. 2022. Octopus bimaculoides' arm recruitment and use during visually evoked prey capture. Current Biology 32:4727–4733.

Budelmann, B. U. 1996. Active marine predators: The sensory world of cephalopods. Marine and Freshwater Behaviour and Physiology 27:59–75.

Budelmann, B. U., and J. Z. Young. 1985. Central pathways of the nerves of the arms and mantle of *Octopus*. Philos Trans R Soc Lond B Biol Sci 310:109–122.

Buresch, K. C., N. D. Huget, W. C. Brister, E. Y. Zhou, A. S. Lineaweaver, C. Rifai, J. Hu, Z. E. Stevenson, J. G. Boal, and R. T. Hanlon. 2024. Evidence for tactile 3D shape discrimination by octopus. Journal of Comparative Physiology A: Neuroethology, Sensory, Neural, and Behavioral Physiology 210:815–823.

Buresch, K. C., K. Sklar, J. Y. Chen, S. R. Madden, A. S. Mongil, G. V. Wise, J. G. Boal, and R. T. Hanlon. 2022. Contact chemoreception in multi-modal sensing of prey by Octopus. Journal of Comparative Physiology A: Neuroethology, Sensory, Neural, and Behavioral Physiology 208:435–442.

Ten Cate, J. 1928. Contribution a l'innervation des ventouses chez Octopus vulgaris. Archives neerlandaises de physiologie de l'homme et des animaux 12:188.

Chang, W., and M. E. Hale. 2023. Mechanosensory signal transmission in the arms and the nerve ring, an interarm connective, of Octopus bimaculoides. iScience 26:106722.

Di Clemente, A., F. Maiole, I. Bornia, and L. Zullo. 2021. Beyond muscles: Role of intramuscular connective tissue elasticity and passive stiffness in octopus arm muscle function. Journal of Experimental Biology 224:jeb242644.

Dou, W., G. Zhong, J. Cao, Z. Shi, B. Peng, and L. Jiang. 2021. Soft Robotic Manipulators: Designs, Actuation, Stiffness Tuning, and Sensing. Advanced Materials Technologies 6:2100018.

Elfferich, J. F., D. Dodou, and C. Della Santina. 2022. Soft Robotic Grippers for Crop Handling or Harvesting: A Review. IEEE Access 10:75428–75443.

Feinstein, N., N. Nesher, and B. Hochner. 2011. Functional morphology of the neuromuscular system of the Octopus vulgaris arm. Vie et Milieu - Life and Environment 61:219–229.

Fiorito, G., A. Affuso, D. B. Anderson, J. Basil, L. Bonnaud, G. Botta, A. Cole, L. D'Angelo, P. De Girolamo, N. Dennison, L. Dickel, A. Di Cosmo, C. Di Cristo, C. Gestal, R. Fonseca, F. Grasso, T. Kristiansen, M. Kuba, F. Maffucci, A. Manciocco, F. C. Mark, D. Melillo, D. Osorio, A. Palumbo, K. Perkins, G. Ponte, M. Raspa, N. Shashar, J. Smith, D. Smith, A. Sykes, R. Villanueva, N. Tublitz, L. Zullo, and P. Andrews. 2014. Cephalopods in neuroscience: Regulations, research and the 3Rs. Invertebrate Neuroscience 14:13–36.

Fiorito, G., A. Affuso, J. Basil, A. Cole, P. de Girolamo, L. D'angelo, L. Dickel, C. Gestal, F. Grasso, M. Kuba, F. Mark, D. Melillo, D. Osorio, K. Perkins, G. Ponte, N. Shashar, D. Smith, J. Smith, and P. lr Andrews. 2015. Guidelines for the Care and Welfare of Cephalopods in Research –A consensus based on an initiative by CephRes, FELASA and the Boyd Group. Laboratory Animals 49:1–90.

Flash, T., and L. Zullo. 2023. Biomechanics, motor control and dynamic models of the soft limbs of the octopus and other cephalopods. Journal of Experimental Biology 226:jeb245295.

Forsythe, J. W., and R. T. Hanlon. 1997. Foraging and associated behavior by *Octopus cyanea* Gray, 1849 on a coral atoll, French Polynesia. Journal of Experimental Marine Biology and Ecology 209:15–31.

Fossati, S., F. Benfenati, and L. Zullo. 2011. Morphological characterization of the *Octopus vulgaris* arm. Vie et Milieu - Life and Environment 61:191–195.

Friard, O., and M. Gamba. 2016. BORIS: a free, versatile open-source event-logging software for video/audio coding and live observations. Methods in Ecology and Evolution 7:1325–1330.

Girod, P. 1884. Recherches sur la peau des céphalopodes. La ventouse. Arch. zool. exp. gén 2:379–401.

Grasso, F. W., and J. A. Basil. 2009. The evolution of flexible behavioral repertoires in cephalopod molluscs. Brain, behavior and evolution 3:231–245.

Grasso, F. W. 2008. Octopus sucker-arm coordination in grasping and manipulation. American Malacological Bulletin 24:13–23.

Graziadei, P. 1962. Receptors in the Suckers of Octopus. Nature 195:57–59.

Graziadei, P. 1964. Electron microscopy of some primary receptors in the sucker of *Octopus vulgaris*. Zeitschrift für Zellforschung und Mikroskopische Anatomie 64:510–522.

Graziadei, P. 1971. The nervous system of the arms. Pages 45–62 In: Young JZ (ed) The anatomy of the nervous system of *Octopus vulgaris*. Oxford University Press, Oxford.

Graziadei, P., and H. T. Gagne. 1976. Sensory innervation in the rim of the octopus sucker. Journal of Morphology 150:639–679.

Gutfreund, Y. 1998. Patterns of arm muscle activation involved in octopus reaching movements. Journal of Neuroscience 18:5976–5987.

Gutfreund, Y., T. Flash, Y. Yarom, G. Fiorito, I. Segev, and B. Hochner. 1996. Organization of Octopus Arm Movements: A Model System for Studying the Control of Flexible Arms. The Journal of Neuroscience 16:7297–7307.

Gutfreund, Y., H. Matzner, T. Flash, and B. Hochner. 2006. Patterns of Motor Activity in the Isolated Nerve Cord of the Octopus Arm. The Biological Bulletin 211:212–222.

Gutnick, T., L. Zullo, B. Hochner, and M. J. Kuba. 2020. Use of Peripheral Sensory Information for Central Nervous Control of Arm Movement by *Octopus vulgaris*. Current Biology 30:4322–4327.

Hague, T., M. Florini, and P. L. R. Andrews. 2013. Preliminary in vitro functional evidence for reflex responses to noxious stimuli in the arms of *Octopus vulgaris*. Journal of Experimental Marine Biology and Ecology 447:100–105.

Hanassy, S., A. Botvinnik, T. Flash, and B. Hochner. 2015. Stereotypical reaching movements of the octopus involve both bend propagation and arm elongation. Bioinspiration and Biomimetics 10:035001.

Hanke, F. D., and A. Kelber. 2020. The Eye of the Common Octopus (*Octopus vulgaris*). Frontiers in Physiology 10:1637.

Hanlon, R. T., and J. B. Messenger. 2018. Cephalopod behaviour. II. Cambridge University Press, Cambridge, UK.

Hochner, B., L. Zullo, T. Shomrat, G. Levy, and N. Nesher. 2023. Embodied mechanisms of motor control in the octopus. Current Biology 33:R1119–R1125.

Imperadore, P., M. G. Lepore, G. Ponte, H. J. Pflüger, and G. Fiorito. 2019. Neural pathways in the pallial nerve and arm nerve cord revealed by neurobiotin backfilling in the cephalopod mollusk *Octopus vulgaris*. Invertebrate Neuroscience 19:5.

Iqbal, F., M. Esfandiari, G. Amirkhani, H. Hoshyarmanesh, S. Lama, M. Tavakoli, and G. R. Sutherland. 2025. Continuum and Soft Robots in Minimally Invasive Surgery: A Systematic Review. IEEE Access 13:24053–24079.

Kawashima, S., and Y. Ikeda. 2025. Cross-Modal Object Recognition and Reliability Between Visual and Tactile Senses in Octopus (*Callistoctopus aspilosomatis*). Zoological science 42:260–269.

Kennedy, E. B. L., K. C. Buresch, P. Boinapally, and R. T. Hanlon. 2020. Octopus arms exhibit exceptional flexibility. Scientific Reports 10:20872.

Kier, W. M. 2016. The musculature of coleoid cephalopod arms and tentacles. Frontiers in Cell and Developmental Biology 4:10.

Kier, W. M., and A. M. Smith. 1990. The Morphology and Mechanics of Octopus Suckers. The Biological Bulletin 178:126–136.

Kier, W. M., and A. M. Smith. 2002. The Structure and Adhesive Mechanism of Octopus Suckers. Integrative And Comparative Biology 42:1146–1153.

Kier, W. M., and K. K. Smith. 1985. Tongues, tentacles and trunks: the biomechanics of movement in muscular-hydrostats. Zoological Journal of the Linnean Society 83:307–324.

Kier, W. M., and M. P. Stella. 2007. The Arrangement and Function of Octopus Arm Musculature and Connective Tissue. Journal of Morphology 268:831–843.

Van Leeuwen, J. L., and W. M. Kier. 1997. Functional design of tentacles in squid: Linking sarcomere ultrastructure to gross morphological dynamics. Philosophical Transactions of the Royal Society B: Biological Sciences 352:551–571.

Levy, G., and B. Hochner. 2017. Embodied Organization of *Octopus vulgaris* Morphology, Vision, and Locomotion. Frontiers in Physiology 8:164.

Longren, L. L., L. Eigen, A. Shubitidze, O. Lieschnegg, D. Baum, J. A. Nyakatura, T. Hildebrandt, and M. Brecht. 2023. Dense reconstruction of elephant trunk musculature. Current Biology 33:1–8.

Maloisel, G., E. Knoop, C. Schumacher, and M. Bächer. 2021. Automated Routing of Muscle Fibers for Soft Robots. IEEE Transactions on Robotics 37:996–1008.

Martini, M., E. Solfiti, A. Mondini, E. Del Dottore, A. Parmiggiani, E. Sinibaldi, and B. Mazzolai. 2026. Routing Optimization of Cable-Driven Octopus-Inspired Manipulators

With Minimal Actuation via Genetic Algorithm and Finite Element Method. Advanced Intelligent Systems 8.

Mather, J., and R. K. O`Dor. 1991. Foraging strategies and predation risk shape the natural history of juvenile *Octopus vulgaris*. Bulletin of Marine Science 49 49:256–269.

Mathis, A., P. Mamidanna, K. M. Cury, T. Abe, V. N. Murthy, M. W. Mathis, and M. Bethge. 2018. DeepLabCut: markerless pose estimation of user-defined body parts with deep learning. Nature Neuroscience 21:1281–1289.

Mazzolai, B., L. Margheri, P. Dario, and C. Laschi. 2013. Measurements of octopus arm elongation: Evidence of differences by body size and gender. Journal of Experimental Marine Biology and Ecology 447:160–164.

Neacsu, D., and R. J. Crook. 2024. Repeating ultrastructural motifs provide insight into the organization of the octopus arm nervous system. Current biology 34:4767–4773.

Nesher, N., G. Levy, F. W. Grasso, and B. Hochner. 2014. Self-recognition mechanism between skin and suckers prevents octopus arms from interfering with each other. Current Biology 24:1271–1275.

Nesher, N., G. Levy, L. Zullo, and B. Hochner. 2020. Octopus Motor Control. Oxford University Press USA.

Olson, C. S., A. Moorjani, and C. W. Ragsdale. 2025. Molecular and Morphological Circuitry of the Octopus Sucker Ganglion. Journal of Comparative Neurology 533:e70055.

Packard, A. 1988. The Skin of Cephalopods (Coleoids): General and Special Adaptations. Pages 37–67 Form and Function. Elsevier.

Qadrie, Z., M. Maqbool, M. A. Dar, and A. Qadir. 2025. Navigating challenges and maximizing potential: Handling complications and constraints in minimally invasive surgery. Open Health 6:20250059.

R Core Team. 2021. R: language and environment for statistical computing. R Foundation for Statistical Computing, Vienna, Austria.

Raman, R., and C. Laschi. 2024. Soft robotics for human health. Device 2:100432.

Rowell, C. H. F. 1963. Excitatory and Inhibitory Pathways in the Arm of Octopus. Journal of Experimental Biology 40:257–270.

Rowell, C. H. F. 1966. Activity of interneurons in the arm of octopus in response to tactile stimulation. Journal of Experimental Biology 44:589–605.

Rus, D., and M. T. Tolley. 2015. Design, fabrication and control of soft robots. Nature 521:467–475.

Della Santina, C., C. Duriez, and D. Rus. 2023. Model-Based Control of Soft Robots: A Survey of the State of the Art and Open Challenges. IEEE Control Systems 43:30–65.

Smith, A. M. 1991. Negative pressure generated by octopus suckers: A study of the tensile strength of water in nature. Journal of Experimental Biology 157:257–271.

Smith, K. K., and W. M. Kier. 1989. Trunks, Tongues, and Tentacles: Moving with Skeletons of Muscle. Source: American Scientist 77:28–35.

Sumbre, G., G. Fiorito, T. Flash, and B. Hochner. 2006. Octopuses Use a Human-like Strategy to Control Precise Point-to-Point Arm Movements. Current Biology 16:767–772.

Sumbre, G., Y. Gutfreund, G. Fiorito, T. Flash, and B. Hochner. 2001. Control of octopus arm extension by a peripheral motor program. Science 293:1845–1848.

Tekinalp, A., N. Naughton, S. H. Kim, U. Halder, R. Gillette, P. G. Mehta, W. Kier, and M. Gazzola. 2024. Topology, dynamics, and control of a muscle-architected soft arm. Proceedings of the National Academy of Sciences 121:e2318769121.

Tonutti, M., D. S. Elson, G. Z. Yang, A. W. Darzi, and M. H. Sodergren. 2017. The role of technology in minimally invasive surgery: state of the art, recent developments and future directions. Postgraduate Medical Journal 93:159–167.

Tramacere, F., L. Beccai, M. Kuba, A. Gozzi, A. Bifone, and B. Mazzolai. 2013. The Morphology and Adhesion Mechanism of Octopus vulgaris Suckers. PLoS ONE 8:e65074.

Tramacere, F., N. M. Pugno, M. J. Kuba, and B. Mazzolai. 2015. Unveiling the morphology of the acetabulum in octopus suckers and its role in attachment. Interface Focus 5:20140050.

Uexküll, J. 1893. Physiologische Untersuchungen an Eledone moschata. II. Die Reflexe des Armes. Zeitschrift für Biologie 12:179–183.

Villanueva, R., V. Perricone, and G. Fiorito. 2017, August 17. Cephalopods as predators: A short journey among behavioral flexibilities, adaptions, and feeding habits. Frontiers Media S.A.

Vincent, T. L. S., D. Scheel, and K. R. Hough. 1998. Some Aspects of Diet and Foraging Behavior of *Octopus dofleini* (Wülker, 1910) in its Northernmost Range. Marine Ecology 19:13–29.

Walderon, M. D., K. J. Nolt, R. E. Haas, K. N. Prosser, J. B. Holm, G. T. Nagle, and J. G. Boal. 2011. Distance chemoreception and the detection of conspecifics in *Octopus bimaculoides*. Journal of Molluscan Studies 77:309–311.

Walker, I. D., D. M. Dawson, T. Flash, F. W. Grasso, R. T. Hanlon, B. Hochner, W. M. Kier, C. C. Pagano, C. D. Rahn, and Q. M. Zhang. 2005. Continuum Robot Arms Inspired by Cephalopods. Unmanned Ground Vehicle Technology VII 5804:303–314.

Weertman, W. L., V. Gopal, D. M. Sivitilli, D. Scheel, and D. H. Gire. 2025. Octopus track chemosensory plumes to find food. PLOS ONE 20:e0330262.

Wells, M. 1978. Octopus: physiology and behaviour of an advanced invertebrate. Springer Science & Business Media.

Wells, M. J. 1964. Tactile Discrimination of Surface Curvature and Shape by the Octopus. Journal of Experimental Biology 41:433–445.

Wells, M. J., and J. Wells. 1957. The Function of the Brain of Octopus in Tactile Discrimination. Journal of Experimental Biology 34:131–142.

Wilson, G. J., G. A. Wood, and B. C. Elliott. 1991. Optimal stiffness of series elastic component in a stretch-shorten cycle activity. Journal of applied physiology 70:825–833.

Yarnall, J. L. 1969. Aspects of the behaviour of *Octopus cyanea* gray. Animal Behaviour 17:747–754.

Young, J. Z. 1963. the Number and Sizes of Nerve Cells in Octopus. Proceedings of the Zoological Society of London 140:229–254.

Young, J. Z. 1971. The anatomy of the nervous system of *Octopus vulgaris*. Oxford University Press, Oxford.

Zullo, L., A. Di Clemente, and F. Maiole. 2022. How octopus arm muscle contractile properties and anatomical organization contribute to arm functional specialization. Journal of Experimental Biology 225:jeb243163.

Zullo, L., S. Fossati, and F. Benfenati. 2011. Transmission of sensory responses in the peripheral nervous system of the arm of *Octopus vulgaris*. Vie et Milieu - Life and Environment 61:197–201.

Zullo, L., G. Sumbre, C. Agnisola, T. Flash, and B. Hochner. 2009. Nonsomatotopic Organization of the Higher Motor Centers in Octopus. Current Biology 19:1632–1636.

7. Appendix A Thesis related papers

Sucker Attachment and Detachment Patterns in *Octopus Vulgaris*

Janina Leonie Röckner, Mariana Díaz Arellano, and Letizia Zullo

July 2023 in Conference on Biomimetic and Biohybrid Systems (pp. 266-280). Cham: Springer Nature Switzerland.

DOI: 10.1007/978-3-031-38857-6_20

Octopus vulgaris has become an important model for motor control studies in soft robotics, due to its highly developed neural system and complexity in motion. For the past ten years, research on octopus arm motor system has provided advancements in understanding the control system of these hyper-redundant and flexible structures with further implementation in the field of soft robotics. In this work, we performed a correlation study of the sucker size and structure with their pattern of “attachment and detachment” using morphological and *in-vivo* behavior observational approaches.

Three main patterns of sucker attachment and detachment were identified and coded as ‘Contraction Attachment/Detachment’ (CA/CD), ‘Orientation-Contraction Attachment’ (OCA), and ‘Wave-Like Attachment/Detachment’ (WLA/WLD). The first two were more frequently used in attachment and the third one in detachment. Suckers involved in these motions showed a similar morphology and no correlation between the use of a specific strategy and their size was found.

We interestingly found indications of a possible association between the sucker strategy of attachment/detachment and overall arm movement. This suggests that the control of the sucker motion pattern may be linked to the suckers’ functional use and interpreted within the framework of the animal behavior.

Proprioception in Muscle Hydrostats

Letizia Zullo, Janina Leonie Röckner, Beatrice Pistolato

December 2025 in Integrative and Comparative Biology, Volume 65, Issue 6, Pages 1477–1488

DOI: 10.1093/icb/icaf046

Proprioception can be seen as a somatic sense stimulated by the action of the body itself. It is perceived through proprioceptors and is tightly linked to the animal body, as it is influenced by the biomechanical properties of the structures in which it is embedded. A specific class of these receptors, the muscle proprioceptors, project at several levels of the nervous system and provide information about limb position, whether in the presence or absence of movement, as well as muscle length, the sense of effort, and the sense of balance. In skeletal systems, proprioception is involved in postural maintenance, reflex actions, and rhythmic behaviors, but also in higher functions such as action planning and prediction. Proprioception can also be found in structures that are capable of movement without any real skeleton and are therefore called hydrostatic skeletons, both in humans and other animals. Hydrostatic bodies, including cephalopod limbs, the elephant trunk, and the human tongue, use muscle contractile forces to generate hydrostatic pressure, which acts as a skeleton to stabilize the structure and create motion. To provide online motion control of these bodies, the animal nervous system must cope with a huge amount of information coming from variables (such as length, angle, stiffness, and orientation) that continuously change throughout the entire structure. To limit this central burden, these structures may benefit from the presence of a muscle proprioceptive system used locally to control muscle contraction. Based on the current knowledge, many of the basic components of the proprioceptive system of soft-bodied and skeletal animals are essentially the same. Here, we aim to provide a forward-looking perspective on the role of muscle proprioception in motion, with a special focus on proprioception in muscular hydrostats. We wish to highlight the relevance of this topic across several fields of investigation, from human sensorimotor pathologies to soft robotics, where a high degree of autonomy in soft structures, combined with a reduced control demand, remains an unmet need. To address these gaps, we emphasize the need for improved knowledge and methodological assessment of this “sixth sense.”

8. Appendix B Other publications during the PhD

Octopus crawling on land: physiological and biochemical responses of *Octopus vulgaris* to emersion

Janina Leonie Röckner, Vanessa M. Lopes, José Ricardo Paula, Maria Rita Pegado, Martim Costa Seco, Mário Diniz, Tiago Repolho, Rui Rosa

November 2023 in Marine Biology, Volume 171, Issue 1, article 14

DOI: 10.1007/s00227-023-04333-x

Cephalopods are well known for their cognitive capabilities and unique behavioural repertoires. Yet, certain life strategies and behaviours are still not fully understood. For instance, coastal octopuses have been documented (mainly through citizen science and TV documentaries) to occasionally leave the water and crawl in intertidal areas. Yet, there is a complete lack of knowledge on this behaviour's physiological and biochemical basis. Within this context, this study aimed to investigate, for the first time, physiological (routine and maximum metabolic rates and aerobic scope) and biochemical (i.e., antioxidant enzymes activities, heat shock protein and ubiquitin levels, DNA damage, lipid peroxidation) responses of the common octopus, *Octopus vulgaris*, to emersion. The octopuses' physiological performance was determined by measuring metabolic rates in different emersion treatments and biochemical markers. The size-adjusted maximum metabolic rates (MMRadj) of octopuses exposed to 2:30 min of air exposure followed by re-immersion did not differ significantly from the MMRadj of the chased individuals (control group). Yet, most biochemical markers revealed no significant differences among the different emersion treatments. Our findings showed that O. vulgaris could tolerate exposure to short-term emersion periods due to an efficient antioxidant machinery and cellular repair mechanisms. Alongside, we argue that the use of atmospheric air through the mucus-covered gills and/or cutaneous respiration may also help octopus withstand emersion and crawling on land.

Collection, handling and care of cephalopod eggs

Roger Villanueva, Anne-Sophie Darmaillacq, …, Janina Leonie Röckner, …, Gjendine Voss

December 2025 in Reviews in Fish Biology and Fisheries, Volume 36, Issue 1, article umber 17

DOI: 10.1007/s11160-025-10017-0

Research on cephalopod early ontogeny has significantly advanced in recent decades, including embryo organogenesis and neurogenesis and early behavioural adaptations, particularly in commercially important and coastal species. Within this context, here we compiled current knowledge on the collection, handling and care under experimental conditions and monitoring in the field of cephalopod eggs and egg masses. It covers field observations and egg collection methods, as well as laboratory incubation protocols for eggs maintained with and without maternal care. It is emphasized how abiotic and biotic factors, including temperature, salinity, oxygen and maternal condition, shape embryonic development and hatchling survival and viability. Monitoring methods for cephalopod egg masses in the wild and the effects of natural threats such as storms and predators are reviewed. Anthropogenic impacts such as pollution, fisheries and climate change are also discussed. Technological advances have enabled finer analysis of neural development as the embryo grows, while ethical considerations regarding embryonic sentience capacity and welfare conditions are becoming central to current experimental designs. Based on current knowledge, it is recommended to apply ethical considerations and the 3Rs principle (Replacement, Reduction, Refinement) for cephalopod embryos following the onset of organogenesis. Thus, a list of potential indicators of health and welfare that could be used for assessing and monitoring cephalopod embryos and hatchlings is proposed. Overall, this synthesis aims to serve as a guide for advancing egg collection and laboratory incubation methodologies, as well as adopting ethical handling protocols to improve cephalopod embryo care and quality.

9. Acknowledgements

Working on a PhD thesis is very challenging. In a short time, you must adapt to a new environment, learn new techniques, develop and conduct experiments independently, and place the results into a clear context. Above all, you need the guidance and encouragement of your supervisors and labmates, and I consider myself lucky to have had both. I would therefore like to express my sincere appreciation to my supervisor, Letizia Zullo, who shared her expertise and guidance throughout my PhD. She encouraged me to develop my own ideas and interests, included me in other projects, and nurtured my interest in teaching through activities such as supervising students. With her help, I grew personally and professionally and gained the confidence to further develop my academic career.

I am also truly grateful to Barbara Mazzolai for allowing me to be part of her BSR group at IIT. This interdisciplinary PhD would not have been possible without the welcoming group she created and the inspiring environment it provided. Her Chief Technician, Alessio Mondini, was always willing to develop my ideas further, helping me truly combine biology and engineering in my work.

This work would also not have been possible without Fabio Benfenati. I am very thankful that he allowed me to join the NSYN group, encouraged me, and provided me with the necessary resources to complete my PhD. His group was always there to help, be it with technical problems or helpful input during lab meetings.

I would also like to warmly thank my PhD mate, Beatrice Pistolato. We started in this lab together, went through all the ups and downs, and kept each other afloat when experiments tended to fail. She never hesitated to help, even when her own schedule was overloaded. Bea, Letizia, and all the other members who were and still are part of our “Polpesse” group, Cosimo, Marta, Gaia, Edoardo, Victoria, Jadan, and Davide, helped me overcome the obstacles that came my way.

Finally, I cannot put into words how much I appreciate my family and close friends, who always found the right words when times were tough. This PhD was shaped not only by the science, but by the people who stood beside me throughout it. To all of you, thank you for being such an important part of these years and for making them unforgettable.